Universidad de La Laguna
Physics degree
Bachelor Thesis

A 2D extinction map of the thin disc of the Milky Way as revealed by the O stars and B supergiants surveyed by the IACOB project

Carlota Méndez Lápido

Supervisor:	Sergio Simón-Díaz
Date final version:	9th July 2023

Abstract

The study presented in this BSc thesis is part of a small research initiation project in Astrophysics developed in the framework of the *IACOB project* of the Instituto de Astrofísica de Canarias.

The gas and dust that make up the **interstellar medium (ISM)** absorb and scatter the light reaching us from distant stars, a process which is known as **interstellar extinction**.
This physical phenomenon is also called as **reddening**, as it is more susceptible to short wavelengths, so blue light is more absorbed than red light, thus the interstellar extinction is wavelength-dependent. Furthermore, this phenomenon is related to the amount of material present in the medium between the emitter and the observer; therefore, to characterise the clumpy interstellar medium, as well as the molecular clouds and other regions with high dust density that compose it, and also to quantify the extinction to which the objects immersed in them are subject, two interstellar extinction parameters are defined: (1) the **amount of light that is absorbed and/or scattered by the medium**: A_λ and (2) the **type of dust present** in different regions of the ISM: R_λ. In parallel, reddening is defined as the **colour excess**: $E(\lambda_1 - \lambda_2)$, i.e. the difference in the light reaching our detectors from a star observed at two different wavelengths. In general terms, these parameters are defined for the UBV (Johnson-Morgan) photometric system, so that the above quantities result in: A_V, R_V and $E(B-V)$. As a consequence of this dependence on λ, it is not possible to attack the interstellar extinction phenomenon from a bolometric point of view, since a strong effect in the ultraviolet range results weak in the optical and undetectable in the infrared band. A set of extinction laws are then proposed for different ranges of the electromagnetic spectrum; some of the best known are those proposed by Cardelli, Clayton, and Mathis 1989, Fitzpatrick 1999 and Maız Apellániz, Evans, et al. 2014 (the latter will be the ones used in the theoretical development of the thesis).

The aim of this BSc thesis is to develop a 2D map of the interstellar extinction characterizing a region of the thin disc of the Milky Way by means of a sample of about 762 Galactic O stars and B suprgiants located at distances of up to 4 kpc.
The sample of stars under study has been extracted from the **IACOB spectroscopic database** which includes OB Galactic stars observed from multi-epocal photometric and spectropolarimetric, high-resolution spectroscopic observations from both the Northern and Southern Hemispheres (led by the IACOB and OWN projects respectively).

Since OB stars are characterised as hot, massive objects with short lifetimes, they are associated to regions of recent (or even active) star formation. Their study in the Milky Way allows the identification of these regions, which mainly are the **spiral arms of the Galaxy and the Gould belt**. The distances to our sample of stars under study are taken from the **Bailer-Jones catalogue** and derived from parallax values obtained from Gaia data.

Interstellar extinction does not modify the stellar parameters, but it does modify the apparent magnitude and spectral energy distribution of each object: **SED**. From an IDL code developed by Miguel Urbaneja (University of Innsbruck), the interstellar extinction parameters are calculated by comparing the observed spectral distribution with the synthetic SED resulting from applying a stellar atmosphere code (**FASTWIND**) by

applying a **Markov chain in the Monte Carlo Method** to the respective photometry values for each star. In particular, the program tries to relate the observed and the synthetic SED by fitting the **photometric values** of the filters in the visible spectrum: B,V (extracted from the Simbad astronomical catalogue) and in the infrared: J,H,K (extracted from the 2MASS near-infrared photometric catalogue) by applying the set of extinction laws of Maíz Apellániz et al. (2015).
A previous study by Maız Apellániz and R. H. Barbá 2018 for these stars in the solar neighbourhood is also taken as a comparative anchor for the subsample of O-type stars.

From the interstellar extinction values of each object, the members of the research group will be able to complete the information on the physical characteristics of each star, such as radius, mass and luminosity, among others. More generally, the study will have an impact on future large-scale physical analyses of the characterisation of the properties of the Milky Way disc.

Resumen

El estudio presentado en este Trabajo de Fin de Grado es parte de un proyecto de investigación en astrofísica dentro del proyecto IACOB del Instituto de Astrofísica de Canarias.

El gas y polvo que componen el medio interestelar (ISM) absorben y dispersan la luz que nos llega de las estrellas lejanas, proceso que se conoce como extinción interestelar.
Este fenómeno físico también recibe el nombre de enrojecimiento, ya que es más susceptible a las longitudes de onda cortas, luego la luz azul es absorbida en mayor cantidad que la roja, por lo que la extinción interestelar depende de la longitud de onda. Además, este fenómeno se relaciona con la cantidad de material presente en el medio que hay entre el emisor y el observador; por tanto, para caracterizar el medio interestelar grumoso, así como las nubes moleculares y otras regiones con alta densidad de polvo que lo componen y además cuantizar la extinción a la que están sujetos los objetos inmersos en ellas, se definen dos parámetros de extinción interestelar: (1) la cantidad de luz que es absorbida y/o dispersada por el medio: A_λ y (2) la cantidad y tipo de polvo presente en diferentes regiones del ISM: R_λ. Paralelamente se define el enrojecimiento como el exceso de color: $E(\lambda_1 - \lambda_2)$, es decir, la diferencia de la luz que nos llega de una estrella observada en dos longitudes de onda diferente. En términos generales estos parámetros se definen para el sistema fotométrico de UBV (Johnson-Morgan), de forma que las cantidades anteriores resultan: A_V, R_V y $E(B-V)$.
Como consecuencia de dicha dependencia con λ, no es posible atacar el fenómeno de la extinción estelar desde un punto de vista bolométrico, ya que un efecto fuerte en el rango del ultravioleta se convierte en débil en el óptico e indetectable en la banda infrarroja. Se proponen entonces un conjunto de leyes de extinción para diferentes rangos del espectro electromagnético; algunas de las más conocidas son las propuestas Cardelli, Clayton y Mathis 1989, Fitzpatrick 1999 y Maız Apellániz, Evans et al. 2014 (estas últimas serán las que se usarán en el desarrollo teórico de la tesis).

Se pretende realizar un mapa 2D de la extinción interestelar a partir de la caracterización de una región del disco delgado de la Vía Láctea mediante una muestra de unas 762 estrellas galácticas O y suprgigantes B situadas a distancias de hasta 4 kpc.
La muestra de estrellas estudiadas ha sido extraída de la base de datos espectroscópica IACOB, que incluye estrellas galácticas OB observadas a partir de espectroscopía multi-época y de alta resolución observables tanto desde el Hemisferio Norte como del Sur (lideradas por los proyectos IACOB y OWN respectivamente).

Dado que las estrellas OB se caracterizan por ser estrellas masivas y calientes con poco tiempo de vida, se asocian a regiones de formación estelar reciente (o incluso activa). Su estudio en la Vía Láctea permite identificar estas regiones que resultan ser principalmente los brazos espirales de la Galaxia y el cinturón de Gould. Las distancia de las estrellas que componen la muestra de estudio son tomadas del catálogo de Bailer-Jones que han sido derivadas a su vez de los valores de paralaje obtenidos a partir de datos de Gaia.

La extinción interestelar no modifica los parámetros estelares, pero sí la magnitud aparente y la distribución espectral de energía de cada objeto: SED (por sus siglas en inglés). A partir de un código en IDL desarrollado por Miguel Urbaneja (Universidad de Innsbruck) se calculan los parámetros de extinción interestelar a partir de la comparación de la distribución espectral observada con la SED sintética resultante

de aplicar un código de atmósfera estelar (FASTWIND) aplicando una cadena de Markov en el Método de Monte Carlo que ajusta los valores de fotometría respectivos a cada estrella. Concretamente, el programa trata de relacionar la SED observada y la sintética ajustando los valores fotométricos de los filtros en el espectro visible:B,V (extraídos del catálogo astronómico Simbad) y en el infrarojo: J,H,K (extraídos del catálogo fotométrico del infrarrojo cercano 2MASS) aplicando el conjunto de leyes de extinción de Maíz Apellániz et al. (2015)
Asimismo, se toma como anclaje comparativo para la submuestra de estrellas de tipo O un estudio previo realizado por Maız Apellániz y R. H. Barbá 2018 para dichas estrellas en la vecindad solar.

A partir de los valores de extinción interestelar de cada objeto, los integrantes del grupo IACOB serán capaces de completar la información referente a las características físicas de cada estrella, como son el radio, la masa y la luminosidad entre otros. En términos más generales, el estudio repercutirá en futuros análisis físicos a gran escala de la caracterización de las propiedades del disco de la Vía Láctea.

Agradecimientos

A mi tutor, por precisamente tutorizarme de la manera más didáctica y atenta posible. Por no ponerme límites y dejarme explorar la física que más me atrae; por confiar en mí y en mi proceso.
Al grupo IACOB en general, por acogerme y enseñarme pacientemente los conocimientos necesarios, además de compartir su apasionada visión conmigo.

A Miguel Urbaneja por compartir conmigo sus códigos y por su espléndida disposición para solventar las dudas que me surgieron en la utilización de los mismos.

A mi familia y amigos por su apoyo incondicional. Gracias.

Contents

List of Figures

List of Tables

Chapter 1
INTRODUCTION

En esta sección se da una definición general de la extinción interestelar, ahondando en los elementos del medio interestelar que causan la absorción y dispersión de la luz que nos llega de estrellas lejanas. Concretamente, se debe a regiones del espacio en las que se acumulan densidades altas de polvo y gas, que junto a otros requisitos propios de la nebulosa, dan lugar a la formación de estrellas.
Paralelamente se introduce el tratamiento de la extinción interestelar dependiente de la longitud de onda y se presentan las expresiones matemáticas de filtro integrado que se emplean en el desarrollo teórico.

1.1. Stars and ISM in the disc of the Milky Way

The main components of the structure of our spiral Galaxy, the Milky Way, are the disc, the Galactic bulge, the Galactic halo, the spiral arms, the Central Bar and the Dark Matter Halo. The Galaxy contains regions with higher densities of dust and gas, which are typically associated with active star formation and also features molecular clouds as well as billions of stars, ranging from small and faint to massive and luminous stars, both of them mainly located in the spiral arms and the Galactic thin disc.
Molecular clouds are made up of interstellar gas and dust that is slowly collapsing under its own gravity. When the density and temperature of a region of the cloud reach a critical point, nuclear fusion reactions are triggered and a new star is born, which remain embedded in the molecular cloud for a short period of time while they continue accreting material from the surrounding cloud. During this time (a few million years), those stars born with masses above $\sim$15 solar masses releases intense radiation, which ionizes the gas in the cloud and creates H II regions.

The characterisation of the main components of the Milky Way can be done attending first to the stars which are in the regions of study or, alternatively, by analysing the material between the stars within the Galaxy, i.e. the **interstellar medium (ISM)**. Thanks to data on distances, positions and velocities from space missions such as *Gaia* [Gaia Collaboration 2018], many studies have been carried out on the basic features of the stars in order to determine the properties, history and evolution of the Milky Way; however, such measurements of stellar parameters are subject to various sources of error, but the most decisive is the

one induced by the gas and dust present in the ISM which varies the path of light from stars in the line of sight between the objects and the observer. The way in which the light is absorbed or scattered depends on the characteristics of the ISM it passes through, such as the chemical composition, size and shape of the dust grains that make up the clouds among others.
On the other hand, in order to study the ISM it is necessary to take into account the Galactic objects that compose it which are: gas in ionic, atomic, and molecular form, as well as dust, cosmic rays, magnetic fields and interstellar medium components. Gas accounts a 99% of the ISM where 91% of it is hydrogen, then an 8.9% is from helium and the remaining 1% is composed of metals [Fitzpatrick 1996], therefore the ISM is dominated by hydrogen regions as well as regions with helium and traces of carbon, oxygen and nitrogen. The denser regions of the interstellar medium are ideal for star formation, which in turn contributes to the formation of molecular clouds and the replenishment of the ISM with energy and matter from supernovae, stellar winds, and planetary nebulae ejecta.
From the study of the main components of the ISM, physico-chemical properties of the ISM itself can be determined through the absorption and scattering of the light emitted by distant stars or through the neutral gas present in the ISM (H I regions).

Interstellar extinction is commonly defined as the physical quantity which describes the absorption and scattering of electromagnetic radiation as a function of the wavelength. Two different spectral ranges are used to study gas and dust in the ISM, depending on the component under study: Gas and molecular clouds are observable in the optical wavelength range, while Galactic dust absorbs and scatters radiation in the ultraviolet (UV) and optical. Measurements in these spectral ranges must be taken from space, so they are subject to certain biases, and therefore, extinction of dust grains is better studied through the emission of the radiation in the infrared bands (IR).
So interstellar extinction can be understood as a corrective parameter to observational data, since the original results will be more or less affected depending on the wavelength at which it is observed. Values derived from the absolute magnitude of the object (which cannot be obtained directly from e.g. spectroscopic methods) such as luminosity, radius or mass, must take into account how much extinction the star under study is subject to.

The German physicist Gustav Mie, showed that the interstellar extinction is inversely proportional to the size of dust grains when the wavelength, λ, is of the order of magnitude of those grains they pass through: *Mie scattering*. Then, for longer wavelengths, the extinction of light will be smaller, and in contrast, for smaller values of λ: red light is less absorbed or scattered than blue light. This effect is also known as **interstellar reddening**.
As a consequence of the dependence of the interstellar extinction with the wavelength, there is a chronic problem in extinction studies: a strong effect in the UV becomes a weak one in the optical and undetectable in the IR band. Likewise for a star with a strong effect in the IR is hard to be observed in the optical and impossible in the UV, so extinction cannot be treated from a wavelength bolometric study point of view.
Ideally, data should be collected in the infrared and near-infrared (NIR) bands, due to the fact that extinction is lower there than in the optical range (see Deno Stelter and Eikenberry 2020), and as it is mentioned before, are the bands where the study of dust have to be done. Despite this, the amount of spectroscopic data in the infrared is currently scarce, which is an obstacle for scientific studies in this field.

Hot ($T_{\rm eff} \approx$ 10000-55000 K) and high-mass stars, i.e. **OB stars**, have several characteristics that make them ideal candidates for the study of ISM properties through the interstellar extinction treatment. Firstly, this group of stars, particularly for O-type, have short lifetimes (a few million years), so they are expected to be located near its birthplace , i.e., their natal molecular cloud. Therefore, the study of OB stars is crucial to locate active star-forming regions and is a way to characterise the stellar evolution of a galaxy (see Hoogerwerf 2000, Elias, Cabrera-Caño, and Alfaro 2006, Quintana, Wright, and Jeffries 2023 and Blaauw 1964).
Moreover, OB stars are extremely luminous due to their large size and high rates of nuclear fusion in their cores, thus they emit a huge amount of energy, making them easily detectable even at great distances. Lastly, it is important to note that because of their high surface temperature, they emit light at shorter wavelengths, including ultraviolet and blue light, which are the bands of the electromagnetic spectrum most sensitive to the phenomenon of interstellar extinction.
Alluding now to the Hertzsprung-Russell diagram [Arp 1958], these stars belong to the group which cover the first part of the evolution of massive stars, fully including the main sequence (MS) as well as some early phases of the post-MS evolution.

There is a large body of studies attempting to identify the distribution of massive stars in order to accurately map the Milky Way distribution of matter and therefore, the star-forming regions.
The first description of the Galactic spiral structure of the Galaxy using OB stars was done by Morgan, Sharpless, and Osterbrock 1952; since then, tracers at different wavelengths have been used to study the configuration of the spiral arms. Due to the difficulty of obtaining accurate distances, the knowledge of the Galactic spiral structure today is unreliable and most of the current models are based on the kinematic distances of ionized H II regions, H I neutral gas and CO molecular clouds, all subjecting large errors.
From different studies carried out in recent years to identify the accumulations of OB stars in the Milky Way, it has been found that they are mainly distributed in regions associated with **Giant Molecular Clouds** (GMCs), spiral arms, HII regions, and stellar associations (see Zhang and Kainulainen 2022, Bouy and Alves 2015). Chen et al. 2019, proposed OB associations in three spiral arms: Outside of the solar circle, the **Perseus arm** ($l = 100° - 140°$), the **Orion-Cygnus** or local arm ($l = 240° - 250°$) and finally the **Carina-Sagittarius arm**, which is the best traced by OB stars as expected by the richness of the different star formation episodes present within it.
. Figure 1.1 shows the location of the population of OB stars under study in an artist impression image of the Milky Way.

In parallel, it is believed that this group of hot massive stars is also located along a ring tilted toward from the Galactic plane by about $16° - 20°$, the **Gould belt** [Taylor, Dickman, and Scoville 1987]. The origin of this region in the Milky Way is unclear nowadays, and there are several theories that try to explained it; one of them postulates that it was formed from an explosive event, while the other holds that it was the result of a shock wave produced by the collision of some cloud with the Galactic disc 50 to 60 million years ago, where the constellation Perseus is currently located. Moreover, it was long speculated that the belt was a physical structure in the Galactic disc, but data from the *Gaia* survey and the subsequent analysis done by Bouy and Alves 2015 revealed that it may be a simple projection effect produced by the Sun's vantage point between two large streams of young stars in the stellar solar neighborhood.

Figure 1.1 shows a superimposition of an artist impression image of the Milky Way next to a diagram which locates in the solar circle the stars of the full sample used in this BSc thesis (see Chapter 2). The bright region in the center corresponds to the Galactic bulge, which is a dense bulging region. The Galactic centre is located at 8178 kpc from the Sun, which is taken as the origin of the coordinate system in most star mapping studies. In addition, the four major spiral arms are also shown: First, Perseus Arm also known as the Local Arm, which is the closest major spiral arm to the Solar System and is where the stars of the current study are located. The Sagittarius-Carina, Norma and the Scutum-Centaurus arms are also presented in lighter colours, representing regions of the Universe with high densities of interstellar gas and dust. In addition, the small pink populations illustrate the ionised regions of the Milky Way.
Note that the overlay diagram with the stars taken for the study are located in the solar neighbourhood, including part of the Carina, Perseus and Sagittarius spiral arms.

Finally, it is worth mentioning the case of **runaway stars**, which are objects pushed out of their birth-place into the surrounding ISM as a consequence of dynamical interaction with other stars during the star formation process, or by the subsequent disruption of binary systems due to the supernova explosion of the initially more massive component.

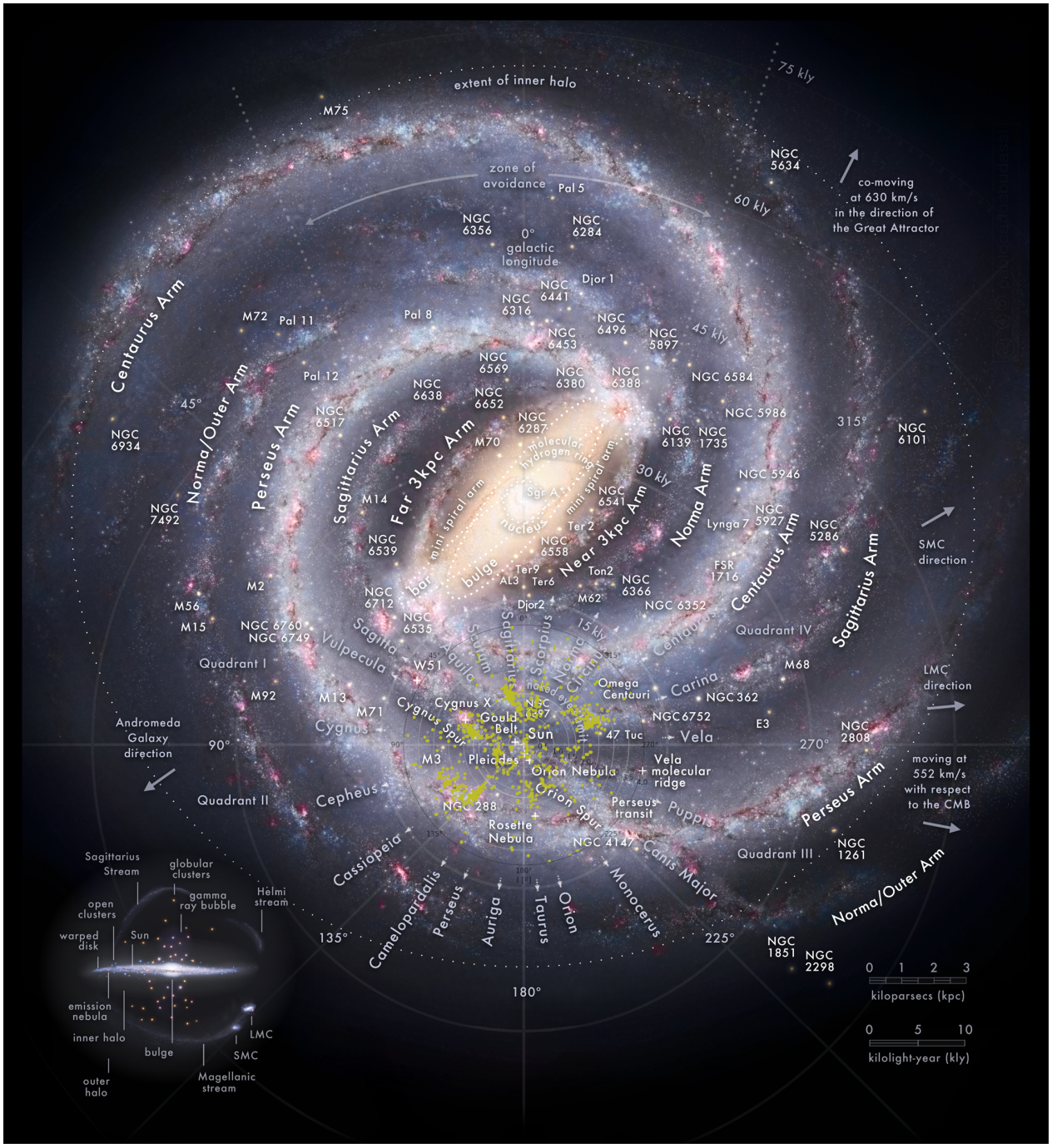

Figure 1.1: Overlaying of an artist impression image of the Milky Way with a polar diagram that locates the stars of the complete sample of the study (green dots).

1.2. Effect of the interstellar extinction

The interstellar extinction does not modify the stellar properties of the object itself, while it does have an impact on the information about the stars reaching our detectors. Therefore, the presence of gas and dust will cause the observed flux to be different from what it would be in the absence of extinction; the SED is therefore modified.
Extinction has different effects on the observed SED of the object such as, and as it would be expected, an overall dimming of the spectral energy distribution for the complete range of spectrum. Moreover, extinction could attenuate or even completely obscure specific spectral features in the SED, as well as modify their change and depth (e.g. emission and absorption lines). As extinction is wavelength-dependent, for shorter wavelengths the flux could present a steeper decrease which would alter the flux of the object (see Figure 1.2 to notice the effects of interstellar extinction.)
To mitigate the biases induced by the interstellar extinction in the spectral energy distribution, different techniques can be applied, such as measuring the colour excess, using reddening laws, or applying general extinction corrections based on specific wavelengths or filters. These corrections allow to obtain accurate values of the intrinsic properties of the star (e.g. its luminosity, temperature and distance).

Figure 1.2 is an example of the variation of the SED of a B Supergiant star when changing the extinction parameters arbitrarily. Blue line, shows the flux distribution versus wavelength without applying extinction corrections, thus it corresponds to the synthetic SED obtained from the stellar atmosphere code FASTWIND (see Chapter 2). The rest of the SEDs which are plotted are taken as an example of the effect of the type and dust present in the ISM the light of the object of study goes through (R_V) and the amount of interstellar extinction it is then subject to (A_V).
The sensitivity of the filters used is also printed at the bottom of the figure: optical (BV) and infrared (JHK). Moreover, the photometry values obtained for the star are also shown in the upper quadrant, specifically, above the SED line obtained from the code developed for the determination of the extinction parameters (see Section 2.2). It should be noted that the photometry in the U filter is obtained for verification purposes but is not incorporated in the interstellar extinction code.

Moreover, interstellar extinction presents different effects in the observational data obtained from astronomical objects. Again, the obscuration and absorption effect by the ISM the light of the star passes through, and finally, as the ISM is a dynamic medium, data is subject to temporal variability, as the amount of interstellar dust or gas may vary from one measurement to another.
On the other hand, either the quantity or the type of extinction the light emitted by early-type stars experience along its way to our detectors in Earth or space, should be different from the typical extinction of late-type stars which is dominated by the diffuse Galactic ISM; thus the light we received from O-type stars is expected to have crossed a more local, clumpy and diverse ISM than the light from late-type stars which would travelled more distance, and so, light would have been scattered and absorbed more times.

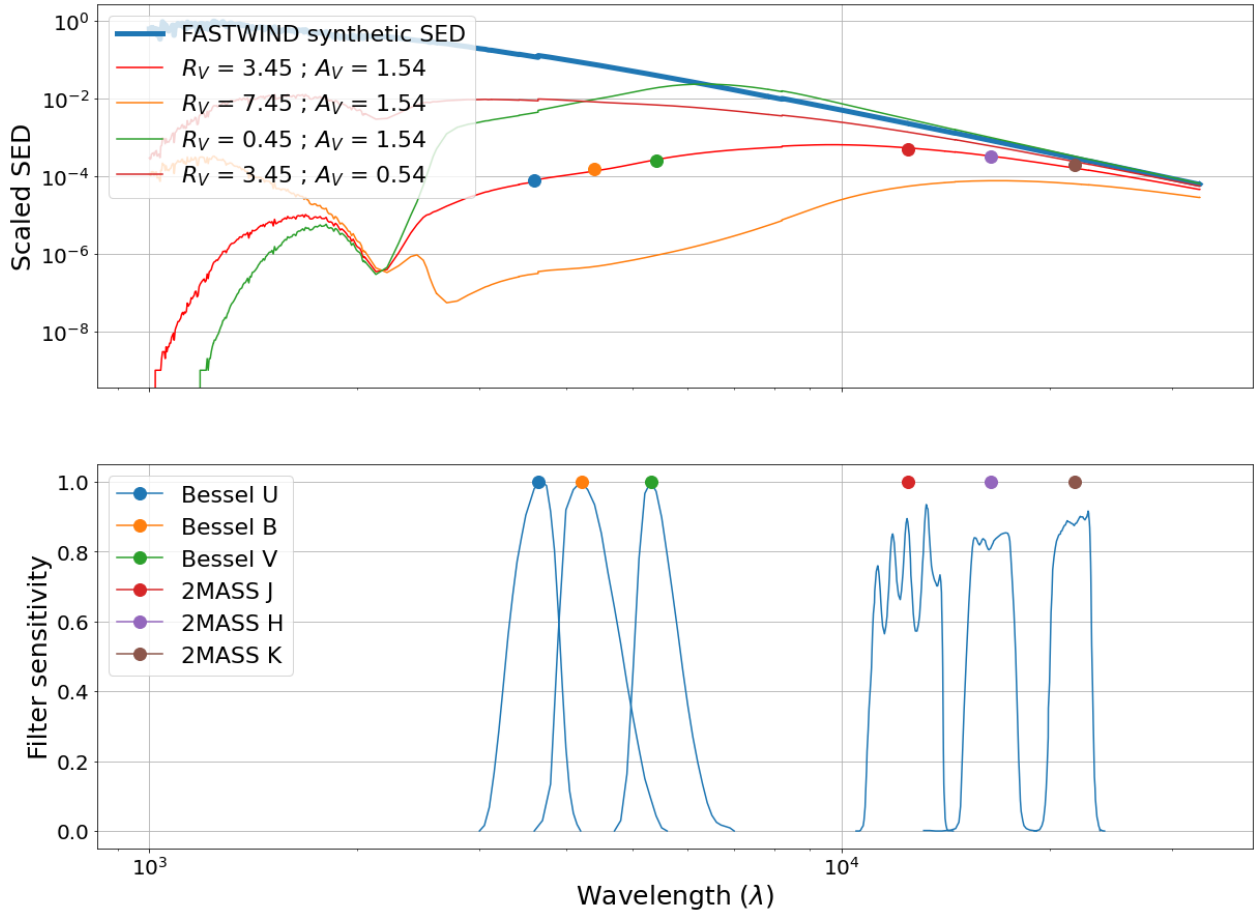

Figure 1.2: Variation of the synthetic SED (blue) obtained from FASTWIND (see Section 2.1) from arbitrary combination of extinction parameters (R_V and A_V), together with the sensitivity of the filters used for the photometric values.

Regarding to the interstellar spatial distribution of extinction, recent studies showed that there is more quantity of interstellar dust towards the inner Milky Way than in the opposite direction. One possible explanation for this is the existence of the **Local Bubble**, which is a cavity filled with hot gas in the solar neighborhood (see Maız Apellániz and R. H. Barbá 2018, Maız Apellániz, R. H. Barbá, et al. 2021, Bouy and Alves 2015).

1.3. Treatment of interstellar extinction

Astronomers of the twentieth century struggled to find a way to quantify extinction in order to either obtain information about the ISM or to eliminate its effect from the observed photometry. It was not until the seminal work Cardelli, Clayton, and Mathis 1989 (CCM hereafter), that a **family of UV-optical-NIR extinction laws** were produced. It counts with a parameter which characterizes the type of extinction and which is associated with the average dust grain size. Fitzpatrick 1999, and later on Maız Apellániz, Evans, et al. 2014 (MA14 hereafter) developed alternative families of laws based on CCM but adding some improvements and correcting previous errors (Maız Apellániz, Pantaleoni González, et al. 2020 and Maız Apellániz, R. H. Barbá, et al. 2021).

Attending to the formalism of the characterization of extinction, a definition of it has been created for different filters. For observed photometric magnitudes such as Johnson $U_J B_J V_J$ it is defined as:

$$V_J = -2.5\ log_{10}\left(\frac{\int P_{V_J}(\lambda) f_\lambda(\lambda)\lambda\, d\lambda}{\int P_{V_J}(\lambda) f_{\lambda,Vega}(\lambda)\lambda\, d\lambda}\right) + ZP_{V_J} \tag{1.1}$$

where $P_{V_J}(\lambda)$ is the total-system dimensionless sensitivity function; $f_\lambda(\lambda)$ refers to the SED of the object and $f_{\lambda,Vega}(\lambda)$ is the Vega SED, which is used as a standard. Last, ZP_{V_J} is the photometric zero-point, that defines the calibration of astronomical observations and relates the observed flux of an object to its corresponding magnitude or intensity.
If the equivalent unextinguished SED, $f_{\lambda,0}(\lambda)$ has a Johnson V_J magnitude of $V_{J,0}$, then the extinction in that filter can be written as:

$$A_{V_J} \equiv V_J - V_{J,0} = -2.5\ log_{10}\left(\frac{\int P_{V_J}(\lambda) f_\lambda(\lambda)\lambda d\lambda}{\int P_{V_J}(\lambda) f_{\lambda,0}(\lambda)\lambda d\lambda}\right) \tag{1.2}$$

Taking into account the difference between the extinction for two different magnitudes, the filter-integrated color excess, or reddening, can be obtained as:

E(B-V)$\equiv A_{B_J} - A_{V_J} = (B_J - B_{J,0}) - (V_J - V_{J,0})$(1.3)

The ratio between total extinction in the Johnson's V filter and the color excess is a value of crucial importance in terms of interstellar extinction, because it represents the properties of interstellar dust:

$$R_V \equiv \frac{A_{V_J}}{}$$

E(B-V)(1.4)

Therefore, the excess of color $E(B-V)$ and R_V are quantities that depend in a complex way on the amount and type of dust, as well as on the type of the star of study.

Extinction by dust alters $f_{\lambda,0}(\lambda)$ to yield $f_\lambda(\lambda)$ and is usually expressed in magnitude form where $A(\lambda)$ is the **total monochromatic extinction**:

$$A(\lambda) = -2.5\ log_{10}\left(\frac{f_\lambda(\lambda)}{f_{\lambda,0}(\lambda)}\right) \tag{1.5}$$

The last expression for $A(\lambda)$ is a function of the dust properties and of the amount of extinction. It is usually normalized by the latter and so it is renamed as $a(\lambda)$, now referring to as the extinction law and being a complete function of the dust properties.

It is important to note that working with monochromatic quantities is not equivalent to work with their filter-integrated quantities; however for low-extinction OB stars both quantities can be considered as an approximation (see Section 2.2); but in general terms, confusing the two types of quantities can easily lead to biases in photometric measurements of extinction.

MA14 provides the best fitting to the optical-NIR extinction to date, even though it was constructed with

O stars on **30 Doradus** instead of Galactic data. The aim to use young, massive stars from this massive star-forming region in the **Large Magellanic Cloud** (LMC) seems to be equally valid because those stars are also formed from the gas and dust within the nebula as the OB stars of the Milky Way do.
Moreover, $R_{5495} = 3.1$ has been determined by MA14 for the closest value of the average Galactic extinction (although it is not necessarily the case for every sightline, as it is discussed in Chapter 3).

Green et al. 2015 analysed the differences between the extinction experienced by O-type stars and cooler stars and the results revealed that for most low-extinction O stars there appears to be nothing special about the surrounding ISM, making their reddenings similar to those of the late-type stars in their neighbourhood. In contrast, high-extinction O stars have an additional reddening component that is not found in the line of sight to the surrounding late-type stars, which is likely related to the dense clumps of gas remaining in the molecular cloud where the star was born.

1.4. Objectives

Throughout this study, a characterization of the extinction and the type/amount of Galactic dust present in the solar neighbourhood is done using a sample of O-type and B Supergiant stars (762 targets) surveyed spectroscopically in the framework of the *IACOB project* [Simón-Dıaz et al. 2011] (see Chapter 2).
Once the extinction parameters are obtained (A_V, $E(B-V)$ and R_V), a 2D extinction map of the region of the Galactic plane where these OB stars are located is done. Presentation and discussion of results are shown in the Chapter 3, as well as a comparison with a research done by Maız Apellániz and R. H. Barbá 2018 for a sample of Galactic O stars in the optical-NIR range (see Section 3.2.2).

Chapter 2
SAMPLE and METHODOLOGY

En esta sección se presenta la muestra de estrellas que se utiliza en la tesis: 262 estrellas O y 500 Supergigantes B que han sido observadas espectroscópicamente como parte del proyecto IACOB liderado por Sergio Simón-Díaz en el Instituto de Astrofísica de Canarias.

Se introduce además la metodología seguida para la obtención de parámetros de extinción (A_V, $E(B-V)$ and R_V) para cada una de ellas; concretamente se habla de la preparación de los datos a partir de un análisis espectroscópico cuantitativo para determinar los parámetros espectroscópicos de cada objeto: $T_{\rm eff}$, $\log g$. A continuación se introducen la SEDs sintéticas (extraídas de la base datos de IACOB) en un código que modela el espectro óptico observado de cada objeto, **FASTWIND** y da como resultado una distribución espectral sintética. Dicha SED junto a la información fotométrica de cada objeto es introducida en un programa de IDL que calcula los valores de extinción interestelar basándose en técninas de **Monte Carlo de Cadenas de Markov**.

The sample of stars selected for this BSc thesis is compound of 262 O-type stars and 500 B Supergigants surveyed in the framework of the IACOB project [Simón-Dıaz et al. 2011]. Data is taken from the IACOB spectroscopic database which includes OB Galactic stars observed from multi-epocal photometric and spectropolarimetric, high-resolution spectroscopic observations from both the Northern and Southern Hemispheres.

Figure 2.1 plot the OB sample of stars used in this study in 2D diagrams; firstly in terms of equatorial coordinates as a way to contextualize the stars in the Northern and Southern Hemisphere. Next, using galactic coordinates in order to show that these stars are distributed throughout the Galactic plane (and hence the Galactic disc); in particular, they populate the **thin disc**. Such a distribution corresponds to what is expected since the thin Galactic disc hosts the spiral arms of the Galaxy and is also the main region of star formation as it is composed of young stars and dense accumulations of dust and gas. There is also a histogram for the values of the galactic longitude which takes into account the location of the spiral arms proposed by Chen et al. 2019, which shows that the population of OB stars is higher at those star-forming regions.
Finally a polar diagram for the stars is presented, as well as a limit on distance (4 kpc) for accuracy issues

in the distance data obtained from astronomical catalogues (see Section 2.1).

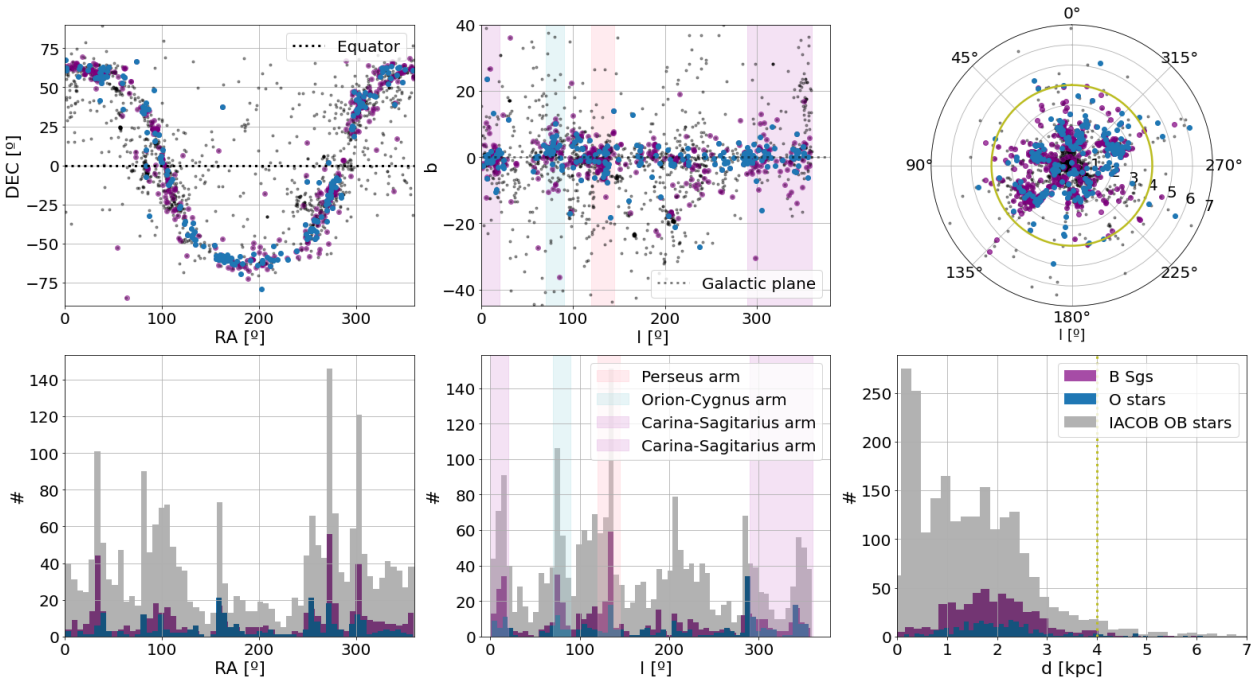

Figure 2.1: Distribution of the total number of stars in the IACOB sample (grey) and the O-type stars (blue) and finally, B Supergiant (purple) stars used in this BSc thesis. Spiral arms of the Milky Way where the study stars are immmerse are represented as coloured bands. Distance limitation in 4 kpc is also shown (green circumference in the polar diagram and vertical line in its corresponding histogram).

2.1. Preparation of required data

In order to obtain the 2D extinction map aimed in this BSc thesis, different physics parameters of each target of study have to be known. Therefore, thanks to previous studies carried out by the IACOB project, concretely by Abel de Burgos (presently PhD student) and Gonzalo Holgado (postdoc at IAC) (AdB and GH hereafter), thanks to the stellar atmosphere code: FASTWIND (see below) and finally from the distance and photometry data for each star taken from astronomical catalogues, the starting point for the determination of the extinction parameters is configured.

- **Distances and coordinates**
  In order to obtain the distance of the star from the Sun several methodologies can be followed. The best known technique is the direct method of parallax, which is simply the measurement of the angle formed by the lines of observation drawn to an object from two points sufficiently far apart. The distance will therefore be the inverse of the parallax: $d(pc) = 1/parallax$ (arcsec). The disadvantage of using this methodology is that because the stars are so far apart, the angle they subtends is small, therefore their quotient can induce remarkable biases, so a limit is set in our study at 4 kpc to maintain a commitment to data reliability. In this BSc thesis, two sources of information are used to obtain the distance of the objects: First and mainly the **Bailer-Jones catalogue**, and secondly data from the Gaia database of the European Space Agency.

Bailer-Jones et al. 2021 calculates the distance in two different ways: applying probabilistic and geometric models (geometric distance) or from photometric values (photogeometric distance) as does Gaia. Because the photometry of OB stars is subject to aberrant factors such as interstellar extinction, field contamination or the intrinsic variability of these stars, as long as the catalogue value of geometric distance is found, this will be taken, if not, the Gaia mission database will be used.
Data of the galactic and equatorial coordinates is taken from the **Simbad** astronomical database [Egret, Wenger, and Dubois 1991].

- **Photometry**
  Knowledge of the broadband photometry in the optical (B and V filters) and in the near-infrared bands (J, H and K filters) is required (see filters sensitivity in Figure 1.2). This information is also obtained from the Simbad database. Those stars in the sample that did not have such complete information were removed from the study, reducing the size of the original sample from 283 to 262 (in the case of the O-type stars) and from 536 to 500 (in the case of the B-Sgs).
  As photometric data for each star is needed for the determination of the extinction parameters, the near-infrared photometry catalogue ***2MASS*** [Skrutskie et al. 2006] (obtained from the VizieR astronomical database) was used to check the quality of the values in this spectral range. It provides a distinction on the basis of how reliable the values given are, therefore those stars whose infrared photometry had three negative indicators were excluded from the original sample.

- **SEDs**
  From spectra taken from the IACOB database, AdB and GH have obtained spectroscopic parameters for the O and B Sgs stars of the sample used in this study respectively by using **quantitative spectroscopic analysis**, QSA (see Section 5.1): effective temperature (T_{eff}) and surface gravity ($\log g$).
  Once these important stellar properties are know, they can be implemented in stellar atmosphere models, such as the one used in this study: **FASTWIND** [Holgado, Simón-Dıaz, and R. Barbá 2017], in order to model the spectrum of the star, i.e. the **synthetic SED**.
  The FASTWIND stellar atmosphere code is a theoretical tool developed in FORTRAN used to describe the structure and composition of the atmosphere of a star, relying on the laws of physics and chemistry to predict a star's radiation and spectrum while taking into account temperature, pressure, density and chemical composition.

Once the synthetic SED and the photometry of each star are known, these parameters are set as fixed and the program for a specific reddening law (MA14) can be run.
A flow chart is presented below as a way of illustrating the main steps followed to obtain the interstellar extinction coefficients for the sample of OB-type stars.

Spectra (IACOB) $\xrightarrow{\text{QSA (GH, AdB)}}$ **Spectroscopic parameters** $\xrightarrow{\text{FASTWIND model}}$ **Synthetic SED** $\xrightarrow{\text{comparison with BV+HJK phot.}}$ **Extinction parameters**

2.2. Treatment and modelling

The family of extinction laws selected for the current work are the ones elaborated by Maız Apellániz, Evans, et al. 2014 which are parameterized in terms of the central wavelengths of the B_J and V_J filters which are 4405Å and 5495Å respectively. Therefore, the monochromatic (or single-wavelength) equivalents to Equations 1.2 and 1.3 are:

$$E(4405-5495) \equiv A_{4405} - A_{5495} = [f_\lambda(4405) - f_{\lambda,0}(4405)] - [f_\lambda(5495) - f_{\lambda,0}(5495)] \tag{2.1}$$

which is now a direct and linear measurement of the amount of extinction. Equation 2.1 illustrates the dependence of dust properties with the type of extinction, or equivalently, the extinction law applied. On the contrary, $E(B-V)$ has a non-linear dependence on the amount of extinction.

$$R_{5495} \equiv \frac{A(5495)}{E(4405-5495)} \tag{2.2}$$

Moreover, these values of wavelength approximately satisfies the limits for OB stars and SEDs for an effective temperature of $30000K$. Therefore, as long as this temperature condition is met or, as discussed in Section 2.2, if the star is low-extinguished, the monochromatic and filter integrated quantities can be approximated:

$$\lim_{A(\lambda)\to 0}$$

E(B-V)$\approx E(4405-5495)$

$$\lim_{A(\lambda)\to 0} R_V \approx R_{5495}$$

The IDL program developed by Urbaneja et al. 2017 which is used for the determination of the extinction parameters for a given star, works with the observed photometry values for colors and magnitudes, which will then be compared with those obtained from the synthetic SED generated from the atmosphere model, FASTWIND. The difference between both spectral energy distribution relies on the presence of the interstellar extinction. The program is run repeatably in a **Monte Carlo Markov Chain (MCMC)** procedure for each star in order to characterize the extinction parameters. Such method is a computational technique used for sampling complex probability distributions; it combines elements of the Monte Carlo method, which involves random sampling, and the Markov chain, that entails a sequence of states with transition probabilities.

Figure 2.2 illustrates the operation of the method for the common example, random walk. Without going into details, it refers to the process of iteratively updating the current position in the sampling space based on a random step. The methodology can be summarised as: the particle starts at an initial position in the sampling space, then another candidate position is proposed by taking a random step from the current position with a size and direction determined by a proposal distribution. The acceptance probability of such position is done basing on the target distribution; if the step is accepted, move to the candidate position and make it the new current position for the next iteration, while if rejected, stay at the current position.

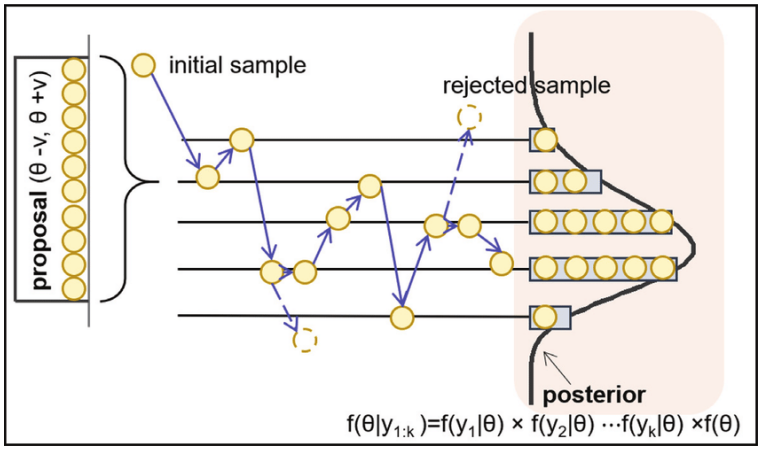

Figure 2.2: Markov chain Monte Carlo sampling using random walk. Figure is extracted from Dong, An, and Kim 2019.

Analogously, the operation of the program used for the determination of extinction parameters (A_V, $E(B-V)$ and R_V) can be summarized as: In a first iteration, it draw the pair of monochromatic $E(4405-5495)$ and R_{5495} values, attending to the family laws of MA14 incorporated in it. Secondly, the synthetic spectral energy distribution predicted by FASTWIND calculated with the results obtained in the spectroscopic analysis is reddened using that family of laws. A value of the **cost function (χ^2)** is obtained. Next, new combinations of the parameters are proposed around the two-dimensional parameter space where χ^2 is smaller (see below), i.e. where the parameters to be determined are most likely to be found. It is important to note that in every iteration the Monte Carlo Markov Chain still proposing values in regions of less probability.
The same procedure is iterated in a similar way n times until these areas of probable values are clearly identified.
Next, the model colors are extracted for that SED: B-V, V-J, V-H and V-Ks and finally the differences between model and observed colors are calculated. The result is a Gaussian-type distribution of values, where the maximum corresponds to the parameter value and the width is the accuracy error of the methodology. The more steps that are included, the more closely the distribution of the sample matches the actual desired distribution. The program used in this BSc thesis does $n = 100$ for each star.

Therefore, the quality fitting of the algorithm is study with the cost function, which theoretical definition is:

$$\chi^2 = \frac{1}{N}\sum_{i=1}^{5}\frac{(M_i - O_i)^2}{\sigma_i^2} \tag{2.3}$$

where i refers to the sequential repetition number for each color-filtered (B,V,J,H,K) and N divides by the total number of them to normalise the measurement, so for this study is equal to 5. M refers to the value of the photometry obtained by the model, and O to the observed one. Finally, the denominator takes into account the intrinsic errors of the measurements, σ^2. For the colour differences of the optical range: $B-V$ and $U-B$ a constant 0.05 mag uncertainty are assumed, while is 0.02 for infrared bands.
As the function takes into account the N number of filters considered in the extinction law, a value of $\chi^2 \approx 1$ means that the fitting quality of the program is optimal.

The MCMC minimizes the two degrees of freedom cost function since five colors are being used to solve simultaneously for three variables. The program sets fixed limits for the calculation of the extinction parameters; in the case of $E(B-V)$, it allows values between $0-2$, for R_V: $0.1-10$, and finally the range of possible values of A_V is between $0.1-7$. The resulting values of $E(4405-5495)$ and R_{5495} are converted to the corresponding filter-integrated quantities using the final model atmosphere SEDs; these values of $E(B-V)$ and R_V are later used to calculate the extinction A_V.

Chapter 3
RESULTS and DISCUSSION

En primer lugar se evalúa la calidad de los resultados obtenidos a partir de la metodología seguida; concretamente se cuantifican los errores de precisión y las incertidumbres características del modelo.
Además se discuten los resultados relativos a los parámetros de extinción. Concretamente, se desarrolla un estudio comparativo de los valores de la cantidad de polvo galáctico obtenido para la submuestra de estrellas O consideradas en esta tesis y las de un estudio bibliográfico. Asimismo se analizan las estrellas que tienen valores de R_V alejados del valor medio de la muestra a la que corresponden, es decir, se caracterizan los ***outlayers***.

De manera paralela se presentan mapas 2D de la extinción interestelar a la que están sujetas las estrellas de la muestra. A partir de la localización en la vecindad solar de estos objetos, se identifican y discuten las regiones de formación estelar dentro de la Vía Láctea. Se ahonda también en la, en términos generales, relación lineal entre distancia y extinción interestelar.

3.1. Evaluation of the quality of the results

The evaluation of the quality of the results obtained when following the methodology described in previous chapter is done by the analysis of the resulting values of χ^2 and the dispersion values which characterize the spread of the Monte Carlo Markov Chain samples (represented by the standard deviation) and the measurement of the discrepancy between predicted values and the true values by the cost function.
Thus, the **cost function** χ^2, which describes how well the MCMC is fitting the proposed pair of extinction parameters for the n number of steps is shown in a histogram for the both groups of spectral type stars of the study (see Figure 3.1). As it is mentioned in the Methodology Section (see 2.2) a value of $\chi^2 \approx 1$ indicates that the MCMC is fitting the best way possible; however, MA14 states that their family of extinction laws provides good results for all stars with $0 < \chi^2 < 4.0$, thus as far as the result is between this uncertainty range, it will be considerate reliable. Concretely, for our OB sample, the volume of stars with such optimal range of the cost function suppose a 84.38% from the total, as it can be expected from the Figure 3.1 which show a concentration of targets with values of χ^2 between 0 and 5.
Values outside this range are neglected for the rest of this work, since probably are indicator of the existence

of problems with one or several points in the considered photometry.

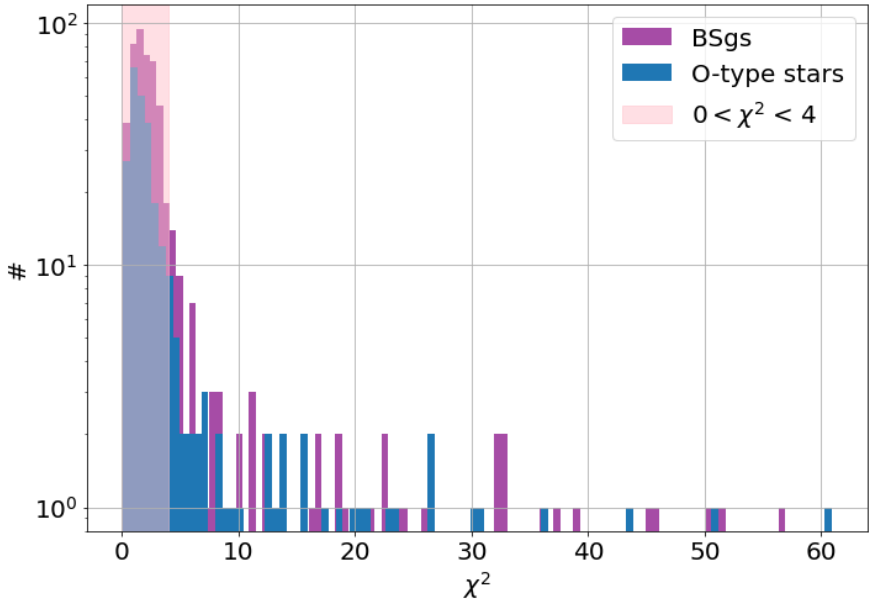

Figure 3.1: Values of the cost function, χ^2, resulted from the extinction parameter determination programme used for the O-B-Sgs sample (Blue and purple respectively). Optimal range of values. Range of optimal values represented as a pink band.

The width of the resulting distribution of the Monte Carlo Markov Chain corresponds with the standard deviation of the parameters determined by the IDL program and quantify the spread or variability of the values obtained from the MCMC method. Figure 3.2 plot the uncertainties values for each extinction parameter (σ_{A_V}, σ_{R_V} and $\sigma_{E(B-V)}$) versus the amount of extinction the object is subject to.

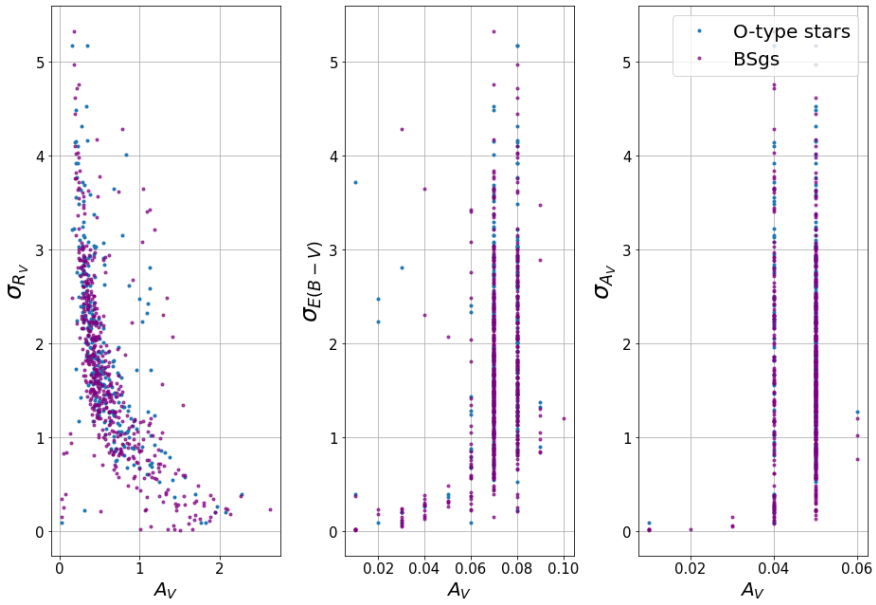

Figure 3.2: Dispersion of the extinction parameters resulting from the MCMC methodology applied.

Inspection of left panel of Figure 3.2 it easily follows that for stars subject to low extinction values, the characterisation of the quantity R_V, i.e., the type of interstellar dust in the region in which they are found will be increasingly difficult and will have indeterminate values each time. This is not surprising since low values of A_V imply low interstellar dust densities, so the quantity R_V remains unconstrained.
The middle panel of the same figure illustrates that the uncertainty of the excess of color ($\sigma_{E(B-V)}$) and the amount of extinction are of inherently tied to a linear dependence; therefore the higher the excess colour can suppose (or not) large values of A_V. The uncertainty of the results will depend on the photometric systems that are considered for the computation of the excess colour, since, as discussed in Section 1.2, blue light is more susceptible to the extinction phenomenon than red light. On the other hand, such uncertainties can be explained as a consequence of errors in the photometry used. Analogously for the uncertainties in the measurement of extinction can arise from various sources and depend on the specific observational setup and analysis techniques employed.

Table 3.1 shows the typical uncertainties achieved for both subsamples of stars. As the values of dispersion uncertainties are smaller than the precision ones, it implies that the methodology used contemplates a considerable range of error; these uncertainties can be introduced by the already mentioned biases in photometry data or by the random nature of the Monte Carlo numerical approximation method.

Table 3.1: Analysis of the uncertainties of the Monte Carlo Markov Chain methodology for the O-BSgs sample. σ represent the dispersion uncertainties and χ^2 is the cost function, which alludes to the precision of the MCMC treatment.

Sample	σ_{R_V}	σ_{A_V}	$\sigma_{E(B-V)}$	$\overline{\sigma}$	χ^2
O	1.00	0.964	0.281	0.749	7.46
B	0.896	0.963	0.295	0.718	6.96

3.2. Extinction parameters

The extinction parameter determination programme return the central values with uncertainties for each parameter under study (A_V, R_V and $E(B-V)$) and the value of the cost function (χ^2). These results are presented in Figures 3.3 and 3.4, where the averaged values of the type of Galactic dust are also shown for the O-type and B Supergiants stars, as well as their uncertainty which corresponds with the width of the distribution obtained from the Monte Carlo Markov Chain method.

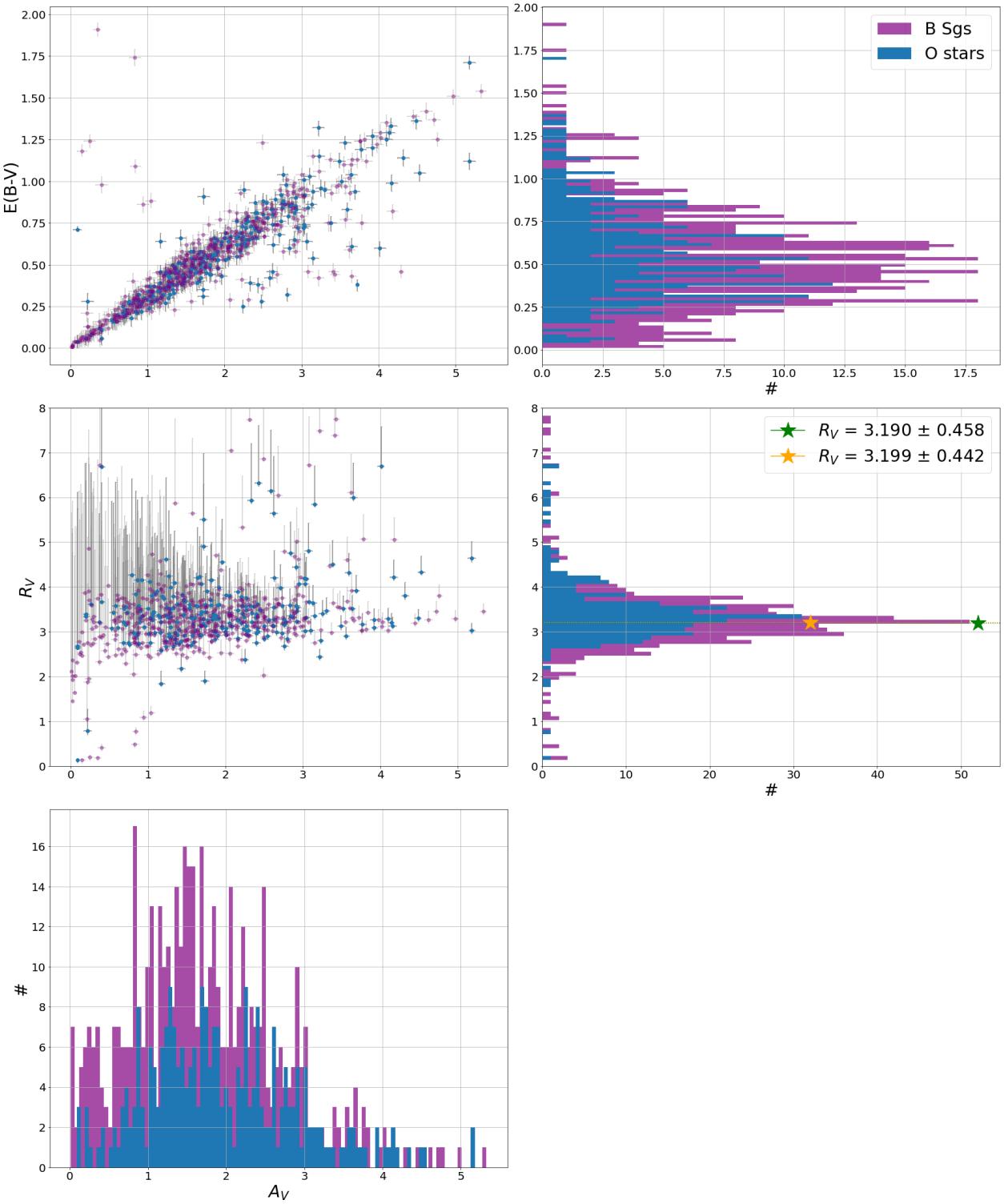

Figure 3.3: Extinction parameters (A_V, R_V and $E(B-V)$) obtained for the O-BSgs sample considering the distribution of values through histograms. Averaged values of R_V are represented with a yellow and green star symbols for the O and B-Sgs sample, respectively.

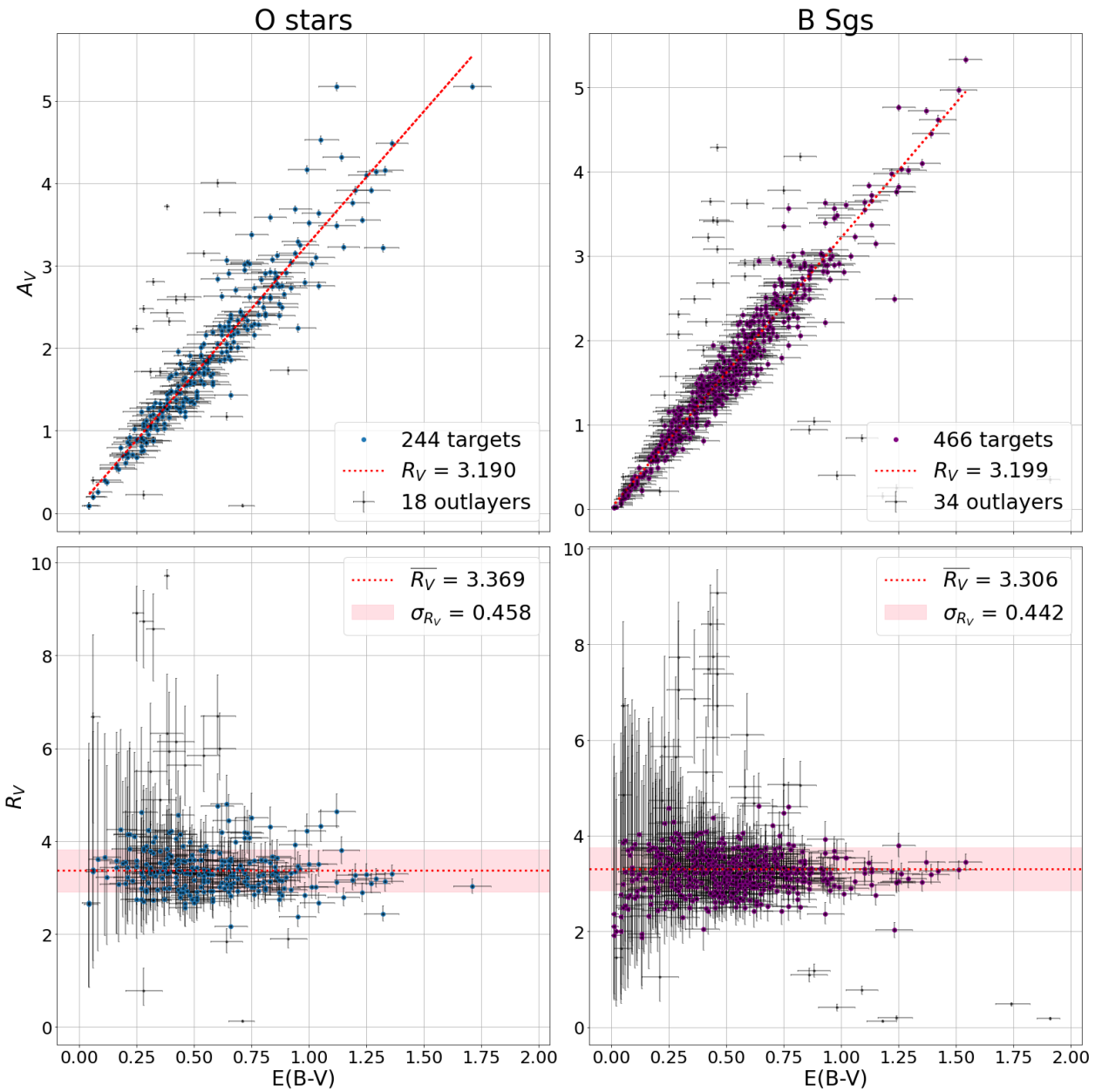

Figure 3.4: Extinction parameters with corresponding error bars (A_V, R_V and $E(B-V)$) obtained for the O-BSgs sample. The values of the slope of the fitted line of A_V and $E(B-V)$ are shown in the figures on the first line, while the figures below show the mean value of the distribution (red dotted line) and the corresponding standard deviation (pink band).

Figures 3.3 and 3.4 clearly shows the linear dependence of the amount of interstellar extinction on the colour excess (see top left diagram of Figure 3.3) as expected from the equation 1.3. Thus, more extinction implies more light absorbed by the interstellar medium between the line of sight of the star and our detectors, A_V, so the more the interstellar medium extinguishes the greater the difference between the light emitted by the object and the light observed, i.e. the colour excess $E(B-V)$.
Middle panels show the semi-gaussian distribution of the Galactic dust type values (R_V), whose values at the peak are likely to the the typical mean value proposed by several studies $R_V \approx 3.1$. Since it is a dust-type dependent parameter, it will be higher in regions of active star formation or molecular clouds; objects with values much higher or lower than the mean value will illustrate that are located in Galactic regions with variations in the different dust properties and extinction behaviour. Characterising the R_V parameter is therefore crucial for the study of the ISM.

In this BSc thesis two different methodologies are developed (see Figure 3.4): First, taking into account the linear dependence of A_V with $E(B-V)$, a linear fitting is performed, where the slope of the straight line will therefore be the value of R_V.
Since there are values that deviate significantly from the means, it is important to apply a rejection criterion so that the statistical measures are not contaminated by them. The **sigma clipping method** is applied to the full sample of O and B stars respectively (three iterations are done considering each time, values three times the sample standard deviation); resulting 18 and 34 **outlayers** are obtained for the O and B star samples respectively.
Alternatively, the mean values and the standard deviation of the terms of the type of dust returned by the extinction determination program are calculated (also excluding outlayers).
The values of R_V determined following the two previous methodologies are listed in Table 3.2 where the final value for the type of Galactic dust in the disc of the Milky Way is considered as the value obtained from the linear fitting plus/minus the data standard deviation: $R_V \pm \sigma_{R_V}$. While $|R_V - \overline{R_V}| > 3\sigma_{R_V}$, the star is excluded from the study and considered as an outlayer.

Table 3.2: Values of the type of dust parameter, obtained by the slope of the linear fitting ($R_V\,slope$) and by the average of the distribution ($\overline{R_V}$) with its width (σ_{R_V}). Range of possible values for each subsample ($R_V \pm \sigma_{R_V}$). Final values used for the BSc thesis development (R_V).

Sample	$R_V\,slope$	$\overline{R_V}$	σ_{R_V}	$R_V \pm \sigma_{R_V}$	R_V
O	3.189	3.369	0.458	2.732 - 3.647	3.189 ± 0.458
B	3.199	3.221	0.442	2.757 - 3.641	3.199 ± 0.442

Most of the values of R_V proposed in the literature, refer to single clusters or associations, not to big samples of Galactic stars, as the case of this BSc thesis and the work of MA14. These studies agree that interstellar dust in the solar neighbourhood is affected by the level of ambient UV radiation; for regions with higher UV incidence, the value of R_V will increase due to the presence of H II regions or cavities filled with hot gas (as the before mentioned, Local Bubble). The regions with the lowest UV incidence have the highest density of interstellar dust in the ISM; they correspond to molecular clouds with small dust grains (hence small R_V). Finally, the regions with intermediate values of R_V do not provide special physical information as they correspond to the typical warm to cold ISM which fills the majority of the volume in the Galactic

disc.
In any case, different values of R_V imply that interstellar dust in different regions of the Universe has different properties and compositions such as: size, shape and structure, amount of dust and the presence of other chemical species mixed in. In star-forming regions, the dust density is higher, so R_V is also higher. From the recent studies it is observed that in the case of young OB stars populating open globular clusters or regions with lower dust density, they have $R_V \approx 3.19$, which is within the range of typical values proposed for the Milky Way. In contrast, stars located in active star-forming regions and dense molecular clouds are characterised by higher values of R_V (up to ≈ 9).

The consistency of the results for the O-star and B Sgs samples shown in Figure 3.4 leads to the conclusion that in general terms, it is not necessary to differentiate between the two spectral classes in terms of interstellar extinction treatment, as they share similar characteristics as temperature and mass and thus, stellar evolution. Therefore, the variation of the interstellar dust type values does not depend on the spectral type of the study star but on its location in the Milky Way.

3.2.1. ISM properties

Through the study of the extinction parameters (A_V, R_V and $E(B-V)$) the characterization of the interstellar medium can be done. As the stars of the sample taken for this BSc thesis are OB types located in the disc of the Milky Way, the solar neighbourhood can be study.

A brief study of stars with dust type values deviating from the mean will be carried out; in addition, the criterion of $A_V > 1$ is imposed. The volume of the new sub-sample is: 5 stars for the total O sample, which means a 1.9% from the total, and for the B Sgs just 9 stars are considered as outlayers (1.8%). These objects are shown in the histogram of the R_V values for the full OB sample and for each sub-sample (O and B Sgs stars) in Figure 3.5.
High values of R_V means that the interstellar dust absorption and dispersion for those stars has a significant impact on the radiation that reaches the detectors, thus, those objects seem to be located in clumpy regions of the Milky Way. Despite of these promising results, the cost function of these stars are between $12-60$, then these objects are probably presenting problems with their photometry information and have to be neglected in future studies.

In any case, a Galactic diagram is shown below (see Figure 3.6) in order to identify those regions in the solar neighbourhood to at least check whether the conflicting stars belong to active formation regions. Such polar diagram plots the outlayers following a size and color code: the bigger the point in the diagram, the higher the extinction increases; the greener the dot, the higher the value of R_V.
The population of the outlayers corresponds to the Sagittarius arm and to the Orion Nebula, so, the subsample is located in stellar forming region with a high density of Galactic dust and so are members of bigger OB stellar populations.

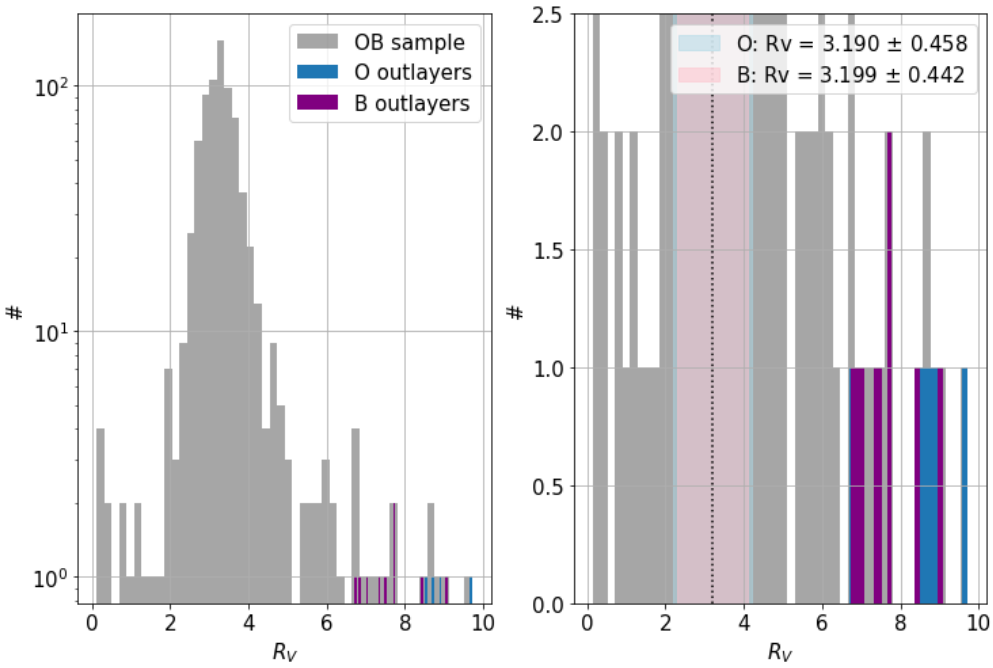

Figure 3.5: Left figure shows a histogram of the R_V values for the total sample (gray), and then for the O-BSgs outlayers (blue and purple respectively). The figure on the right shows the same histogram but limiting the y-axis (number of stars) so that the distribution of outlayers values can be better observed; also includes R_V values (black dotted line) and their corresponding uncertainty (blue or pink bands for O-BSgs sample respectively).

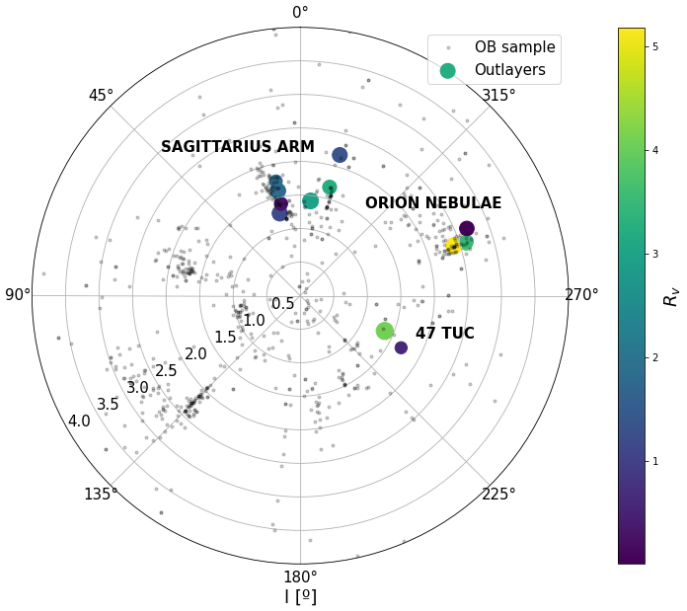

Figure 3.6: A polar diagram which show the distribution of the whole O-BSgs sample (gray) and the outlayers ($R_V \pm \sigma_{R_V}$ and $A_V > 1$). The color code depends on the extinction value of those stars, and the size depends on their R_V values.

3.2.2. Comparison of O stars with literature

Maız Apellániz and R. H. Barbá 2018 (MA18 hereafter) carried out a study of dust extinction towards Galactic O stars using a sample of 509 targets obtained from the Galactic O-star Spectroscopic Survey, GOSS. In it, the determination of extinction parameters was executed in a similar way as in the present study; both studies consider the MA14 family of extinction laws and the main difference lies in the program which calculate these values (for MA18 is called CHORIZOS [Maız-Apellániz 2004].
Both programs were developed following a χ^2 distribution for the parameterised modelling and characterisation of photometry and spectrophotometry. While the proposal of Miguel Urbaneja (Innsbruck University) is the determination of extinction parameters through Markov Chains in the Carlo method, Jesús Maíz Apellániz (Centro de Astrobiología, Madrid) incorporates a multi-purpose Bayesian code, which offers a broader suite of tools and algorithms for Bayesian analysis, including MCMC but not limited to it. In addition, CHORIZOS incorporates default tables of stellar models to select the desired SED family (e.g. Kurucz Kurucz 1993), while Miguel Urbaneja's program works with an input SED (in our case extracted from FASTWIND).

The numerical values obtained for the O-type stars (collected in Appendix 5.1) are compared with those of the MA18 sample. Figure 3.7 represents the values of R_V and A_V respectively obtained in the two surveys along a straight line of unit slope, in order to study the similarity of the results.

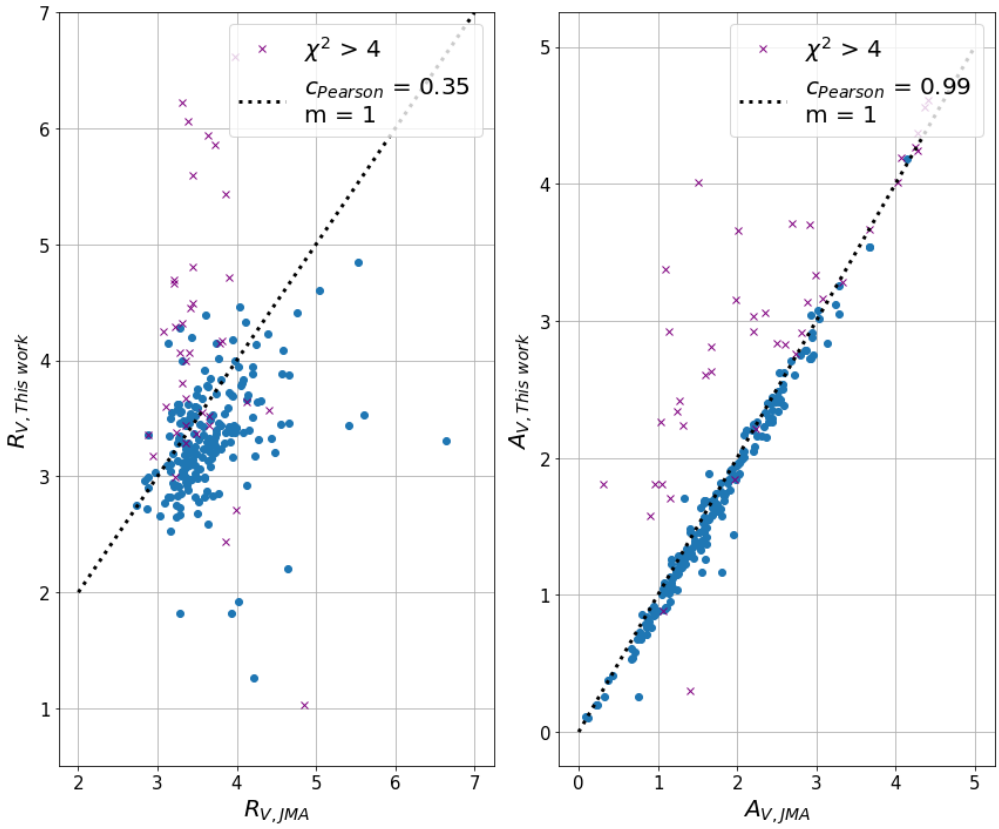

Figure 3.7: Comparison of the results of the characterization of interstellar extinction and type of dust obtained in this BSc thesis and the values taken from MA17 survey. Outlayers are represented with a purple cross. Black dotted line shows a 1:1 relation.

Objects with values of $\chi^2 > 4$ (limit defined by Jesús Maíz Apellániz himself, see Section 3.1), will be excluded from the comparative study, as they are interpreted as being subject to uncertainties related to the methodology followed or the photometric values considered. Once this rejection criterion has been applied (targets shown with purple crosses in Figure 3.7), the dust type and interstellar extinction values are plotted. For the case of R_V a distribution of values around the line of slope one with a Pearson coefficient $c_{Pearson} = 0.35$ is observed, so the data are not fully correlated. Furthermore, a range of values for R_V between 3 and 4 is obtained, as expected. Again, the typical Galactic R_V is 3.1, but since O-type stars are generally located in regions of active star formation or, in some cases, near molecular clouds left over from their births, they have higher extinctions than the average of nearby late-type populations.
The values of the amount of extinction to which the stars common to the two studies are subject follow an almost 1:1 ratio ($c_{Pearson} = 0.99$), so it can be confirmed that both studies provide accurate results for the extinction parameters. This in turn implies that either the Markov Chain Carlo method or more general Bayesian algorithms can be used to study the interstellar extinction of early-type stars in the solar neighbourhood.

3.3. A 2D map of the interstellar extinction in the thin disc of the Milky Way

The determination of extinction parameters serve as an anchor to consolidate a 2D extinction map of the stars of the region of the disc of the Milky Way up where our sample of OB stars are located (covering a distance of up to 4 kpc in various line-of-sights). Thus, the aim of this study is to relate the position of the stars in our Galaxy to the amount of interstellar extinction to which they are subjected.

Figure 3.8 is composed by two maps of the stars in the disc of the Milky Way for each sub-sample (O and B-Sgs stars). First, a 2D representation of the galactic coordinates is shown in addition with the location of the spiral arms (defined in Chapter 1.1) present in the solar neighbourhood up to 4 kpc; then a polar representation is shown. Both diagrams follow a color map code defined by the values of the amount of extinction the stars are involved, the greener the stars are plotted, the higher values of extinction they are subject to.

A better location of the stars in the spiral arms they belong to is shown in Figure 3.9, as the OB distributions are superimposed to a graphical representation of the Milky Way (it is a zoomed version of Figure 2.1 limiting now up to 15 kly $\approx$ 4.5 kpc). From this representation, it can be deduced that there is no noticeable difference in the location of the hot and massive stars under study, so the sample of O and B Supergiant stars can be treated as a set to study the interstellar medium in the solar neighbourhood (see Figure 3.9 below).

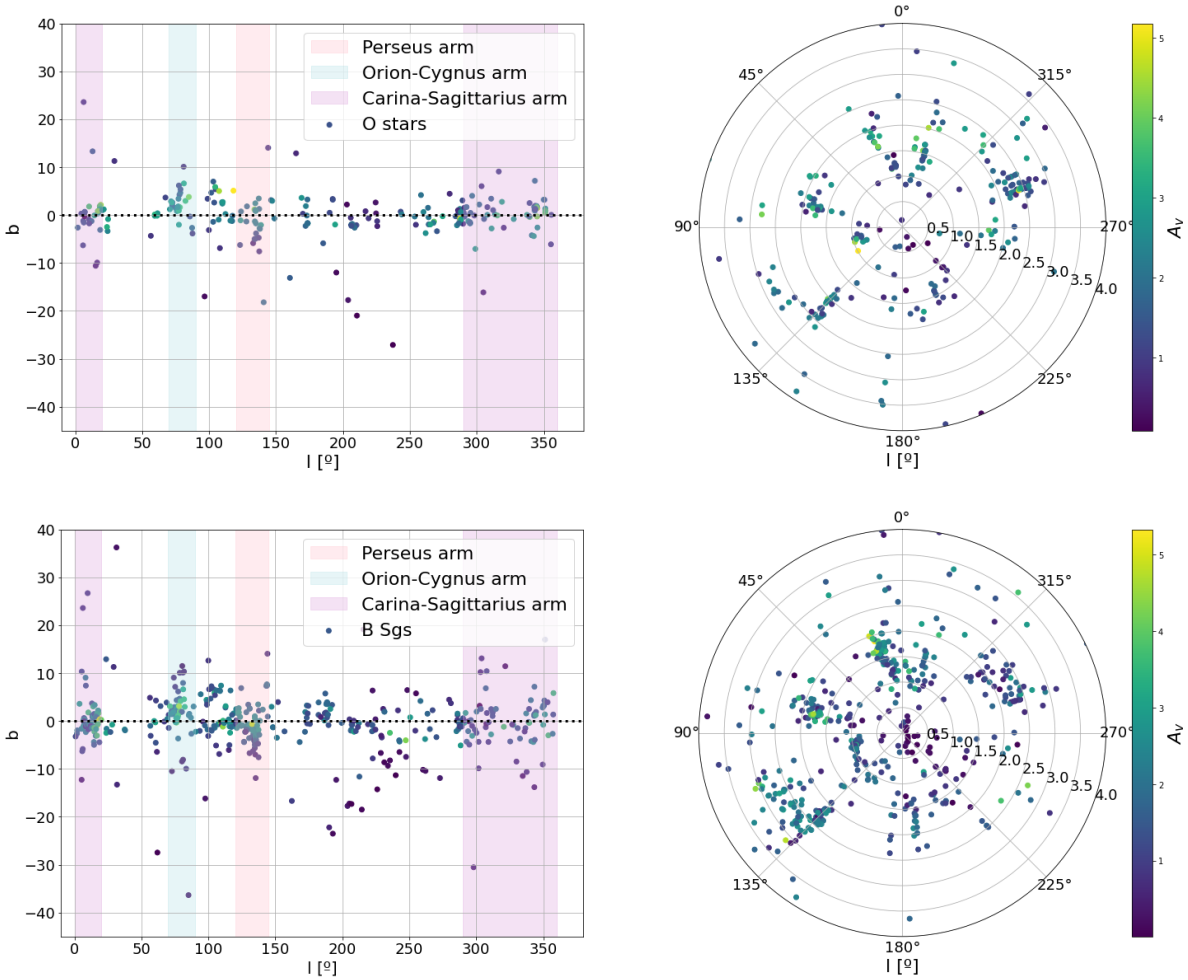

Figure 3.8: Location of the O-type stars (above) and B-Sgs (down) of the sample of stars under study taking to account the interstellar extinction they are exposed to. Left figures shows a 2D diagram in terms of galactic coordinates as well as the location of the spiral arms.

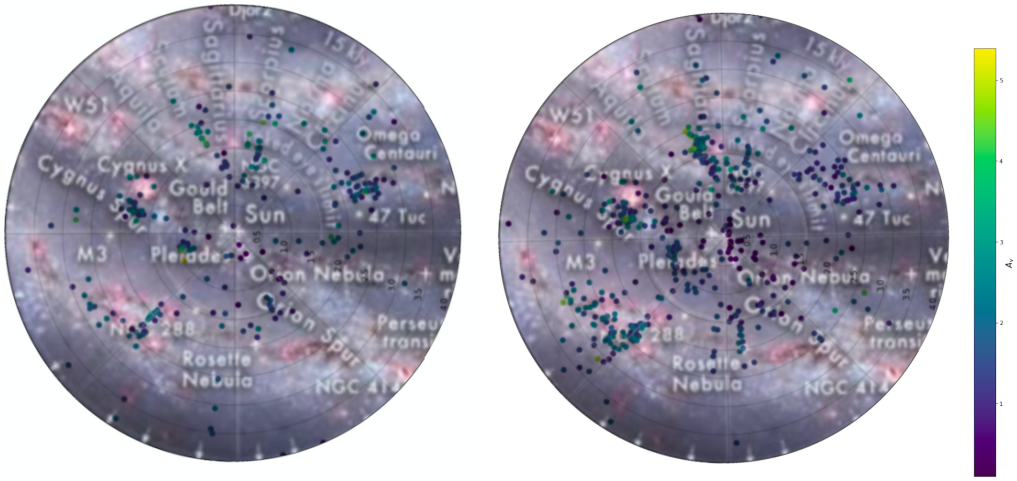

Figure 3.9: An enlarged image of Figure 1.1 for O-BSgs stars (left and right respectively).

As it is expected, OB stars are located in star-forming regions as it is shown in Figure 3.10, where R_V values bigger than 3.2 are considered. The spiral arms of the Milky Way that goes through the solar neighbourhood (Sagittarius, Carina and Perseus arms) and molecular clouds (Cygnus X).
The amount of gas and dust will be greater in those regions, and therefore the light from the stars in or behind them is more likely to be absorbed, thus interstellar extinction is higher than in the low matter density regions of the ISM.

Cygnus X is a molecular cloud in the constellation Cygnus which hosts various astronomical structures and objects such as star clusters, emission nebulae, and regions of dust and gas. This region is known for its intense star formation activity, then the presence of massive OB stars and associated star clusters is high.

The Carina spiral arm, Perseus Arm and the Sagittarius Arm are the regions of the Milky Way where the stars with higher values of A_V are observed. This is in agreement with the prediction throughout the BSc thesis that it is in these regions of active star formation that the density of interstellar dust and gas is highest. Spiral arms are compound by stars, interstellar gas, dust, and star-forming regions which for the aforementioned arms the mainly star-forming regions are:

- **Orion Molecular Cloud Complex**: Located in the constellation Orion, this complex is one of the most well-known and active star-forming regions in our Galaxy. It includes the Orion Nebula (M42) and the Horsehead Nebula (B33), among others.
- **Carina Nebula**: Situated in the constellation Carina. It contains a mix of young and massive stars, as well as pillars of gas and dust resembling those seen in the Eagle Nebula (M16).
- **Perseus Molecular Cloud**: Located in the constellation Perseus, this cloud complex is home to a variety of star-forming regions, such as the California Nebula (NGC 1499).

On the other hand, Figure 3.9 shows that in regions where there is no dense interstellar material, the studied stars have low extinction values, as expected. The light from such objects does not pass through clumpy regions, so it is neither absorbed nor scattered.

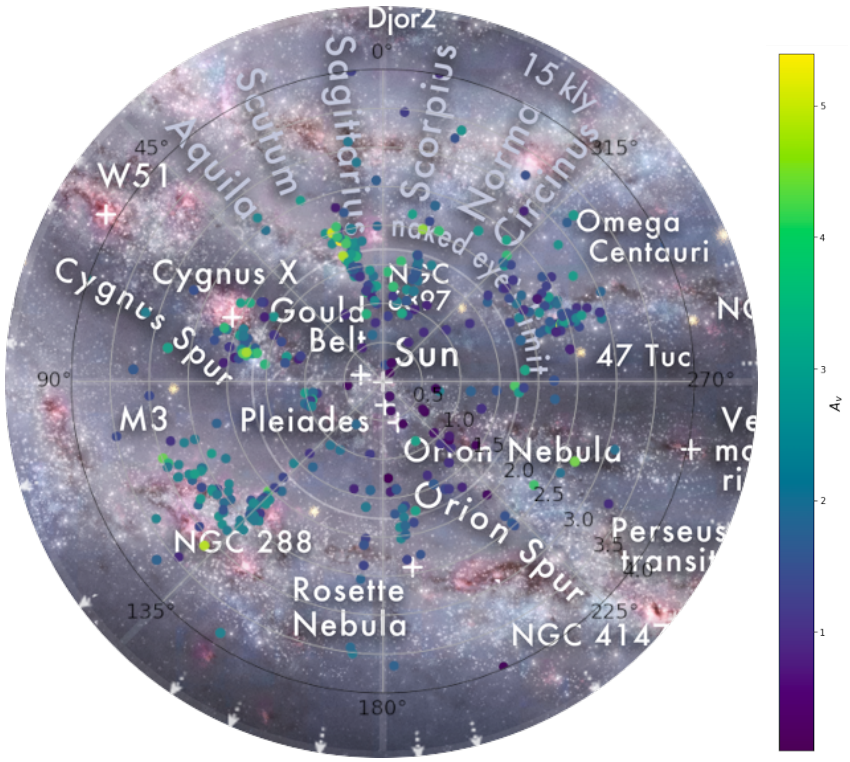

Figure 3.10: Overlaying of an artist impression image of the Milky Way with a polar diagram which locates the regions of O-BSgs population of interest ($R_V > 3.2$) taking into account a colour map of A_v.

A brief study of interstellar extinction with distance is presented in Figure 3.11 in order to check whether there is also a dependence of the light absorbed on distance. The Galactic length range chosen corresponds to some of the regions of interest already discussed:

- $l : 45° - 90°$; includes CygnusX.
- $l : 90° - 180°$; includes Perseus Arm.
- $l : 315° - 45°$; includes part of the Sagittarius Arm.

From distance-extinction diagrams in Figure 3.11, it can be conclude that the extinction grows, in general terms, linearly with distance, since the further away from the Sun the star from which the electromagnetic radiation reaches us is located, the more ISM it will pass through. There does not seem to be a favourable direction for star formation, since, for example, spiral arms extend across the Galactic disc at different distances, including the inner and outer regions of the Milky Way.
Then distance is an additional source of interstellar extinction, along with dense dust regions which produce the highest extinction values (wherever they are).

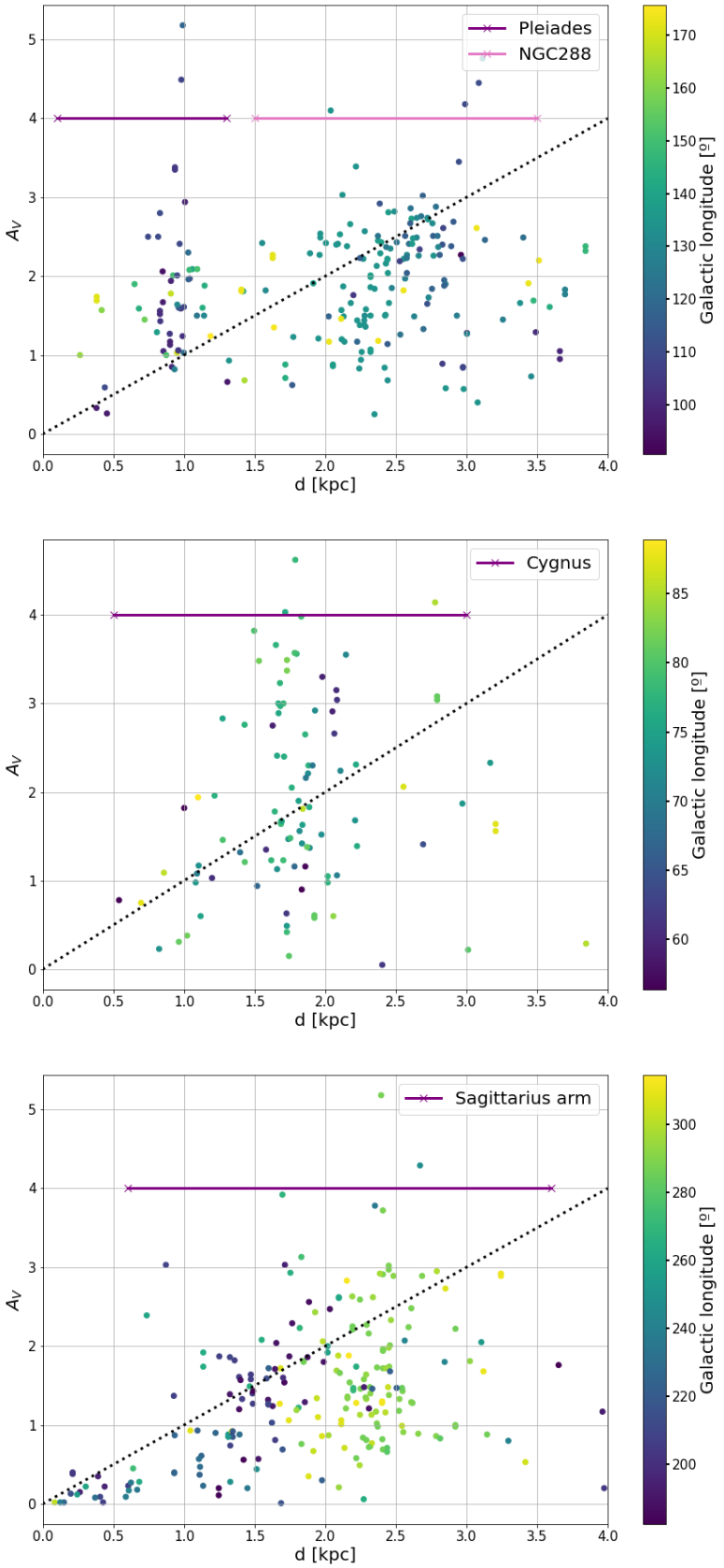

Figure 3.11: Study of the dependence of the parameter extinction A_V with the distance (d) and galactic longitude (l) for the stars located in some of the star-forming regions of interest in the solar neighbourhood.

Chapter 4
CONCLUSIONS AND FUTURE WORK

En esta sección se hace hincapié en los conceptos fundamentales de la extinción interestelar y a su tratamiento; así como una breve descripción de la muestra de estrellas utilizada y las características de la metodología seguida.
Se comentan los resultados principales obtenidos atendiendo en primer lugar a la calidad de los mismos y al respectivo análisis de los parámetros de extinción; por otro lado, se aluden las regiones de formación estelar identificadas en este estudio en la región de la vecindad solar.

Finalmente, se proponen futuras líneas de trabajo para completar la información de las propiedades estelares de cada objeto y la mejora de los datos inciales (volumen de muestra y valores de fotometría) para caracterizar el medio interestelar del disco de la Vía Láctea.

... ---...

The interstellar medium is composed of a large number of astronomical objects that emit, absorb and scatter electromagnetic radiation. The study in terms of wavelength devoted to the absorption and scattering of light emitted by stars by components of the ISM such as interstellar dust and gas is known as interstellar extinction. This physical phenomenon is most susceptible at short wavelengths, then different sets of laws are developed (we use those developed by Maız Apellániz, Evans, et al. 2014). Interstellar extinction can be studied from hot, massive stars, OBs, which, due to their surface temperature, emit large amounts of energy (due to their high mass) mainly in the blue range. Thus, from the spectroscopic database of the IACOB project, a sample of 762 O-type and B Supergiant stars is used (see Chapter 2).

The extinction parameters are determined from input data obtained from astronomical catalogues, from the quantitative spectroscopic study performed by members of the IACOB project, and from observed and synthetic energy distributions (the latter obtained from the stellar atmosphere code FASTWIND) (see Section 2.1). The Markov Chain Carlo method is used to compare the SEDs with the photometry values of each object, giving the quantity for the amount of interstellar extinction A_V, the type of dust present in the region where the star R_V is located, and the difference between the light we observe and the light actually emitted by the object: $E(B-V)$ (see Section 2.2).
The quality of the results obtained is evaluated in Section 3.1 and it is found that this methodology gives reliable results. Furthermore, results are compared with a previous study performed for O-type Galactic

stars and a very good agreement between values derived by means of the two methodologies is obtained (see Section 3.2.2).

First, we conclude that the higher the extinction, the larger the difference in magnitude of the observed light, since there will be more absorbing interstellar material in the line of sight between the observer and the emitter, and then there is also a linear dependence on distance. In contrast, the type of dust in the solar neighbourhood (the region to which our sample of stars is limited, ≈ 4 kpc) is more or less uniform, with values around 3.19 ± 0.45 according to our results (3.1 according to the literature). Two values of R_V were obtained for each of the samples excluding stars that did not deviate significantly from the mean value by applying the sigma clipping method (for three iterations considering values three times the width of the distribution of values obtained from the extinction calculation program). This yields the arithmetic mean of the distribution values, and from the slope of the fitted line relating A_V to $E(B-V)$. Our result implies that the ISM has generally similar physico-chemical characteristics; those regions with values deviating from the typical mean value correspond to areas of active star formation, i.e. with high densities of dust and gas in ionised, atomic and molecular form. In addition, a brief study of these outlayers was performed and although the quality factor χ^2 was bad, these objects were located in star-forming regions, so it follows that the photometry values are wrong for these targets (see Section 3.2).

In parallel, 2D maps of interstellar extinction (Section 3.3) were made in order to identify the active star-forming regions. The results were expected as the highest A_V values in the sample are found for stars immersed in spiral arms, stellar globules or molecular clouds.

From the results obtained in this study, the correction to the absolute magnitude of the stars can be calculated, so that the real value of the light emitted by the stars can be obtained and it is possible to complete information on the physical properties of each star such as radius, mass and luminosity. In any case, the Appendix contains information about each star 5.1 and 5.2.
On the other hand, this study could be extended by delving into the relationship between the R_V parameter and the presence of interstellar or diffuse band lines (DIBs) observed in the star's spectrum.
This thesis serves as an anchor and basic treatment of interstellar extinction that could be improved as future work by expanding the sample of early-type objects with stars from other surveys (e.g. WEAVE and 4MOST). Furthermore, given the susceptibility of the methodology to the photometry used, it would be ideal to repeat the study this time taking the Gaia values.

Chapter 5
APPENDIX

5.1. Spectroscopy of massive OB stars

Brief notes about quantitative spectroscopic analysis applied to the cooler stars in the H-R diagram are presented below, as a way to calculate parameters such as effective temperature, gravity or abundances (see Holgado, Simón-Dıaz, and R. Barbá 2017 and Simón-Dıaz 2020).

Although observing OB stars implies several difficulties, the in-depth study is motivated by the huge impact they have in the physics of the surrounding Cosmos, and because these hot stars have become valuable indicators of present-day abundances in the Milky Way and other external galaxies beyond the Local Group. They cannot only be considered as a reliable alternative to H II regions as abundance indicators, but also these stars are not affected neither by depletion into dust grains, nor the long-standing problem of the discrepancy resulting from the computation of nebular abundances using collisional emission lines or recombination ones.

The interpretation of the light emitted by close-by and distant two times ionized hydrogen regions and the ones with high star formation rates (starburst galaxies) relies on our knowledge of the effect that the strong ionizing radiation emitted by O-types stars produce in the surrounding interstellar medium. Thus, any empirical information extracted from the spectra of OB stars via **quantitative spectroscopy** is crucial to step forward in the understanding of the evolution and final fate of massive stars as well as the chemodynamical impact on the ISM at different scales. Spectroscopic parameters determined from the optical spectrum of OB-type stars are: projected rotational velocities, $vsin(i)$; macroturbulence velocity, v_{mac}; effective temperature, T_{eff}; gravity, $\log g$; wind-strength, $log(Q)$; helium abundance, Y_{He}; microturbulence, ξ_t, and the exponent of the wind-law, β.
The high effective temperature of the massive stars and the gas pressure, favour the presence of electronic transitions between the energy levels of the hydrogen atom involving the main energy level $n = 2$, the so-called **Balmer jump**; typically OBs emit radiation in the H-alpha ($656.3nm$) line and in other lines of the Balmer series. It is precisely the intensity and profile of these reference lines in the spectrum that determine some of the fundamental parameters of the massive star.

Quantitative spectroscopy is a powerful tool which allows to extract information by comparing an observed spectrum with a grid of synthetic spectra obtained by means of a stellar atmosphere code. The analysis of the parameters obtained by this technique, led to a better characterization of the presence of stellar winds,

circumstellar material, spots and surface magnetic fields, faint companions in binary systems and/or sources of stellar activity, as well as the main character in this study: the insterstellar extinction.

There are three main spectral windows commonly used to extract information from OB spectra: (far-)UV, optical range and finally (near-)IR. The main spectroscopic features of OB stars are visible in the ranges mentioned above but not for all luminosity classes OB-type stars. The main identifier is the presence of the He lines in absorption. Since He I and He II lines disappear in the B-type and early-O stars, thus other lines of reference must be sought.
Whatever the case, from the spectra analysis the effective temperature, SED, and gravity of the star can be determined in order to evaluate the stellar atmosphere model that fits better the object.

5.2. Extinction results for the stars in the sample

Results from the extinction parameters determination programme using the MA14 extinction laws for O-BSgs sample as well as complete information relative to each star are shown in Tables 5.1 (O-type stars) and Table 5.2 (for B-Sgs stars).

Table 5.1: Complete list of O-type stars considered in this BSc thesis.

Complete information relative to each star for the O-type sample: SpT and galactic coordinates (l and b) are taken from **Simbad**; distances in kpc from Bailer-Jones and Gaia catalogues (d); photometry values (U Mag, B Mag, V Mag) taken from Simbad catalogue and (J Mag, H Mag, K Mag) taken from 2MASS catalogue. Extinction parameters with corresponding uncertainty ($E(B-V)$, A_V, R_V and χ^2) are obtained from MAUP's programme and absolute magnitude taking into account interstellar extinction: M_V.

ID	**SpT**	**l [º] b**	**d [kpc]**	**U Mag**	**B Mag**	**V Mag**	**J Mag**	**H Mag**	**K Mag**	$E(B-V)$	A_V **[mag]**	R_V	χ^2	M_V **[mag]**
HD164019	O9.5IVp	1.91 -2.62	2.58	8.79	9.49	9.4	8.82	8.78	8.8	0.4 ± 0.07	1.67 ± 0.04	4.23 ± 0.81	2.9	-4.33
HD164438	O9.2IV	10.35 1.79	1.16	7.37	8.89	8.76	6.73	6.65	6.62	0.61 ± 0.07	3.65 ± 0.04	5.99 ± 0.73	36.2	-5.21
HD166546	O9.5IV	10.36 -0.92	1.18	6.4	7.26	7.22	7.12	7.15	7.16	0.34 ± 0.07	1.01 ± 0.04	2.95 ± 0.74	0.8	-4.15
HD167264	O9.7Iab	10.46 -1.74	1.18	4.64	5.42	5.37	5.21	5.21	5.16	0.28 ± 0.07	1.09 ± 0.05	3.85 ± 1.16	1	-6.07
HD207538	O9.7IV	101.6 4.67	0.83	7	7.55	7.3	6.76	6.76	6.76	0.58 ± 0.08	1.56 ± 0.04	2.7 ± 0.41	1.7	-3.86
ALS12370	O6.5Vnn((f))	103.05 -1.41	4.79	9.83	10.49	10.3	9.73	9.65	9.64	0.51 ± 0.08	1.74 ± 0.05	3.44 ± 0.59	0.6	-4.84
HD207198	O8.5II	103.14 6.99	0.98	5.61	6.25	5.94	5.37	5.32	5.32	0.58 ± 0.07	1.59 ± 0.05	2.76 ± 0.4	0.4	-5.6
HD210839	O6.5I(n)fp	103.83 2.61	0.83	4.55	5.29	5.05	4.59	4.62	4.5	0.51 ± 0.08	1.43 ± 0.05	2.79 ± 0.48	2.7	-5.98
HD209339	O9.7IV	104.58 5.87	0.94	5.9	8.73	8.51	6.54	6.62	6.62	0.75 ± 0.07	3.38 ± 0.04	4.51 ± 0.47	50.6	-4.73
HD209975	O9Ib	104.87 5.39	0.96	4.36	5.19	5.11	5.02	4.92	4.93	0.31 ± 0.07	1.06 ± 0.04	3.4 ± 0.88	0.3	-5.86
ALS12619	O7V((f))z	107.18 -0.95	2.67	10.4	10.92	10.56	9.56	9.44	9.38	0.69 ± 0.07	2.34 ± 0.04	3.41 ± 0.37	1	-3.91
BD+622078	O7V((f))z	107.45 5.02	0.98	10.83	10.76	9.78	7.21	6.93	6.76	1.36 ± 0.07	4.49 ± 0.04	3.3 ± 0.2	4.6	-4.67
HD218915	O9.2Iab	108.06 -6.89	2.97	6.32	7.22	7.2	7.13	7.22	7.2	0.29 ± 0.07	0.85 ± 0.04	2.91 ± 0.81	2.4	-6.02
HD216532	O8.5V(n)	109.65 2.68	0.75	8.06	8.46	8	6.83	6.73	6.68	0.8 ± 0.08	2.5 ± 0.05	3.12 ± 0.35	2.2	-3.86
HD216898	O9V	109.93 2.39	0.82	8.1	8.58	8.04	6.88	6.76	6.73	0.88 ± 0.07	2.5 ± 0.04	2.84 ± 0.24	1.3	-4.02
HD217086	O7Vnn((f))z	110.22 2.72	0.83	7.88	8.3	7.66	6.23	6.1	6.03	0.98 ± 0.08	2.8 ± 0.04	2.84 ± 0.28	2.3	-4.74
BD+602522	O6.5(n)fp	112.23 0.22	2.83	8.46	9.08	8.67	7.6	7.47	7.38	0.71 ± 0.08	2.4 ± 0.05	3.39 ± 0.41	0.8	-5.99
BD+602635	O6V((f))	115.9 -1.16	2.81	9.98	10.5	10.1	9.12	9.01	8.96	0.72 ± 0.07	2.27 ± 0.04	3.13 ± 0.33	0.8	-4.41
HD225146	O9.7Iab	117.23 -1.24	2.84	8.32	8.96	8.6	7.78	7.7	7.64	0.62 ± 0.07	1.95 ± 0.05	3.11 ± 0.42	0.9	-5.62
HD225160	O8Iabf	117.44 -0.14	2.76	7.74	8.46	8.19	7.49	7.43	7.34	0.54 ± 0.07	1.84 ± 0.04	3.39 ± 0.51	1.4	-5.85
V747CEP	O5.5V(n)((f))	118.2 5.09	0.99	11.6	11.38	10.07	6.99	6.63	6.42	1.71 ± 0.08	5.18 ± 0.04	3.03 ± 0.15	3.6	-5.09
HD167659	O7II-III(f)	12.2 -1.27	1.4	6.87	7.54	7.4	6.77	6.75	6.67	0.45 ± 0.08	1.76 ± 0.05	3.9 ± 0.73	2.5	-5.09
HD157857	O6.5II(f)	12.97 13.31	2.22	7.16	7.95	7.78	7.31	7.28	7.25	0.46 ± 0.07	1.55 ± 0.05	3.32 ± 0.56	0.9	-5.5
HD5005D	O9.2V	123.12 -6.25	2.53	8.98	9.84	9.78	9.52	9.54	9.55	0.38 ± 0.08	1.26 ± 0.05	3.31 ± 0.78	1.6	-3.5
BD+60134	O5.5V(n)((f))	123.5 -1.11	2.68	11	11.29	10.6	9.2	9.09	9.01	1.04 ± 0.08	2.76 ± 0.04	2.67 ± 0.22	1.7	-4.3
HD5689	O7Vn((f))	123.86 0.75	2.85	8.79	9.41	9.19	8.49	8.38	8.4	0.53 ± 0.07	1.9 ± 0.05	3.59 ± 0.56	0.9	-4.99
BD+60261	O7.5III(n)((f))	127.87 -1.35	2.47	8.27	8.94	8.69	7.92	7.95	7.85	0.56 ± 0.07	1.85 ± 0.05	3.3 ± 0.47	4.3	-5.12
HD10125	O9.7II	128.29 1.82	3.7	7.88	8.52	8.28	7.55	7.57	7.49	0.56 ± 0.08	1.83 ± 0.05	3.28 ± 0.52	3.9	-6.39
HD12323	ON9.2V	132.91 -5.87	2.44	7.95	8.87	8.92	9.06	9.16	9.17	0.25 ± 0.08	0.68 ± 0.05	2.75 ± 0.98	1.6	-3.7
BD+61411	O6.5V((f))z	133.84 1.17	2.04	11.09	11.14	10.28	7.98	7.72	7.61	1.25 ± 0.08	4.1 ± 0.04	3.29 ± 0.23	5.2	-5.37
HD13268	ON8.5IIIn	133.96 -4.99	1.77	7.48	8.24	8.18	7.87	7.94	7.92	0.36 ± 0.08	1.23 ± 0.05	3.36 ± 0.83	3.2	-4.29
HD14442	O5n(f)p	134.21 -1.32	2.56	9.01	9.58	9.27	8.27	8.24	8.18	0.65 ± 0.08	2.22 ± 0.05	3.4 ± 0.45	4.5	-4.99
BD+62424	O6.5V(n)((f))	134.53 2.46	2.09	10.31	9.23	8.9	7.83	7.72	7.67	0.66 ± 0.07	2.41 ± 0.04	3.62 ± 0.39	2.5	-5.11
HD13745	O9.7II(n)	134.58 -4.96	2.28	7.22	7.99	7.9	7.45	7.45	7.43	0.38 ± 0.07	1.44 ± 0.05	3.83 ± 0.76	2.1	-5.33
BD+60498	O9.7II-III	134.63 0.99	2.08	11.61	10.47	9.94	8.79	8.74	8.65	0.87 ± 0.08	2.4 ± 0.05	2.75 ± 0.28	2.8	-4.05
BD+60499	O9.5V	134.64 1	1.97	10.27	10.85	10.31	9.11	9.01	8.93	0.87 ± 0.08	2.54 ± 0.05	2.9 ± 0.29	1.5	-3.7
BD+60501	O7V(n)((f))z	134.71 0.94	1.89	11.06	10.02	9.56	8.54	8.43	8.39	0.78 ± 0.08	2.29 ± 0.04	2.92 ± 0.33	0.9	-4.12
HD15570	O4If	134.77 0.86	2.12	8.4	8.8	8.11	6.48	6.31	6.16	1.01 ± 0.08	3.03 ± 0.04	3.01 ± 0.26	2.2	-6.55
HD15629	O4.5V((fc))	134.77 1.01	1.96	8.23	8.85	8.42	7.42	7.32	7.27	0.75 ± 0.08	2.27 ± 0.05	3.01 ± 0.34	1.2	-5.31
BD+60513	O7Vnz	134.9 0.92	2.01	9.38	9.88	9.39	8.29	8.16	8.1	0.81 ± 0.08	2.42 ± 0.05	3 ± 0.32	0.7	-4.54
HD14947	O4.5If	134.99 -1.74	2.43	7.83	8.44	7.98	7.04	6.95	6.86	0.76 ± 0.07	2.16 ± 0.05	2.85 ± 0.32	0.8	-6.11
HD14434	O5.5Vnn((f))p	135.08 -3.82	2.24	7.87	8.65	8.49	8.13	8.13	8.12	0.47 ± 0.07	1.38 ± 0.04	2.92 ± 0.51	1.2	-4.65
HD15642	O9.5II-IIIn	137.09 -4.73	2.32	9.3	8.56	8.55	8.36	8.41	8.44	0.31 ± 0.08	1.07 ± 0.05	3.44 ± 1.03	2.5	-4.35
HD18409	O9.7Ib	137.12 3.46	2.44	9.83	8.72	8.4	7.36	7.28	7.24	0.62 ± 0.07	2.21 ± 0.05	3.58 ± 0.47	3.1	-5.75
BD+60586	O7Vz	137.42 1.28	1.92	9.63	8.71	8.49	7.75	7.71	7.73	0.58 ± 0.08	1.91 ± 0.05	3.29 ± 0.52	3.4	-4.83
HD15137	O9.5II-IIIn	137.46 -7.58	2.05	7	7.92	7.86	7.8	7.83	7.84	0.32 ± 0.08	0.88 ± 0.05	2.74 ± 0.88	0.8	-4.58
HD16691	O4If	137.73 -2.73	2.37	10.19	9.07	8.7	7.56	7.44	7.36	0.7 ± 0.08	2.45 ± 0.04	3.48 ± 0.41	2.4	-5.63
HD16832	O9.2III	138 -2.88	2.32	10.29	9.21	8.87	8.01	7.95	7.95	0.66 ± 0.08	2.01 ± 0.04	3.07 ± 0.42	2.1	-4.97
HD17603	O7.5Ib(f)	138.77 -2.08	2.61	8.68	9.1	8.45	7.04	6.86	6.76	0.92 ± 0.08	2.73 ± 0.05	2.96 ± 0.28	0.6	-6.36
HD167633	O6.5V((f))	14.34 -0.07	1.84	7.69	9.16	9.07	7.45	7.39	7.35	0.54 ± 0.07	3.15 ± 0.04	5.85 ± 0.82	23.1	-5.41
HD14633	ON8.5V	140.78 -18.2	1.42	6.14	8.79	8.73	7.92	8.05	8.12	0.5 ± 0.08	1.81 ± 0.05	3.59 ± 0.6	20.8	-3.84
HD30614	O9Ia	144.07 14.04	1.72	3.47	4.34	4.29	4.2	4.38	4.24	0.32 ± 0.07	0.88 ± 0.05	2.73 ± 0.75	7.3	-7.76

Table 5.1: Complete information relative to each star for the O-type sample: SpT and galactic coordinates (l and b); distances in kpc (d); photometry values (U Mag, B Mag, V Mag, J Mag, H Mag, K Mag); extinction parameters with corresponding uncertainty ($E(B-V)$, A_V, R_V and χ^2) and absolute magnitude taking into account interstellar extinction: M_V.

ID	**SpT**	**l [º] b**	**d [kpc]**	**U Mag**	**B Mag**	**V Mag**	**J Mag**	**H Mag**	**K Mag**	$E(B-V)$	A_V **[mag]**	R_V	χ^2	M_V **[mag]**
ALS7833	O8Vz	146.25 3.12	3.47	11.25	10.35	10.08	9.49	9.45	9.43	0.58 ± 0.08	1.69 ± 0.05	2.93 ± 0.46	0.9	-4.31
HD237211	O9.5Iab	147.14 2.97	3.84	10.58	9.41	9.05	7.95	7.83	7.77	0.65 ± 0.07	2.32 ± 0.04	3.58 ± 0.42	1.9	-6.19
HD24431	O9III+B1.5V	148.84 -0.71	0.92	6.5	7.11	6.74	5.92	5.84	5.82	0.69 ± 0.08	2.01 ± 0.05	2.92 ± 0.35	1.2	-5.1
HD175876	O6.5III(n)(f)	15.28 -10.58	2.31	5.79	6.82	6.94	7.13	7.2	7.26	0.16 ± 0.08	0.55 ± 0.05	3.43 ± 1.93	1.3	-5.43
HD175754	O8II(n)((f))p	16.39 -9.92	2.02	5.99	6.96	7.03	7.1	7.17	7.17	0.2 ± 0.07	0.71 ± 0.04	3.55 ± 1.47	1.5	-5.21
HD168076	O4III(f)	16.94 0.84	1.65	8.12	8.72	8.25	6.9	6.66	6.38	0.73 ± 0.07	3.04 ± 0.04	4.18 ± 0.46	3.9	-5.87
BD-134927	O7II(f)	16.98 0.85	1.65	10.12	10.14	9.48	7.22	6.87	6.71	0.99 ± 0.08	4.17 ± 0.05	4.22 ± 0.36	2.4	-5.78
HD24912	O7.5III(n)((f))	160.37 -13.11	0.42	3.19	4.08	4.06	3.41	3.06	3.95	0.54 ± 0.07	1.57 ± 0.04	2.91 ± 0.46	15.8	-5.61
HD41161	O8Vn	164.97 12.89	1.43	5.66	6.66	6.76	6.87	7	7.02	0.21 ± 0.07	0.68 ± 0.05	3.22 ± 1.16	3.1	-4.69
BD+391328	O8.5Iab(n)(f)	169.11 3.6	4.99	9.95	10.28	9.92	8.59	8.44	8.36	0.68 ± 0.07	2.71 ± 0.04	3.98 ± 0.48	3.3	-6.28
HD168504	O7.5V(n)z	17.03 0.35	1.63	9	9.64	9.29	8.17	8.11	8.03	0.7 ± 0.08	2.44 ± 0.05	3.48 ± 0.42	4	-4.21
HD34656	O7.5II(f)	170.04 0.27	0.95	5.87	6.77	6.76	6.64	6.63	6.68	0.31 ± 0.08	1.03 ± 0.04	3.3 ± 0.91	0.8	-4.16
HD34078	O9.5V	172.08 -2.26	0.38	5.48	6.18	5.96	5.34	5.36	5.29	0.56 ± 0.07	1.74 ± 0.05	3.13 ± 0.45	2.7	-3.69
HD36483	O9.5IV(n)	172.29 1.88	1.63	8.06	8.55	8.24	7.25	7.15	7.13	0.65 ± 0.07	2.27 ± 0.04	3.48 ± 0.43	2.7	-5.09
HD35619	O7.5V((f))z	173.04 -0.09	3.44	8.08	8.79	8.66	7.93	7.88	7.89	0.48 ± 0.07	1.91 ± 0.05	3.99 ± 0.68	3.8	-5.93
HD37737	O9.5II-III(n)	173.46 3.24	1.41	8.02	8.3	8.06	7.32	7.32	7.25	0.55 ± 0.08	1.83 ± 0.04	3.33 ± 0.5	3.3	-4.51
BD+331025	O7.5V(n)z	173.56 -1.66	2.55	9.84	10.37	10.28	9.65	9.63	9.58	0.44 ± 0.07	1.82 ± 0.04	4.15 ± 0.76	3.1	-3.58
ALS8294	O7V(n)z	173.61 -1.72	3.07	10.17	10.71	10.22	9	8.89	8.79	0.83 ± 0.07	2.61 ± 0.05	3.14 ± 0.32	1.8	-4.83
HD242926	O7Vz	173.65 -1.74	3.51	9.04	9.65	9.4	8.51	8.42	8.37	0.58 ± 0.08	2.2 ± 0.05	3.78 ± 0.52	1.9	-5.53
ALS4880	O6V((f))	18.32 1.87	1.75	11.12	11.28	10.45	8.4	8.15	8.02	1.19 ± 0.08	3.77 ± 0.05	3.16 ± 0.23	2.1	-4.54
HD168112	O5III(f)	18.44 1.62	1.88	8.81	9.21	8.52	6.9	6.72	6.63	1.03 ± 0.08	3.1 ± 0.05	3.02 ± 0.26	2	-5.95
HD168461	O7.5V((f))Nstr	18.57 1.25	1.98	9.8	10.22	9.66	7.99	7.9	7.79	0.94 ± 0.08	3.15 ± 0.04	3.35 ± 0.29	7.3	-4.98
HD171589	O7.5II(f)	18.65 -3.09	1.77	7.91	8.6	8.28	7.58	7.5	7.47	0.61 ± 0.07	1.85 ± 0.05	3.01 ± 0.42	0.6	-4.81
HD93521	O9.5IIInn	183.14 62.15	1.25	5.67	6.79	7.03	7.5	7.65	7.7	0.06 ± 0.04	0.2 ± 0.04	3.39 ± 2.46	1.8	-3.65
HD36879	O7V(n)((f))z	185.22 -5.89	1.71	6.97	7.69	7.58	7.11	7.09	7.09	0.43 ± 0.08	1.54 ± 0.05	3.6 ± 0.73	2.1	-5.13
BD-114586	O8Ib(f)	19.08 2.14	1.9	10.26	10.33	9.52	7.04	6.74	6.54	1.14 ± 0.08	4.32 ± 0.05	3.8 ± 0.29	4.2	-6.19
HD42088	O6V((f))z	190.04 0.48	1.63	6.73	7.58	7.57	7.31	7.37	7.39	0.35 ± 0.07	1.24 ± 0.05	3.54 ± 0.74	3.3	-4.73
HD256725	O5V((fc))	192.32 3.36	3.96	9.34	9.94	9.59	9.34	9.32	9.35	0.64 ± 0.07	1.17 ± 0.04	1.84 ± 0.26	0.1	-4.57
HD44811	O7V(n)z	192.4 3.21	1.86	7.72	8.54	8.48	8.2	8.18	8.25	0.39 ± 0.08	1.29 ± 0.05	3.33 ± 0.77	1.6	-4.15
HD41997	O7.5Vn((f))	194.15 -1.98	1.71	8.16	9.47	9.13	7.54	7.46	7.41	0.74 ± 0.08	3.03 ± 0.05	4.07 ± 0.47	13.3	-5.07
HD36861	O8III((f))	195.05 -12	0.44	2.17	3.48	3.47	3.85	3.99	4.03	0.28 ± 0.08	0.22 ± 0.05	0.78 ± 0.4	1	-4.96
BD-104682	O7Vn((f))	20.24 1.01	1.88	9.64	10.03	9.61	8.4	8.27	8.17	0.74 ± 0.08	2.62 ± 0.05	3.54 ± 0.42	1.8	-4.38
HD47839	O7V+B1.5/2V	202.94 2.2	3.97	3.36	4.45	4.68	5.2	5.32	5.34	0.06 ± 0.04	0.2 ± 0.04	3.34 ± 2.75	1.1	-8.52
HD36486	O9.5IINwk	203.86 -17.74	0.21	0.96	2.02	2.41	2.72	2.84	2.88	0.06 ± 0.02	0.4 ± 0.04	6.68 ± 2.03	5.2	-4.62
HD46966	O8.5IV	205.81 -0.55	1.65	5.91	6.83	6.87	6.92	6.97	7.02	0.27 ± 0.07	0.81 ± 0.04	2.98 ± 0.96	1.1	-5.02
HD46149	O8.5V	206.22 -2.04	1.49	7.03	7.8	7.61	7.24	7.25	7.25	0.51 ± 0.08	1.4 ± 0.05	2.74 ± 0.47	1.1	-4.65
HD46150	O5V((f))z	206.31 -2.07	1.49	6.03	6.86	6.73	6.45	6.47	6.44	0.44 ± 0.07	1.27 ± 0.05	2.89 ± 0.56	1.4	-5.4
HD46202	O9.2V	206.31 -2	1.47	7.6	8.33	8.27	7.78	7.78	7.72	0.39 ± 0.08	1.64 ± 0.05	4.2 ± 0.95	2.4	-4.21
HD46056	O8Vn	206.34 -2.25	1.41	7.6	8.36	8.16	7.84	7.83	7.82	0.5 ± 0.08	1.33 ± 0.05	2.67 ± 0.47	0.7	-3.92
HD46223	O4V((f))	206.44 -2.07	1.39	6.73	7.5	7.28	6.74	6.7	6.68	0.53 ± 0.07	1.61 ± 0.05	3.02 ± 0.47	1	-5.05
HD46485	O7V((f))nzvar?	206.9 -1.84	1.25	7.92	8.6	8.27	7.56	7.51	7.45	0.63 ± 0.07	1.87 ± 0.05	2.99 ± 0.39	1	-4.08
HD46573	O7V((f))z	208.73 -2.63	1.33	7.61	8.27	7.93	7.2	7.17	7.13	0.66 ± 0.07	1.86 ± 0.04	2.82 ± 0.36	1.6	-4.54
HD169582	O6Iaf	21.33 1.2	2.03	8.74	9.24	8.7	7.34	7.22	7.08	0.86 ± 0.07	2.78 ± 0.05	3.22 ± 0.31	2.1	-5.62
HD47432	O9.7Ib	210.03 -2.11	1.6	5.67	6.44	6.31	5.93	5.95	5.87	0.38 ± 0.07	1.26 ± 0.05	3.34 ± 0.75	2.2	-5.97
HD36512	O9.7V	210.44 -20.98	0.41	3.3	4.36	4.63	5.23	5.35	5.38	0.04 ± 0.03	0.09 ± 0.04	2.64 ± 2.45	0.9	-3.51
HD52533	O8.5IVn	216.85 0.8	1.7	6.66	7.57	7.68	7.83	7.92	7.94	0.19 ± 0.07	0.69 ± 0.05	3.52 ± 1.46	1.6	-4.16
HD52266	O9.5IIIn	219.13 -0.68	1.35	6.32	7.22	7.23	7.2	7.24	7.26	0.27 ± 0.07	0.92 ± 0.05	3.35 ± 0.97	0.9	-4.33
HD57682	O9.2IV	224.41 2.63	1.11	5.2	6.24	6.43	6.81	6.97	6.94	0.12 ± 0.06	0.37 ± 0.04	3.22 ± 1.93	2.8	-4.17
HD55879	O9.7III	224.73 0.35	0.93	4.88	5.85	6.03	6.36	6.45	6.5	0.11 ± 0.06	0.4 ± 0.04	3.66 ± 2.18	1.1	-4.22
HD54879	O9.7V	225.55 -1.28	1.22	6.8	7.6	7.65	7.65	7.68	7.73	0.25 ± 0.08	0.9 ± 0.05	3.47 ± 1.54	1.3	-3.69
HD53975	O7.5Vz	225.68 -2.32	1.12	5.38	6.4	6.5	6.7	6.81	6.82	0.2 ± 0.08	0.61 ± 0.04	3.09 ± 1.33	1.8	-4.36

Table 5.1: Complete information relative to each star for the O-type sample: SpT and galactic coordinates (l and b); distances in kpc (d); photometry values (U Mag, B Mag, V Mag, J Mag, H Mag, K Mag); extinction parameters with corresponding uncertainty ($E(B-V)$, A_V, R_V and χ^2) and absolute magnitude taking into account interstellar extinction: M_V.

ID	**SpT**	**l [º] b**	**d [kpc]**	**U Mag**	**B Mag**	**V Mag**	**J Mag**	**H Mag**	**K Mag**	$E(B-V)$	A_V **[mag]**	R_V	χ^2	M_V **[mag]**
HD173010	O9.7Ia	23.73 -2.49	4.18	9.64	9.87	9.21	7.38	7.18	7.03	0.96 ± 0.08	3.25 ± 0.05	3.4 ± 0.29	3.3	-7.15
HD38666	O9.5V	237.29 -27.1	0.59	3.84	4.9	5.18	5.74	5.89	5.99	0.04 ± 0.04	0.09 ± 0.04	2.68 ± 2.63	1.9	-3.76
HD173783	O9Iab	24.18 -3.34	4.61	9.3	9.69	9.31	8.22	8.11	8.02	0.66 ± 0.07	2.36 ± 0.05	3.57 ± 0.45	1.3	-6.37
HD172175	O6.5I(n)fp	24.53 -0.85	2.55	9.63	10	9.54	8.04	7.92	7.84	0.81 ± 0.08	2.91 ± 0.05	3.58 ± 0.38	5.9	-5.4
HD64568	O3V((f*))z	243.14 0.71	4.26	8.64	9.5	9.39	9.13	9.12	9.12	0.42 ± 0.07	1.29 ± 0.05	3.1 ± 0.58	0.8	-5.05
CPD-262716	O6.5Iabf	243.82 0.14	5.72	9.37	10	9.67	8.75	8.62	8.55	0.62 ± 0.07	2.16 ± 0.05	3.48 ± 0.43	0.6	-6.28
HD69464	O7Ib(f)	253.61 -0.3	3.11	8.47	9.11	8.8	7.93	7.87	7.77	0.6 ± 0.07	2.05 ± 0.04	3.41 ± 0.46	1.8	-5.71
HD68450	O9.7II	254.47 -2.02	1.31	5.58	6.42	6.44	6.43	6.44	6.47	0.25 ± 0.06	0.88 ± 0.04	3.58 ± 1.11	0.4	-5.03
HD75222	O9.7Iab	258.29 4.18	2.02	7.24	7.8	7.42	6.53	6.49	6.4	0.66 ± 0.08	2 ± 0.05	3 ± 0.4	2.5	-6.1
HD73882	O8.5IV	260.18 0.64	0.74	7.07	7.59	7.19	6.11	6.02	5.92	0.72 ± 0.07	2.39 ± 0.05	3.32 ± 0.37	2.1	-4.54
HD71304	O9II	261.76 -3.77	2.1	8.52	8.98	8.45	7.13	7.02	6.93	0.83 ± 0.07	2.62 ± 0.05	3.13 ± 0.3	2.2	-5.78
HD76341	O9.2IV	263.53 1.52	1.14	6.88	7.39	7.16	6.44	6.41	6.32	0.53 ± 0.08	1.92 ± 0.05	3.6 ± 0.59	2.3	-5.04
HD75211	O8.5II((f))	263.96 -0.47	1.55	7.35	7.9	7.5	6.58	6.54	6.4	0.67 ± 0.08	2.08 ± 0.05	3.11 ± 0.41	2.4	-5.53
HD74194	O8.5Ib-II(f)p	264.04 -1.95	2.22	7.05	7.77	7.55	6.93	6.89	6.81	0.48 ± 0.07	1.74 ± 0.05	3.59 ± 0.62	1.3	-5.92
HD74920	O7.5IVn((f))	265.29 -1.95	1.75	6.64	9.46	9.09	7.41	7.45	7.47	0.83 ± 0.08	2.93 ± 0.05	3.54 ± 0.4	30.3	-5.06
HD76556	O6IV(n)((f))p	267.58 -1.63	1.82	8.03	8.61	8.2	7.22	7.14	7.05	0.73 ± 0.07	2.23 ± 0.04	3.06 ± 0.33	1.4	-5.33
CPD-472963	O5Ifc	267.98 -1.36	1.7	9.11	9.41	8.54	6.33	6.06	5.9	1.2 ± 0.08	3.92 ± 0.05	3.27 ± 0.23	2.6	-6.53
HD76968	O9.2Ib	270.22 -3.37	2.2	6.53	7.33	7.21	6.75	6.76	6.66	0.4 ± 0.08	1.47 ± 0.05	3.67 ± 0.8	2.4	-5.97
HD298429	O8.5V	274.47 -0.25	1.83	9.78	10.46	9.97	8.3	8.22	8.1	0.86 ± 0.08	3.13 ± 0.04	3.64 ± 0.35	8.6	-4.47
HD89137	ON9.7II(n)	279.69 4.45	2.44	7.02	7.93	7.97	8.07	8.13	8.12	0.23 ± 0.07	0.71 ± 0.05	3.15 ± 1.18	1.1	-4.68
HD90273	ON7V((f))	284.18 -0.25	2.54	8.35	9.25	9.05	8.64	8.62	8.59	0.51 ± 0.07	1.47 ± 0.04	2.91 ± 0.48	0.6	-4.45
HD90087	O9.2III(n)	285.16 -2.13	2.19	6.91	9.49	8.92	7.72	7.74	7.76	0.95 ± 0.08	2.25 ± 0.05	2.37 ± 0.22	8.8	-5.04
HD91572	O6.5V((f))z	285.52 -0.05	2.62	7.44	8.29	8.24	7.96	7.99	7.99	0.37 ± 0.07	1.28 ± 0.05	3.43 ± 0.74	1.8	-5.13
HD91824	O7V((f))z	285.7 0.07	1.83	7.17	8.11	8.14	8.21	8.3	8.35	0.28 ± 0.07	0.76 ± 0.05	2.71 ± 0.86	1.6	-3.93
HD92504	O8.5V(n)	285.92 0.99	2.32	7.47	8.38	8.46	8.56	8.62	8.68	0.21 ± 0.08	0.73 ± 0.05	3.43 ± 1.44	1.1	-4.1
HD91651	ON9.5IIIn	286.55 -1.72	1.85	7.96	9.64	9.52	8.76	8.81	8.81	0.49 ± 0.07	1.81 ± 0.05	3.7 ± 0.6	9.4	-3.62
HD94024	O8IV	287.34 1.27	2.59	8.03	9.15	9.45	8.45	8.49	8.48	0.25 ± 0.03	2.24 ± 0.04	8.92 ± 0.8	26.4	-4.86
CPD-582611	O6V((f))z	287.39 -0.59	2.29	9.16	9.88	9.59	8.66	8.52	8.5	0.61 ± 0.08	2.27 ± 0.05	3.75 ± 0.5	1.1	-4.48
HD93128	O3.5V((fc))z	287.4 -0.58	2.31	8.82	8.97	8.77	7.91	7.86	7.79	0.55 ± 0.08	2.16 ± 0.05	3.89 ± 0.6	3.3	-5.21
ALS15196	O8.5V	287.41 -0.58	2.25	9.28	10.1	9.9	8.97	8.77	8.38	0.42 ± 0.08	2.59 ± 0.05	6.15 ± 1.25	12.5	-4.44
HD93160	O7III((f))	287.44 -0.59	2.55	7.27	7.99	7.6	7.18	7.14	7.08	0.66 ± 0.07	1.43 ± 0.05	2.17 ± 0.29	1.2	-5.86
HD303311	O6V((f))z	287.48 -0.54	2.25	8.3	9.04	8.98	8.59	8.59	8.56	0.39 ± 0.08	1.46 ± 0.05	3.71 ± 0.88	1.8	-4.24
HD93250	O4III(fc)	287.51 -0.54	2.37	6.73	8.12	7.5	6.78	6.72	6.71	0.91 ± 0.08	1.73 ± 0.05	1.9 ± 0.21	0.1	-6.1
ALS15210	O3.5If*Nwk	287.52 -0.71	2.4	11.03	11.51	10.71	7.84	7.38	7.06	1.12 ± 0.08	5.18 ± 0.05	4.64 ± 0.36	1.7	-6.37
HD93204	O5.5V((f))	287.57 -0.71	2.32	7.63	8.52	8.42	8.03	7.99	7.97	0.4 ± 0.08	1.48 ± 0.05	3.68 ± 0.79	0.8	-4.88
HD303308	O4.5V((fc))	287.59 -0.61	2.17	7.45	8.3	8.17	7.71	7.71	7.62	0.43 ± 0.07	1.54 ± 0.05	3.53 ± 0.65	2.3	-5.06
CPD-592600	O6V((f))	287.6 -0.74	2.46	8.07	8.79	8.57	7.8	7.74	7.64	0.53 ± 0.08	2.01 ± 0.04	3.81 ± 0.6	1.7	-5.39
HD93027	O9.5IV	287.61 -1.13	2.92	7.86	8.72	8.72	8.67	8.72	8.67	0.29 ± 0.07	1 ± 0.05	3.51 ± 1.03	1.6	-4.61
HD305523	O9II-III	287.66 -0.9	2.41	7.82	8.64	8.5	7.78	7.69	7.63	0.43 ± 0.07	1.96 ± 0.04	4.56 ± 0.84	1.1	-5.37
CPD-592551	O9V	287.67 -1.05	2.52	8.42	9.37	9.36	9.19	9.2	9.18	0.31 ± 0.08	1.18 ± 0.05	3.79 ± 1.11	0.9	-3.83
HD93222	O7V((f))z	287.74 -1.02	2.41	7.26	8.18	8.1	7.59	7.5	7.44	0.35 ± 0.08	1.72 ± 0.05	4.9 ± 1.17	0.5	-5.53
HD305532	O6.5V((f))z	287.78 -0.84	2.41	9.8	10.54	10.2	8.87	8.66	8.54	0.65 ± 0.08	2.91 ± 0.05	4.44 ± 0.55	1	-4.62
HD305525	O5.5V(n)((f))z	287.79 -0.71	6.12	10.26	10.68	10	8.18	7.96	7.77	1 ± 0.08	3.52 ± 0.04	3.51 ± 0.29	1.9	-7.45
HD94370	O7.5III(f)	288.01 0.63	2.61	7.19	8.69	8.92	7.73	7.76	7.69	0.28 ± 0.03	2.48 ± 0.04	8.74 ± 0.83	26.7	-5.64
HD93632	O5Ifvar	288.03 -0.87	2.41	7.89	8.69	9.1	7.19	7.06	6.85	0.38 ± 0.01	3.72 ± 0.04	9.72 ± 0.21	43.4	-6.53
HD303492	O8.5Iaf	288.05 0.4	4.74	9	9.45	8.85	7.31	7.11	6.95	0.85 ± 0.07	2.84 ± 0.05	3.35 ± 0.32	1.3	-7.37
HD305619	O9.7II	288.22 -0.96	2.45	9.28	9.86	9.44	7.96	7.77	7.62	0.72 ± 0.08	3.02 ± 0.05	4.19 ± 0.51	1.9	-5.53
HD93843	O5III(fc)	288.24 -0.9	2.37	6.37	7.29	7.33	7.23	7.27	7.23	0.24 ± 0.07	1.02 ± 0.04	4.11 ± 1.48	1.7	-5.56
HD96917	O8Ib(n)(f)	289.28 3.06	2.61	6.46	7.29	7.21	6.82	6.82	6.77	0.32 ± 0.07	1.29 ± 0.05	3.99 ± 1.02	1.8	-6.16
HD94963	O7II(f)	289.76 -1.81	2.79	6.35	7.17	7.26	7.26	7.35	7.33	0.21 ± 0.07	0.86 ± 0.04	4.15 ± 1.54	2.6	-5.82
HD165174	O9.7IIn	29.27 11.29	0.98	5.23	6.08	6.15	6.15	6.22	6.24	0.22 ± 0.08	0.84 ± 0.05	3.84 ± 1.81	2.1	-4.65

Table 5.1: Complete information relative to each star for the O-type sample: SpT and galactic coordinates (l and b); distances in kpc (d); photometry values (U Mag, B Mag, V Mag, J Mag, H Mag, K Mag); extinction parameters with corresponding uncertainty ($E(B-V)$, A_V, R_V and χ^2) and absolute magnitude taking into account interstellar extinction: M_V.

ID	**SpT**	**l [º] b**	**d [kpc]**	**U Mag**	**B Mag**	**V Mag**	**J Mag**	**H Mag**	**K Mag**	$E(B-V)$	A_V **[mag]**	R_V	χ^2	M_V **[mag]**
HD96622	O9.2IV	290.09 0.57	2.16	8.37	9.05	8.87	8.48	8.53	8.5	0.49 ± 0.08	1.36 ± 0.04	2.75 ± 0.47	2.4	-4.16
HD96715	O4V((f))z	290.27 0.33	2.53	7.51	8.32	8.28	7.95	7.98	7.96	0.35 ± 0.08	1.33 ± 0.05	3.79 ± 0.96	2.3	-5.06
HD96946	O6.5III(f)	290.73 -0.34	2.45	7.93	8.69	8.55	7.95	7.91	7.92	0.48 ± 0.07	1.74 ± 0.04	3.6 ± 0.59	2.4	-5.14
HD97848	O8V	290.74 1.53	2.66	7.66	8.59	8.6	8.61	8.63	8.65	0.28 ± 0.08	0.89 ± 0.05	3.22 ± 1.06	0.4	-4.41
HD97253	O5III(f)	290.79 0.09	2.29	6.42	7.24	7.09	6.69	6.71	6.7	0.45 ± 0.07	1.35 ± 0.05	2.98 ± 0.52	1.9	-6.06
HD97434	O7.5III(n)((f))	291.04 -0.15	2.32	7.45	8.24	8.07	7.66	7.65	7.62	0.46 ± 0.08	1.4 ± 0.05	3.04 ± 0.58	1.2	-5.16
HD99546	O7.5V((f))Nstr	292.33 1.68	3.02	7.33	9.06	9.02	8.28	8.35	8.38	0.44 ± 0.07	1.81 ± 0.05	4.15 ± 0.73	12.5	-5.19
HD99897	O6.5IV((f))	293.61 -1.28	2.19	7.74	9.39	9.18	7.84	7.85	7.82	0.62 ± 0.08	2.63 ± 0.05	4.2 ± 0.59	17.4	-5.15
HD101190	O6IV((f))	294.78 -1.49	2.36	6.58	7.37	7.33	7.12	7.17	7.16	0.36 ± 0.07	1.17 ± 0.05	3.21 ± 0.7	2	-5.7
HD308813	O9.7IV(n)	294.79 -1.61	2.43	8.46	9.68	9.73	9.15	9.16	9.14	0.31 ± 0.07	1.72 ± 0.04	5.5 ± 1.31	6.3	-3.92
HD101223	O8V	294.81 -1.49	2.34	8.12	9.55	9.51	8.24	8.22	8.23	0.46 ± 0.08	2.62 ± 0.05	5.64 ± 1.07	19.8	-4.95
HD101191	O8V	294.84 -1.68	2.47	7.69	9.32	9.36	8.29	8.32	8.34	0.39 ± 0.07	2.33 ± 0.04	5.93 ± 1.19	20.3	-4.93
HD101298	O6.5IV((f))	294.94 -1.69	2.29	7.33	8.15	8.07	7.76	7.75	7.77	0.38 ± 0.08	1.33 ± 0.06	3.53 ± 0.98	1.5	-5.06
HD101413	O8V	295.03 -1.71	1.93	7.62	9.16	9.21	8.11	8.13	8.1	0.38 ± 0.07	2.43 ± 0.04	6.32 ± 1.2	18.6	-4.65
HD102415	ON9IIInn	295.3 0.45	2.08	8.51	9.44	9.35	8.8	8.78	8.76	0.42 ± 0.07	1.69 ± 0.04	4.06 ± 0.8	2.3	-3.93
HD104565	OC9.7Iab	296.51 4.02	4.76	9	9.55	9.27	8.36	8.29	8.2	0.54 ± 0.07	2.05 ± 0.04	3.8 ± 0.55	2	-6.17
HD105627	O9III	298.15 -0.1	2.25	7.31	8.21	8.19	7.98	8.05	8.05	0.34 ± 0.08	1.13 ± 0.05	3.36 ± 0.89	2.6	-4.7
HD105056	ON9.7Iae	298.95 -7.06	2.79	6.57	9.07	8.74	7.16	7.14	7.05	0.72 ± 0.07	2.95 ± 0.04	4.07 ± 0.44	15.7	-6.44
HD110360	ON7V	301.8 2.2	2.09	8.69	9.79	9.58	8.85	8.82	8.83	0.57 ± 0.07	1.88 ± 0.05	3.29 ± 0.47	3.7	-3.9
HD112244	O8.5Iab(f)p	303.55 6.03	1.34	4.49	5.33	5.32	5.3	5.28	5.22	0.22 ± 0.07	0.92 ± 0.05	4.15 ± 1.52	1.3	-6.23
HD116852	O8.5II-III((f))	304.88 -16.13	3.42	8.29	8.38	8.47	8.72	8.81	8.78	0.17 ± 0.08	0.53 ± 0.05	3.08 ± 2.04	1.6	-4.73
HD114737	O8.5III	305.41 -0.82	4.12	7.43	8.19	8	7.5	7.49	7.44	0.5 ± 0.08	1.58 ± 0.04	3.17 ± 0.55	1.5	-6.66
HD117797	O7.5fp	307.86 0.04	2.85	9.13	9.68	9.2	7.87	7.69	7.58	0.76 ± 0.07	2.73 ± 0.05	3.58 ± 0.38	0.8	-5.8
HD117490	ON9.5IIInn	307.88 1.66	2.11	8.13	8.94	8.92	8.78	8.84	8.83	0.33 ± 0.07	1.06 ± 0.05	3.26 ± 0.87	2	-3.77
HD120521	O7.5Ib(f)	310.73 3.42	3.12	8.06	8.79	8.58	7.98	7.93	7.86	0.5 ± 0.08	1.68 ± 0.05	3.39 ± 0.58	1.3	-5.57
HD123008	ON9.2Iab	311.02 -2.8	3.24	8.58	10	9.5	7.91	7.84	7.71	0.85 ± 0.07	2.92 ± 0.05	3.45 ± 0.33	8.1	-5.98
HD123056	O9.5IV(n)	312.17 1.03	2.4	7.54	8.28	8.14	7.81	7.79	7.84	0.45 ± 0.07	1.3 ± 0.04	2.89 ± 0.53	1	-5.06
HD125241	O8.5Ib(f)	313.54 0.14	2.15	8.6	9.08	8.6	7.1	6.99	6.86	0.79 ± 0.07	2.83 ± 0.05	3.59 ± 0.36	4.8	-5.9
CPD-595634	O9.2Ib	315.37 -0.08	2.26	9.95	10.35	9.89	7.92	7.76	7.62	0.83 ± 0.07	3.59 ± 0.04	4.31 ± 0.41	10.4	-5.47
HD124979	O7.5IV(n)((f))	316.4 9.08	3.61	7.81	8.61	8.51	8.35	8.35	8.37	0.37 ± 0.08	1.03 ± 0.05	2.75 ± 0.64	0.5	-5.31
HD130298	O6.5III(n)(f)	318.77 2.77	2.41	9.14	10.06	9.83	8.27	8.19	8.11	0.64 ± 0.07	3.07 ± 0.05	4.81 ± 0.58	13.7	-5.15
HD135591	O8IV((f))	320.13 -2.64	0.82	4.46	5.36	5.46	5.58	5.58	5.62	0.18 ± 0.07	0.79 ± 0.05	4.26 ± 1.77	0.2	-4.89
CPD-546791	O9.5V	327.56 -0.83	2.29	10.51	10.95	10.41	9.03	8.86	8.75	0.86 ± 0.08	2.87 ± 0.05	3.33 ± 0.33	1	-4.26
HD149452	O9IVn	337.47 0.03	1.39	9.2	10.39	9.4	7.6	7.48	7.34	1.32 ± 0.08	3.22 ± 0.04	2.44 ± 0.16	2.2	-4.53
HD150574	ON9III(n)	339 -0.2	2.2	8.01	8.74	8.5	7.93	7.89	7.86	0.54 ± 0.07	1.68 ± 0.04	3.12 ± 0.47	0.8	-4.9
HD149038	O9.7Iab	339.38 2.51	0.91	4.05	4.99	4.94	4.74	4.68	4.61	0.27 ± 0.08	1.23 ± 0.05	4.62 ± 1.51	1	-6.07
HD151018	O9Ib	339.51 -0.41	2.05	8.9	9.93	9.37	7.28	7.17	7.02	0.94 ± 0.07	3.69 ± 0.04	3.92 ± 0.33	13.7	-5.88
HD154811	OC9.7Ib	341.06 -4.22	1.22	6.71	7.32	6.98	5.95	5.85	5.79	0.63 ± 0.08	2.26 ± 0.05	3.56 ± 0.48	2.1	-5.71
HD155756	O9Ibp	342.57 -4.39	3.37	9.39	9.81	9.55	8.14	8.03	7.92	0.6 ± 0.07	2.84 ± 0.04	4.76 ± 0.63	6.9	-5.93
HD151515	O7II(f)	342.81 1.7	1.46	6.77	7.48	7.3	6.71	6.71	6.65	0.49 ± 0.08	1.69 ± 0.05	3.44 ± 0.59	2.4	-5.21
HD152147	O9.7IbNwk	343.15 1.1	1.57	7.2	7.76	7.34	6.35	6.25	6.17	0.69 ± 0.07	2.2 ± 0.04	3.19 ± 0.4	1.2	-5.84
HD152003	O9.7IabNwk	343.33 1.41	1.54	6.9	7.47	7.08	6.1	6.01	5.91	0.67 ± 0.07	2.17 ± 0.04	3.25 ± 0.4	1.7	-6.03
HD152424	OC9.2Ia	343.36 0.89	1.56	6.11	6.69	6.27	5.32	5.22	5.06	0.66 ± 0.07	2.15 ± 0.05	3.26 ± 0.41	1.9	-6.85
HD148546	O9Iab	343.38 7.15	2.35	7.28	7.99	7.71	6.96	6.9	6.81	0.56 ± 0.07	1.88 ± 0.04	3.37 ± 0.49	1.4	-6.02
HD152200	O9.7IV(n)	343.41 1.22	1.39	7.74	8.49	8.39	8.12	8.08	8.06	0.37 ± 0.07	1.29 ± 0.05	3.51 ± 0.76	0.4	-3.62
CPD-417721A	O9.7V	343.44 1.18	1.57	8.11	8.85	8.72	8.31	8.29	8.27	0.44 ± 0.07	1.46 ± 0.05	3.36 ± 0.62	1.1	-3.71
HD152249	OC9Iab	343.45 1.16	1.47	5.91	6.65	6.45	5.9	5.84	5.75	0.45 ± 0.08	1.62 ± 0.05	3.58 ± 0.68	1.1	-6
HD326329	O9.7V	343.46 1.17	1.53	8.14	9.18	9.01	8.38	8.4	8.36	0.52 ± 0.08	1.71 ± 0.05	3.28 ± 0.56	3.7	-3.63
HD152233	O6II(f)	343.48 1.22	1.38	5.93	6.72	6.59	6.17	6.14	6.1	0.43 ± 0.08	1.46 ± 0.05	3.38 ± 0.69	1	-5.56
HD326331	O8IVn((f))	343.49 1.14	1.36	6.89	7.68	7.5	6.97	6.93	6.91	0.48 ± 0.08	1.57 ± 0.05	3.3 ± 0.59	1	-4.74
HD152247	O9.2III	343.61 1.3	1.38	6.62	7.35	7.16	6.65	6.61	6.59	0.48 ± 0.07	1.6 ± 0.05	3.31 ± 0.54	1	-5.14

Table 5.1: Complete information relative to each star for the O-type sample: SpT and galactic coordinates (l and b); distances in kpc (d); photometry values (U Mag, B Mag, V Mag, J Mag, H Mag, K Mag); extinction parameters with corresponding uncertainty ($E(B-V)$, A_V, R_V and χ^2) and absolute magnitude taking into account interstellar extinction: M_V.

ID	**SpT**	**l [º] b**	**d [kpc]**	**U Mag**	**B Mag**	**V Mag**	**J Mag**	**H Mag**	**K Mag**	$E(B-V)$	A_V **[mag]**	R_V	χ^2	M_V **[mag]**
HD151804	O8Iaf	343.62 1.94	2.14	4.45	5.29	5.22	4.94	4.95	4.79	0.33 ± 0.07	1.34 ± 0.05	4.09 ± 1.01	3.8	-7.77
HD152405	O9.7II	344.56 1.89	1.68	6.71	7.42	7.29	6.83	6.86	6.8	0.42 ± 0.07	1.47 ± 0.05	3.5 ± 0.7	2.7	-5.3
HD152623	O7V(n)((f))z	344.62 1.61	5.28	5.95	8.7	8.64	6.34	6.34	6.3	0.6 ± 0.08	4.01 ± 0.04	6.7 ± 0.86	60.9	-8.98
HD152723	O6.5III(f)	344.81 1.61	2.55	6.43	7.24	7.1	6.84	6.74	6.81	0.43 ± 0.07	1.27 ± 0.05	2.95 ± 0.53	0.4	-6.2
HD152590	O7.5Vz	344.84 1.83	1.68	7.87	9.11	9.29	7.98	7.9	7.92	0.32 ± 0.04	2.81 ± 0.04	8.57 ± 0.95	23.7	-4.64
HD326775	O6.5V(n)((f))z	345.01 -0.3	1.55	11.42	11.54	10.55	8.23	7.93	7.75	1.33 ± 0.08	4.16 ± 0.05	3.13 ± 0.2	1	-4.57
HD322417	O6.5IV((f))	345.26 1.47	2.02	10.65	10.9	10.22	7.7	7.37	7.16	1.05 ± 0.08	4.53 ± 0.05	4.33 ± 0.34	5.7	-5.83
HD155913	O4.5Vn((f))	345.29 -2.61	1.21	8.2	8.81	8.34	7.15	7	6.91	0.8 ± 0.08	2.62 ± 0.04	3.28 ± 0.35	0.8	-4.7
HD154368	O9.5Iab	349.97 3.22	1.03	6.1	6.63	6.13	5.02	4.85	4.75	0.73 ± 0.07	2.34 ± 0.04	3.21 ± 0.31	0.4	-6.27
HD154643	O9.7III	350.54 3.19	0.93	6.76	7.42	7.2	6.57	6.54	6.53	0.54 ± 0.07	1.71 ± 0.05	3.18 ± 0.49	1.9	-4.36
HD156738	O6.5III(f)	351.18 0.48	1.76	10.06	10.27	9.35	7.18	6.92	6.76	1.27 ± 0.08	3.92 ± 0.04	3.09 ± 0.22	1.7	-5.8
HD156154	O7.5Ib(f)	351.22 1.36	1.59	8.19	8.64	8.04	6.67	6.48	6.37	0.87 ± 0.07	2.75 ± 0.04	3.17 ± 0.29	0.5	-5.72
HD319699	O5V((fc))	351.32 0.92	1.56	10.17	10.31	9.63	7.66	7.45	7.29	1.04 ± 0.08	3.64 ± 0.04	3.51 ± 0.28	3.9	-4.97
HD163758	O6.5Iafp	355.36 -6.1	3.46	6.46	7.35	7.32	7.19	7.16	7.16	0.28 ± 0.07	1.05 ± 0.05	3.8 ± 1.07	0.3	-6.43
HD159176	O7V((f))+O7V((f))	355.67 0.05	0.84	4.88	5.74	5.7	5.53	5.52	5.54	0.34 ± 0.08	1.15 ± 0.05	3.33 ± 0.81	0.6	-5.06
HD162978	O8II((f))	4.54 0.3	1	5.35	6.24	6.2	5.97	5.97	5.95	0.32 ± 0.08	1.2 ± 0.05	3.74 ± 1.01	1	-5
HD168941	O9.5IVp	5.82 -6.31	4	8.53	9.36	9.37	9.19	9.21	9.22	0.29 ± 0.07	1.12 ± 0.04	3.9 ± 1.07	1.3	-4.76
HD188001	O7.5Iabf	56.48 -4.33	1.83	5.32	6.24	6.23	6.11	6.17	6.15	0.27 ± 0.07	0.9 ± 0.05	3.32 ± 0.99	2	-5.99
HD344784	O6.5V((f))	59.4 -0.15	1.63	9.38	9.86	9.37	8.03	7.89	7.84	0.84 ± 0.07	2.75 ± 0.05	3.28 ± 0.32	2.8	-4.44
HDE344777	O7.5Vz	59.41 0.11	1.98	9.83	10.13	9.54	7.77	7.6	7.55	0.95 ± 0.08	3.3 ± 0.05	3.46 ± 0.3	6.3	-5.24
HD164794	O4V((f))z	6.01 -1.2	1.22	5.08	5.97	5.97	5.75	5.75	5.73	0.3 ± 0.08	1.27 ± 0.06	4.24 ± 1.29	1.2	-5.73
HD149757	O9.2IVnn	6.28 23.59	0.14	1.73	2.58	2.56	2.59	2.59	2.62	0.29 ± 0.07	0.86 ± 0.05	2.96 ± 0.87	0.2	-4.01
HD165246	O8V(n)	6.4 -1.56	1.19	6.9	7.7	7.6	7.31	7.29	7.23	0.38 ± 0.08	1.38 ± 0.05	3.62 ± 0.94	1	-4.15
HDE338931	O6III(f)	61.19 -0.14	2.08	9.38	9.72	9.14	7.59	7.41	7.32	0.92 ± 0.08	3.04 ± 0.05	3.31 ± 0.3	2.1	-5.49
HDE338916	O7.5Vz	61.47 0.38	2.06	10.36	10.7	10.17	8.85	8.79	8.71	0.89 ± 0.08	2.66 ± 0.05	2.99 ± 0.29	4	-4.06
HD186980	O7.5III((f))	67.39 3.66	1.78	6.72	7.56	7.48	7.24	7.27	7.29	0.39 ± 0.07	1.16 ± 0.05	2.98 ± 0.61	1.7	-4.94
HD164492	O7.5Vz	7 -0.25	1.42	6.49	7.49	6.8	7.4	7.39	7.3	0.71 ± 0.06	0.09 ± 0.01	0.13 ± 0.03	30.5	-4.06
HD163800	O7.5III((f))	7.05 0.69	1.25	6.61	7.27	7	6.33	6.3	6.22	0.54 ± 0.08	1.77 ± 0.04	3.25 ± 0.51	1.7	-5.26
HD163892	O9.5IV(n)	7.15 0.62	1.27	6.81	7.61	7.44	7.08	7.1	7.08	0.48 ± 0.08	1.35 ± 0.05	2.84 ± 0.55	1.5	-4.43
HDE227465	O7V((f))	70.73 1.21	4.04	10.21	10.75	10.33	9.1	9.04	8.97	0.78 ± 0.08	2.56 ± 0.04	3.26 ± 0.34	4.8	-5.26
HDE227018	O6.5V((f))z	71.58 2.87	2.11	8.75	9.35	9	8.04	7.95	7.9	0.67 ± 0.07	2.24 ± 0.05	3.33 ± 0.39	1.8	-4.86
HDE227245	O7V((f))z	72.17 2.62	1.93	9.92	10.25	9.69	8.21	8.07	7.99	0.9 ± 0.08	2.92 ± 0.05	3.23 ± 0.31	3.2	-4.66
HD190864	O6.5III(f)	72.47 2.02	1.82	7.18	7.93	7.78	7.26	7.28	7.26	0.47 ± 0.08	1.56 ± 0.05	3.31 ± 0.58	3.1	-5.08
HD190429	O4If+O9.5II	72.59 2.61	1.89	5.98	6.78	6.63	6.25	6.19	6.18	0.42 ± 0.08	1.37 ± 0.05	3.22 ± 0.66	0.4	-6.12
HD192639	O7.5Iabf	74.9 1.48	1.81	6.83	7.46	7.11	6.3	6.27	6.22	0.65 ± 0.07	1.9 ± 0.05	2.91 ± 0.38	2.1	-6.08
HD193682	O4.5IV(f)	75.92 0.82	1.66	8.44	8.87	8.42	7.3	7.19	7.14	0.78 ± 0.08	2.41 ± 0.05	3.07 ± 0.33	1.8	-5.09
HD228841	O6.5Vn((f))	76.6 1.68	1.71	9.08	9.5	9.01	7.91	7.78	7.75	0.81 ± 0.07	2.4 ± 0.05	2.96 ± 0.3	1.1	-4.55
HD193595	O7V((f))	76.86 1.62	1.76	8.5	9.08	8.78	7.92	7.87	7.85	0.64 ± 0.08	2.05 ± 0.05	3.19 ± 0.43	2.6	-4.5
HD193514	O7Ib(f)	77 1.8	1.88	7.32	7.83	7.38	6.35	6.24	6.18	0.76 ± 0.07	2.3 ± 0.05	3.02 ± 0.32	0.8	-6.29
HD192281	O4.5V(n)((f))	77.12 3.4	1.22	7.32	7.85	7.55	6.74	6.72	6.7	0.64 ± 0.07	1.96 ± 0.04	3.07 ± 0.39	3	-4.84
HD229232	O4Vn((f))	77.4 0.93	1.68	10.17	10.3	9.5	7.77	7.6	7.5	1.15 ± 0.07	3.23 ± 0.04	2.8 ± 0.19	1.9	-4.86
HD189957	O9.7III	77.43 6.17	2.02	6.93	7.84	7.82	7.72	7.71	7.74	0.31 ± 0.08	1.05 ± 0.05	3.34 ± 0.96	0.5	-4.75
BD+364145	O8.5V(n)	77.45 -2.02	1.43	9.23	9.47	8.96	7.57	7.46	7.43	0.88 ± 0.08	2.76 ± 0.05	3.15 ± 0.32	4.5	-4.58
HD191978	O8Vz	77.87 4.25	1.62	7.38	8.15	8.03	7.76	7.8	7.8	0.44 ± 0.08	1.23 ± 0.05	2.79 ± 0.58	1.8	-4.25
HDE229202	O7.5V(n)((f))	78.19 1.63	1.8	10.28	10.44	9.58	7.6	7.43	7.31	1.23 ± 0.08	3.56 ± 0.04	2.9 ± 0.2	3.5	-5.25
HD192001	O9.5IV	78.53 4.66	1.69	7.97	8.52	8.29	7.68	7.68	7.68	0.57 ± 0.07	1.67 ± 0.04	2.93 ± 0.43	2.7	-4.52
HD191423	ON9II-IIInn	78.64 5.37	1.7	7.43	8.19	8.03	7.73	7.74	7.77	0.46 ± 0.08	1.23 ± 0.05	2.66 ± 0.52	1.1	-4.36
HD188209	O9.5Iab	80.99 10.09	1.92	4.61	5.55	5.63	5.72	5.83	5.82	0.16 ± 0.08	0.58 ± 0.05	3.58 ± 2.17	2.5	-6.37
HD191781	ON9.7Iab	81.18 6.61	2.79	10.1	10.06	9.53	8	7.76	7.66	0.84 ± 0.08	3.08 ± 0.04	3.67 ± 0.35	0.9	-5.78
HD195592	O9.7Ia	82.36 2.96	1.73	7.75	7.95	7.08	5.08	4.8	4.62	1.12 ± 0.08	3.49 ± 0.04	3.12 ± 0.24	0.6	-7.6
LSIII+4612	O4.5IV(f)	84.88 3.78	2.78	11.07	11.22	10.26	7.93	7.62	7.47	1.29 ± 0.08	4.14 ± 0.04	3.2 ± 0.21	1.5	-6.1

Table 5.1: Complete information relative to each star for the O-type sample: SpT and galactic coordinates (l and b); distances in kpc (d); photometry values (U Mag, B Mag, V Mag, J Mag, H Mag, K Mag); extinction parameters with corresponding uncertainty ($E(B-V)$, A_V, R_V and χ^2) and absolute magnitude taking into account interstellar extinction: M_V.

ID	**SpT**	**l [º] b**	**d [kpc]**	**U Mag**	**B Mag**	**V Mag**	**J Mag**	**H Mag**	**K Mag**	$E(B-V)$	A_V **[mag]**	R_V	χ^2	M_V **[mag]**
HD199579	O6.5V((f))z	85.7 -0.3	0.86	5.16	6.01	5.96	5.8	5.83	5.86	0.37 ± 0.08	1.09 ± 0.04	2.98 ± 0.69	1.5	-4.8
HD202124	O9Iab	87.29 -2.66	3.21	7.33	7.94	7.76	7.18	7.13	7.09	0.46 ± 0.07	1.64 ± 0.05	3.56 ± 0.62	1.2	-6.41
HD203064	O7.5IIIn((f))	87.61 -3.84	0.7	4.05	4.99	5	5.04	5.11	5.11	0.27 ± 0.07	0.75 ± 0.05	2.75 ± 0.81	1.4	-4.96
HD214680	O9V	96.65 -16.98	0.45	3.65	4.67	4.88	5.39	5.44	5.5	0.08 ± 0.05	0.26 ± 0.04	3.61 ± 2.46	0.1	-3.67
HD206183	O9.5IV-V	98.89 3.4	0.9	6.75	7.55	7.41	7.19	7.19	7.23	0.46 ± 0.07	1.17 ± 0.04	2.57 ± 0.44	0.8	-3.54
HD210809	O9Iab	99.85 -3.13	3.66	6.7	7.61	7.56	7.37	7.4	7.41	0.3 ± 0.07	0.95 ± 0.04	3.1 ± 0.84	1.7	-6.21

Table 5.2: Complete list of B-Sgs stars considered in this BSc thesis.

Complete information relative to each star for the B-Sgs sample: SpT and galactic coordinates (l and b) are taken from **Simbad**; distances in kpc from Bailer-Jones and Gaia catalogues (d); photometry values (U Mag, B Mag, V Mag) taken from Simbad catalogue and (J Mag, H Mag, K Mag) taken from 2MASS catalogue. Extinction parameters with corresponding uncertainty ($E(B-V)$, A_V, R_V and χ^2) are obtained from MAUP's programme and absolute magnitude taking into account interstellar extinction: M_V.

ID	**SpT**	**l [º] b**	**d [kpc]**	**U Mag**	**B Mag**	**V Mag**	**J Mag**	**H Mag**	**K Mag**	$E(B-V)$	A_V **[mag]**	R_V	χ^2	M_V **[mag]**
HD164032	B1/2Ib	0.88 -3.24	1.62	6.84	7.53	7.45	7.14	7.18	7.15	0.34 ± 0.07	1.07 ± 0.04	3.09 ± 0.77	2.5	-4.67
HD164019	O9.5IVp	1.91 -2.62	2.58	8.79	9.49	9.4	8.82	8.78	8.8	0.41 ± 0.07	1.66 ± 0.04	4.08 ± 0.77	3	-4.32
HD164438	O9.2IV	10.35 1.79	1.16	7.37	8.89	8.76	6.73	6.65	6.62	0.59 ± 0.07	3.62 ± 0.05	6.11 ± 0.79	37.2	-5.18
HD166546	O9.5IV	10.36 -0.92	1.18	6.4	7.26	7.22	7.12	7.15	7.16	0.33 ± 0.07	0.97 ± 0.05	2.95 ± 0.81	0.8	-4.11
HD167264	O9.7Iab	10.46 -1.74	1.18	4.64	5.42	5.37	5.21	5.21	5.16	0.28 ± 0.07	1.04 ± 0.05	3.66 ± 1.12	0.9	-6.02
HD205139	B1Ib	100.55 6.62	0.85	4.92	5.6	5.52	5.56	5.22	5.26	0.22 ± 0.06	1.05 ± 0.04	4.73 ± 1.52	9.9	-5.19
HD207538	O9.7IV	101.6 4.67	0.83	7	7.55	7.3	6.76	6.76	6.76	0.57 ± 0.08	1.52 ± 0.05	2.66 ± 0.45	1.8	-3.82
HD235783	B1Ib	101.69 -1.87	3.49	8.14	8.82	8.74	8.28	8.28	8.26	0.35 ± 0.07	1.29 ± 0.05	3.66 ± 0.82	2.4	-5.26
HD206165	B2Ib	102.27 7.25	0.99	4.49	5.03	4.73	4.28	4.21	4.13	0.48 ± 0.07	1.24 ± 0.05	2.6 ± 0.46	1.2	-6.49
HD235813	B0III	102.47 -2.03	4.14	8.33	9	8.87	8.35	8.3	8.28	0.4 ± 0.08	1.52 ± 0.05	3.86 ± 0.83	1.2	-5.74
HD208218	B1III	103.98 6.62	0.9	6.3	6.89	6.71	6.23	6.24	6.26	0.47 ± 0.08	1.27 ± 0.05	2.72 ± 0.52	2.4	-4.33
HD239967	B3II	104.23 -1	2.2	9.2	9.66	9.43	8.59	8.53	8.51	0.51 ± 0.08	1.76 ± 0.05	3.43 ± 0.58	3.2	-4.04
HD209339	O9.7IV	104.58 5.87	0.94	5.9	8.73	8.51	6.54	6.62	6.62	0.75 ± 0.07	3.35 ± 0.05	4.47 ± 0.47	51.4	-4.7
HD209975	O9Ib	104.87 5.39	0.96	4.36	5.19	5.11	5.02	4.92	4.93	0.29 ± 0.08	1.06 ± 0.05	3.71 ± 1.19	0.4	-5.86
HD216438	B1II	105.72 -5.12	2.83	7.76	8.5	8.48	8.34	8.37	8.36	0.27 ± 0.07	0.89 ± 0.05	3.29 ± 0.99	1.3	-4.67
HD210386	B1.5II-III	106 6.38	1.04	7.79	8.27	8.02	7.11	7.02	6.99	0.55 ± 0.08	1.97 ± 0.05	3.57 ± 0.59	2.7	-4.04
HD215806	O	107.14 -0.7	2.53	9.05	9.52	9.23	8.25	8.16	8.07	0.59 ± 0.07	2.19 ± 0.04	3.72 ± 0.51	2	-4.97
HD216411	B0	108.03 -0.35	2.84	7.38	7.81	7.2	5.77	5.59	5.46	0.86 ± 0.08	2.61 ± 0.05	3.01 ± 0.3	1.2	-7.67
HD218915	O9.2Iab	108.06 -6.89	2.97	6.32	7.22	7.2	7.13	7.22	7.2	0.29 ± 0.08	0.84 ± 0.05	2.85 ± 0.89	2.4	-6.01
HD213087	B0.5Ib	108.5 6.39	1	5.24	5.81	5.51	4.95	4.81	4.74	0.49 ± 0.07	1.61 ± 0.04	3.25 ± 0.53	0.7	-6.09
HD213405	B0.5V	108.69 6.25	0.95	7.98	8.39	8.02	7.05	6.99	6.98	0.69 ± 0.07	2.01 ± 0.04	2.92 ± 0.36	3.4	-3.88
HD217490	B0	109.28 -0.27	2.99	9.26	9.64	9.21	6.79	6.56	6.41	0.82 ± 0.07	4.18 ± 0.04	5.06 ± 0.48	19	-7.35
HD213481	B8	109.44 7.39	0.97	8.42	8.66	8.23	6.97	6.88	6.77	0.72 ± 0.07	2.41 ± 0.05	3.34 ± 0.39	3.5	-4.11
HD218376	B0.5III	109.95 -0.78	0.44	3.93	4.77	4.84	4.93	5.01	5.05	0.2 ± 0.07	0.59 ± 0.04	2.92 ± 1.12	1.6	-3.97
HD166787	B0.5Ia	11.06 -0.8	1.8	8.27	8.75	8.31	7.01	6.83	6.7	0.71 ± 0.07	2.65 ± 0.05	3.73 ± 0.43	1.1	-5.61
HD166628	B3Ia/ab	11.26 -0.51	1.81	7.6	7.93	7.32	5.73	5.56	5.41	0.81 ± 0.08	2.64 ± 0.05	3.27 ± 0.35	2.3	-6.61
HD166922	B2Ib	11.54 -0.72	1.65	9.05	9.49	9.28	8.42	8.35	8.27	0.47 ± 0.08	1.82 ± 0.05	3.85 ± 0.67	2.3	-3.62
HD166569	B1II	11.55 -0.26	1.99	8.85	9.34	8.96	7.88	7.77	7.71	0.66 ± 0.07	2.19 ± 0.05	3.29 ± 0.41	2.2	-4.73
HD166965	B2Ib	11.83 -0.63	1.73	8.4	9.37	9.37	8.05	8.01	7.93	0.36 ± 0.07	2.49 ± 0.04	6.86 ± 1.39	16.8	-4.31
HD167287	B1Iab	11.99 -0.93	1.63	6.38	8.7	8.76	6.82	6.8	6.78	0.44 ± 0.07	3.43 ± 0.04	7.75 ± 1.08	50.2	-5.74
HD219287	B0	110.81 -1.19	3.09	10.12	10.3	9.23	6.54	6.25	6.05	1.39 ± 0.08	4.45 ± 0.04	3.19 ± 0.2	4.3	-7.67
HD218941	O	110.93 0.06	2.95	10.34	10.34	9.68	7.7	7.48	7.34	0.97 ± 0.07	3.45 ± 0.04	3.55 ± 0.29	4.4	-6.12
HD240256	B0	111.76 -0.42	2.97	9.12	9.18	8.8	7.6	7.42	7.32	0.6 ± 0.07	2.22 ± 0.05	3.69 ± 0.48	1	-5.79
BD+602525	B3	112.23 -0.15	2.72	9.3	9.85	9.6	8.95	8.92	8.89	0.56 ± 0.08	1.65 ± 0.05	2.98 ± 0.48	1.9	-4.22
BD+631962	B5	112.74 2.8	0.96	8.16	8.66	8.4	7.75	7.76	7.72	0.58 ± 0.08	1.6 ± 0.05	2.77 ± 0.4	3	-3.12
BD+631964	B0	112.89 3.1	2.39	8.79	9.05	8.5	6.9	6.71	6.59	0.84 ± 0.07	2.92 ± 0.05	3.48 ± 0.33	2.9	-6.31
BD+602615	B0	115.1 -0.18	2.91	9.24	9.62	9.14	7.76	7.62	7.48	0.74 ± 0.08	2.69 ± 0.05	3.61 ± 0.43	2.3	-5.87
BD+612509	B3	115.13 0.32	2.89	8.35	8.8	8.5	7.35	7.31	7.21	0.63 ± 0.07	2.38 ± 0.05	3.78 ± 0.49	6	-6.19
HD224257	B0.2IV	115.25 -6.06	1.77	7.03	7.91	7.99	8.08	8.17	8.24	0.24 ± 0.07	0.62 ± 0.04	2.61 ± 0.9	2.5	-3.87
BD+612526	B3	115.54 0.09	2.58	8.63	9.09	8.8	7.84	7.74	7.69	0.58 ± 0.08	2.04 ± 0.05	3.52 ± 0.51	2.1	-5.3
BD+612529	B0	115.62 0.01	2.76	8.74	9.07	8.68	7.4	7.25	7.17	0.67 ± 0.08	2.51 ± 0.05	3.73 ± 0.46	2.6	-6.04
HD224436	B1II	115.68 -5.03	2.44	8.36	9.03	8.93	8.61	8.63	8.61	0.37 ± 0.07	1.14 ± 0.04	3.05 ± 0.73	1.7	-4.15
BD+602631	B0.5III	115.8 -1.13	2.57	9.68	10.05	9.7	8.43	8.36	8.23	0.67 ± 0.07	2.51 ± 0.05	3.76 ± 0.46	5.1	-4.86
HD223987	B0	116.18 -0.51	2.25	7.59	8	7.6	6.48	6.38	6.26	0.66 ± 0.07	2.23 ± 0.05	3.39 ± 0.43	2.3	-6.39
HD224424	B0e	116.21 -2.45	2.69	8.61	8.76	8.1	6.42	6.15	6.07	0.91 ± 0.08	3.02 ± 0.05	3.3 ± 0.31	0.9	-7.07
HD224055	B3Ia	116.29 -0.3	2.6	7.67	7.85	7.23	5.59	5.44	5.27	0.81 ± 0.08	2.67 ± 0.05	3.3 ± 0.37	3.5	-7.51
HD222568	B1IV	116.5 6.37	1.03	7.59	8.03	7.71	6.74	6.71	6.67	0.63 ± 0.08	1.96 ± 0.05	3.13 ± 0.44	4.3	-4.32
HD225146	O9.7Iab	117.23 -1.24	2.84	8.32	8.96	8.6	7.78	7.7	7.64	0.62 ± 0.07	1.88 ± 0.05	3.02 ± 0.43	0.9	-5.55
HD225094	B2.9Iab	117.63 1.26	2.02	6.01	6.56	6.22	5.41	5.34	5.27	0.5 ± 0.07	1.49 ± 0.05	2.98 ± 0.49	1.4	-6.8
BD+6312	O9Ib	118.82 1.6	3.13	9.86	10.18	9.72	8.55	8.42	8.36	0.77 ± 0.07	2.46 ± 0.05	3.2 ± 0.34	1.4	-5.22
HD1544	B0.5III(n)	119.27 -0.58	2.23	7.51	8.28	8.12	7.79	7.79	7.8	0.45 ± 0.08	1.17 ± 0.04	2.61 ± 0.51	1.2	-4.79
HD167224	B3Ib/II	12 -0.85	2	7.54	8.96	9.07	7.79	7.78	7.78	0.29 ± 0.04	2.31 ± 0.04	7.73 ± 1.22	26	-4.74

Table 5.2: Complete information relative to each star for the B-Sgs sample: SpT and galactic coordinates (l and b); distances in kpc (d); photometry values (U Mag, B Mag, V Mag, J Mag, H Mag, K Mag); extinction parameters with corresponding uncertainty ($E(B-V)$, A_V, R_V and χ^2) and absolute magnitude taking into account interstellar extinction: M_V.

ID	**SpT**	**l [º] b**	**d [kpc]**	**U Mag**	**B Mag**	**V Mag**	**J Mag**	**H Mag**	**K Mag**	$E(B-V)$	A_V **[mag]**	R_V	χ^2	M_V **[mag]**
HD167375	B2III	12.08 -1.01	1.49	7.44	8.22	8.22	7.86	7.81	7.68	0.23 ± 0.07	1.35 ± 0.04	5.87 ± 1.71	2.3	-4
HD167479	B1/2Ib/II	12.26 -1.03	1.37	7.59	8.18	8.16	7.89	7.92	7.92	0.26 ± 0.08	0.91 ± 0.05	3.5 ± 1.23	2.3	-3.43
HD167336	B0II	12.57 -0.66	1.81	8.7	9.24	8.78	7.42	7.28	7.16	0.74 ± 0.07	2.69 ± 0.05	3.63 ± 0.39	2.2	-5.2
HD168021	B0Ia+B0.2II	12.7 -1.47	0.61	6.46	7.08	6.86	6.08	6.01	5.9	0.48 ± 0.07	1.92 ± 0.05	3.94 ± 0.69	1.7	-3.98
HD2451	B0.5IV	120.32 -0.25	2.7	8.2	8.85	8.74	8.38	8.38	8.36	0.41 ± 0.07	1.33 ± 0.04	3.24 ± 0.62	1.5	-4.74
HD2619	B	120.74 2.49	1.03	8.44	8.78	8.33	7.19	7.12	7.11	0.79 ± 0.07	2.3 ± 0.04	2.9 ± 0.3	3.9	-4.04
HD2905	B1Ia	120.84 0.14	1	3.5	4.3	4.16	3.99	3.81	3.88	0.34 ± 0.07	1.03 ± 0.04	2.98 ± 0.68	1.1	-6.87
BD+6073	B1Ib	121.22 -1.46	3.4	9.79	10.14	9.66	8.39	8.27	8.17	0.76 ± 0.07	2.49 ± 0.05	3.28 ± 0.36	2	-5.49
BD+6476	B1Ib	122.24 2.4	2.59	9.3	9.57	9.16	7.88	7.77	7.73	0.73 ± 0.08	2.41 ± 0.05	3.32 ± 0.39	4.6	-5.32
BD+6389	B1Ib	122.26 1.53	2.79	9.69	10.05	9.5	8.23	8.05	8	0.83 ± 0.08	2.51 ± 0.05	3.04 ± 0.32	0.7	-5.24
HD4613	B1II	122.68 2.68	2.51	9.02	9.32	8.84	7.54	7.44	7.39	0.78 ± 0.07	2.43 ± 0.04	3.1 ± 0.31	3.9	-5.59
HD4694	B3Ia	122.77 1.77	2.6	9.06	9.16	8.55	6.82	6.61	6.48	0.82 ± 0.08	2.86 ± 0.05	3.47 ± 0.34	2.7	-6.39
BD+61175	B3II	122.83 -0.51	2.78	10.25	10.26	9.63	7.91	7.72	7.56	0.87 ± 0.08	2.88 ± 0.04	3.32 ± 0.32	2.4	-5.47
HD5551	B1.5Ib	123.71 0.85	2.37	7.97	8.26	7.76	6.41	6.27	6.14	0.75 ± 0.08	2.51 ± 0.05	3.32 ± 0.39	2.3	-6.63
HD6182	B1	124.42 -1.02	2.58	8.24	8.7	8.3	7.23	7.14	7.04	0.69 ± 0.08	2.23 ± 0.04	3.23 ± 0.39	2	-5.99
HD6675	B0.5III	124.48 6.87	1.09	6.57	7.16	6.94	6.38	6.42	6.38	0.53 ± 0.08	1.5 ± 0.05	2.81 ± 0.46	3.2	-4.75
HD7103	B0k	125.42 -0.88	2.43	8.6	8.82	8.4	7.04	6.91	6.79	0.65 ± 0.07	2.37 ± 0.05	3.66 ± 0.46	3.3	-5.9
BD+57247	O9.5IV	126.57 -4.33	3.26	9.45	10.14	9.93	9.45	9.46	9.47	0.54 ± 0.08	1.45 ± 0.05	2.67 ± 0.43	2.3	-4.08
BD+57252	B1IV	126.64 -4.41	2.93	9.2	9.77	9.51	8.88	8.83	8.84	0.53 ± 0.07	1.5 ± 0.05	2.82 ± 0.44	1.4	-4.33
HD236740	B2Ib	127.38 -2.28	2.57	8	8.28	7.91	6.85	6.75	6.7	0.61 ± 0.08	1.97 ± 0.05	3.22 ± 0.44	2.6	-6.11
HD8965	B0.5V	127.68 -2.27	0.93	6.48	7.27	7.29	7.23	7.3	7.32	0.29 ± 0.07	0.82 ± 0.05	2.84 ± 0.78	2	-3.38
HD10125	O9.7II	128.29 1.82	3.7	7.88	8.52	8.28	7.55	7.57	7.49	0.55 ± 0.08	1.77 ± 0.05	3.2 ± 0.5	4	-6.33
BD+60279	B2II	128.36 -1.42	3	8.65	9.24	9.11	8.64	8.67	8.62	0.4 ± 0.08	1.27 ± 0.05	3.21 ± 0.69	3.3	-4.55
HD236810	B2III	128.68 -1.78	7.82	8.38	8.9	8.73	7.99	7.96	7.89	0.46 ± 0.07	1.71 ± 0.05	3.72 ± 0.64	2.9	-7.45
HD236815	B0.5III	128.82 -1.91	2.63	8.05	8.71	8.56	8.02	8.04	7.96	0.44 ± 0.08	1.49 ± 0.04	3.42 ± 0.67	2.8	-5.03
BD+60333	B5Ib	129.46 -0.95	2.72	9.59	9.6	8.97	7.29	7.05	6.94	0.83 ± 0.08	2.74 ± 0.05	3.31 ± 0.34	1.3	-5.95
BD+60345	B0II:	129.48 -0.66	2.65	9.88	10.26	9.81	8.6	8.47	8.39	0.75 ± 0.07	2.49 ± 0.05	3.34 ± 0.38	1.7	-4.79
BD+60339	B6Iabe	129.49 -0.91	2.58	8.98	9.09	8.47	7.05	6.9	6.78	0.81 ± 0.07	2.27 ± 0.04	2.8 ± 0.28	1.8	-5.85
BD+60343A	B6Ia	129.51 -0.9	2.66	9.58	9.83	9.3	8.06	7.94	7.83	0.77 ± 0.07	2.26 ± 0.05	2.94 ± 0.32	1.5	-5.09
BD+60351	B6Iab	129.63 -1.01	2.8	9.48	9.62	9.1	7.75	7.55	7.51	0.76 ± 0.08	2.37 ± 0.04	3.13 ± 0.36	1.3	-5.51
HD11744	B2III	129.75 3.42	1.14	7.78	8.18	7.81	7	7	6.94	0.62 ± 0.08	1.5 ± 0.05	2.42 ± 0.36	3.5	-3.98
HD164188	B1Ib/II	13.09 3.67	1.65	8.18	8.89	8.71	8.26	8.24	8.24	0.48 ± 0.07	1.35 ± 0.05	2.82 ± 0.49	1.5	-3.72
HD166287	B1Ib	13.36 1.08	1.39	7.42	8.1	7.92	7.31	7.28	7.23	0.46 ± 0.07	1.56 ± 0.05	3.36 ± 0.58	1.8	-4.36
HD166286	B1II	13.42 1.13	1.73	7.91	8.42	8.25	7.6	7.55	7.51	0.47 ± 0.07	1.69 ± 0.05	3.6 ± 0.64	2	-4.63
HD166540	B1Ib	13.43 0.81	1.39	7.57	8.29	8.16	7.71	7.7	7.67	0.43 ± 0.07	1.42 ± 0.04	3.34 ± 0.6	1.7	-3.98
HD165049	B2Ib/II	13.95 3.04	0.89	8.05	9.17	9.14	7.2	7.09	7.05	0.46 ± 0.07	3.41 ± 0.04	7.38 ± 1.12	32.2	-4.01
HD166689	B1Ib	13.96 0.91	1.44	7.55	8.95	8.61	7.08	7.03	7.03	0.73 ± 0.08	2.73 ± 0.05	3.75 ± 0.44	16.5	-4.92
HD10898	B2Ib	130.36 -3.59	2.73	7.23	7.75	7.4	6.55	6.47	6.41	0.57 ± 0.08	1.73 ± 0.05	3.04 ± 0.48	1.2	-6.51
BD+60369	B2II	130.36 -1.13	2.65	10.08	10.33	9.74	8.22	8.03	7.92	0.86 ± 0.07	2.74 ± 0.04	3.19 ± 0.32	1.5	-5.12
HD232522	B1II	130.7 -6.71	3.46	7.76	8.65	8.7	8.72	8.79	8.77	0.23 ± 0.07	0.73 ± 0.05	3.21 ± 1.17	1.8	-4.72
HD12509	B1III	130.78 2.64	0.95	6.9	7.4	7.14	6.44	6.41	6.36	0.54 ± 0.07	1.64 ± 0.05	3.05 ± 0.46	1.9	-4.39
HD12567	B0.5III	130.86 2.56	1.58	8.12	8.63	8.31	7.5	7.46	7.43	0.62 ± 0.07	1.82 ± 0.04	2.91 ± 0.38	2.5	-4.5
BD+59387	B3II	131.7 -1.57	2.76	9.92	10.16	9.72	8.24	8.1	8	0.74 ± 0.08	2.67 ± 0.05	3.63 ± 0.43	4.3	-5.15
BD+59388	B3II	131.73 -1.67	2.46	9.99	10.1	9.62	8.31	8.25	8.11	0.76 ± 0.07	2.35 ± 0.05	3.11 ± 0.33	4.6	-4.69
HD12150	B2IV	132.03 -3.43	2.28	8.36	8.85	8.68	8	8.03	7.92	0.43 ± 0.07	1.5 ± 0.05	3.49 ± 0.64	5.2	-4.61
HD13256	B1Ia	132.6 -0.64	3.11	9.8	9.69	8.68	5.67	5.27	4.95	1.25 ± 0.07	4.76 ± 0.04	3.8 ± 0.24	4.2	-8.55
HD13036	B0.5:III:	132.68 -1.76	1.55	8.67	8.91	8.51	7.33	7.26	7.15	0.72 ± 0.07	2.42 ± 0.04	3.37 ± 0.37	3.5	-4.87
HD232590	B1.5III	133.23 -6.3	2.24	7.99	8.65	8.62	8.45	8.54	8.52	0.3 ± 0.08	0.83 ± 0.05	2.76 ± 0.91	3.2	-3.96
HD236954	B3Ib-II	133.3 -2.04	2.28	9.82	9.95	9.42	7.99	7.81	7.76	0.8 ± 0.08	2.57 ± 0.04	3.22 ± 0.34	2.3	-4.94
BD+59451	B1II	133.45 -1.45	2.49	9.7	9.97	9.37	7.79	7.74	7.58	0.92 ± 0.08	2.82 ± 0.05	3.07 ± 0.28	6.6	-5.43
BD+57520	B1II	133.54 -2.73	3.38	9.5	9.92	9.57	8.86	8.83	8.78	0.65 ± 0.07	1.66 ± 0.04	2.57 ± 0.34	1.6	-4.73

Table 5.2: Complete information relative to each star for the B-Sgs sample: SpT and galactic coordinates (l and b); distances in kpc (d); photometry values (U Mag, B Mag, V Mag, J Mag, H Mag, K Mag); extinction parameters with corresponding uncertainty ($E(B-V)$, A_V, R_V and χ^2) and absolute magnitude taking into account interstellar extinction: M_V.

ID	**SpT**	**l [º] b**	**d [kpc]**	**U Mag**	**B Mag**	**V Mag**	**J Mag**	**H Mag**	**K Mag**	$E(B-V)$	A_V **[mag]**	R_V	χ^2	M_V **[mag]**
BD+59461	B1II	133.81 -1.27	2.77	10.21	10.6	10.19	9.03	8.95	8.85	0.7 ± 0.07	2.26 ± 0.04	3.22 ± 0.36	2.8	-4.28
HD13659	B1Ib	134.2 -4.1	2.36	8.8	9.05	8.71	7.65	7.61	7.53	0.64 ± 0.08	2.13 ± 0.05	3.31 ± 0.45	4.6	-5.29
HD13854	B1Iab	134.38 -3.91	2.18	6.1	6.76	6.48	5.78	5.71	5.61	0.5 ± 0.07	1.66 ± 0.05	3.29 ± 0.54	1.2	-6.87
HD13841	B1.5Ib	134.38 -3.93	2.29	6.95	7.6	7.37	6.82	6.81	6.78	0.48 ± 0.07	1.36 ± 0.04	2.83 ± 0.48	1.9	-5.78
HD13831	O9.5I	134.46 -4.21	2.14	7.56	8.32	8.26	8.04	8.06	7.98	0.3 ± 0.08	1.17 ± 0.05	3.95 ± 1.26	1.8	-4.56
HD13969	B0.5I	134.49 -3.83	5.36	8.56	9.15	8.02	8.28	8.24	8.18	1.18 ± 0.07	0.15 ± 0.04	0.13 ± 0.03	32.8	-5.78
HD13866	B2Ib-II:p	134.5 -4.22	1.95	6.95	7.63	7.51	7.1	7.07	7.06	0.36 ± 0.08	1.21 ± 0.05	3.37 ± 0.8	1.1	-5.15
HD14052	B1Ib	134.54 -3.69	2.25	7.9	8.48	7.79	7.51	7.5	7.42	0.86 ± 0.08	0.94 ± 0.05	1.09 ± 0.15	5.8	-4.92
BD+56501	B0.5I	134.56 -3.74	2.13	8.98	9.63	9.41	8.89	8.83	8.82	0.49 ± 0.08	1.49 ± 0.05	3.05 ± 0.51	0.6	-3.72
HD13745	O9.7II(n)	134.58 -4.96	2.28	7.22	7.99	7.9	7.45	7.45	7.43	0.35 ± 0.07	1.38 ± 0.04	3.87 ± 0.87	2.1	-5.27
HD14053	B0.7I	134.59 -3.88	3.08	8.05	8.67	7.83	7.91	7.9	7.87	0.98 ± 0.08	0.4 ± 0.05	0.41 ± 0.07	12.3	-5.01
BD+60493	B0.5Iae	134.62 0.58	2.22	10.57	9.12	8.48	6.57	6.36	6.2	0.93 ± 0.08	3.39 ± 0.05	3.64 ± 0.32	3.8	-6.64
HD14134	B3Ia	134.64 -3.73	2.13	6.63	7	6.57	5.56	5.43	5.29	0.59 ± 0.07	1.87 ± 0.04	3.17 ± 0.44	1.3	-6.94
HD13621	B1V	134.64 -5.65	1.32	7.35	8.13	8.13	8	8.05	8.03	0.29 ± 0.07	0.93 ± 0.05	3.25 ± 0.97	1.8	-3.4
BD+60499	O9.5V	134.64 1	1.97	10.27	10.85	10.31	9.11	9.01	8.93	0.86 ± 0.07	2.49 ± 0.04	2.88 ± 0.29	1.6	-3.65
BD+56525	B0.5V	134.65 -3.73	2.35	9.24	9.63	9.29	8.39	8.29	8.32	0.63 ± 0.07	1.84 ± 0.04	2.91 ± 0.36	2.5	-4.41
BD+56527	B2.0I	134.65 -3.73	2.32	8.43	8.82	8.48	7.6	7.54	7.46	0.6 ± 0.07	1.86 ± 0.04	3.09 ± 0.38	1.8	-5.21
HD14143	B2Ia	134.65 -3.69	2.27	6.71	7.16	6.7	5.53	5.37	5.31	0.69 ± 0.08	2.22 ± 0.05	3.22 ± 0.41	1	-7.3
HD14162	B0.5V	134.69 -3.71	2.35	9.26	9.61	8.46	8.59	8.52	8.54	1.24 ± 0.08	0.25 ± 0.04	0.2 ± 0.04	22.7	-3.64
HD13544	B0.5IV	134.99 -7.02	2.85	8.05	8.86	8.88	8.99	9.05	9.06	0.23 ± 0.07	0.58 ± 0.05	2.48 ± 0.93	1	-3.98
HD14357	B2.0I	135 -3.89	2.23	8.31	8.83	8.5	7.86	7.83	7.8	0.58 ± 0.07	1.44 ± 0.05	2.49 ± 0.35	1.3	-4.68
HD14476	B1.5I	135 -3.46	2.42	8.62	9.13	8.19	7.97	7.88	7.86	1.09 ± 0.07	0.84 ± 0.04	0.77 ± 0.08	11.1	-4.57
HD14443	BC2Ib	135.01 -3.59	2.26	7.85	8.39	7.69	7.31	7.24	7.23	0.88 ± 0.07	1.04 ± 0.04	1.18 ± 0.14	2.5	-5.12
BD+56574	B1III	135.04 -3.61	2.32	8.27	8.83	8.53	7.87	7.87	7.82	0.56 ± 0.07	1.5 ± 0.05	2.69 ± 0.4	2.3	-4.8
BD+56576	B1.5I	135.04 -3.61	2.43	9.14	9.68	9.4	8.75	8.76	8.71	0.56 ± 0.08	1.51 ± 0.05	2.7 ± 0.44	2.4	-4.04
BD+56578	B2IIIe	135.06 -3.59	2.45	9.02	9.57	9.19	8.48	8.44	8.33	0.63 ± 0.07	1.66 ± 0.05	2.63 ± 0.34	1.8	-4.42
HD14302	B1II-III	135.1 -4.42	2.42	8.27	8.81	8.64	8.01	8.01	7.97	0.45 ± 0.07	1.5 ± 0.04	3.31 ± 0.59	3.2	-4.78
HD14520	B1.5III	135.12 -3.61	2.29	8.92	9.47	9.23	8.54	8.5	8.5	0.53 ± 0.08	1.58 ± 0.04	2.99 ± 0.49	2.5	-4.15
HD14661	B1.5I	135.2 -3.3	2.15	9.31	9.63	9.18	7.94	7.83	7.81	0.76 ± 0.07	2.38 ± 0.05	3.12 ± 0.31	3.6	-4.87
HD12740	B1.5II	135.3 -11.91	2.98	7.04	7.9	7.94	8	8.04	8.09	0.2 ± 0.06	0.57 ± 0.04	2.83 ± 1.18	1	-5
HD15785	B1Iab	135.31 0.19	2.62	10.03	8.82	8.37	7.11	6.95	6.87	0.71 ± 0.08	2.48 ± 0.05	3.47 ± 0.43	1.7	-6.2
HD14331	B0III	135.31 -4.88	2.12	7.82	8.57	8.47	8.12	8.22	8.19	0.41 ± 0.07	1.2 ± 0.05	2.9 ± 0.58	4.8	-4.36
HD14956	B1.5Ia	135.42 -2.86	2.73	7.63	7.92	7.2	5.68	5.47	5.35	0.95 ± 0.08	2.72 ± 0.04	2.86 ± 0.27	0.4	-7.7
HD14818	B2Ia	135.62 -3.93	2.11	5.95	6.56	6.26	5.57	5.49	5.42	0.5 ± 0.08	1.57 ± 0.05	3.14 ± 0.56	0.8	-6.94
HD15325	B1IV	135.99 -3.1	2.44	8.46	8.95	8.63	7.66	7.56	7.5	0.61 ± 0.07	2.04 ± 0.05	3.37 ± 0.42	1.9	-5.35
HD15752	B0III	136.07 -1.82	2.39	10.36	9.17	8.77	7.65	7.57	7.46	0.68 ± 0.08	2.29 ± 0.05	3.38 ± 0.44	2.8	-5.41
HD15571	B1II	136.22 -2.81	6.23	10.17	8.83	8.43	7.2	7.06	7.01	0.7 ± 0.08	2.44 ± 0.05	3.52 ± 0.46	2.3	-7.99
HD15690	B2Iab	136.32 -2.66	2.1	10.05	8.54	8.02	6.59	6.45	6.38	0.78 ± 0.07	2.53 ± 0.05	3.23 ± 0.36	3	-6.13
HD16310	B1II:	136.42 -0.95	2.18	10.03	8.64	8.1	6.68	6.53	6.44	0.83 ± 0.07	2.66 ± 0.04	3.21 ± 0.33	2.3	-6.25
HD16243	B2II:	136.84 -2.13	2.62	8.55	8.69	8.25	6.86	6.7	6.6	0.67 ± 0.08	2.41 ± 0.05	3.59 ± 0.47	2.5	-6.25
HD15642	O9.5II-IIIn	137.09 -4.73	2.32	9.3	8.56	8.55	8.36	8.41	8.44	0.32 ± 0.08	1.04 ± 0.05	3.26 ± 0.91	2.5	-4.32
HD18409	O9.7Ib	137.12 3.46	2.44	9.83	8.72	8.4	7.36	7.28	7.24	0.62 ± 0.07	2.22 ± 0.04	3.57 ± 0.43	3.2	-5.76
HD16779	B2Ib	137.44 -1.85	2.45	9.33	9.59	8.85	7.27	7.12	6.97	1.01 ± 0.07	2.81 ± 0.04	2.79 ± 0.23	1.6	-5.9
HD15137	O9.5II-IIIn	137.46 -7.58	2.05	7	7.92	7.86	7.8	7.83	7.84	0.32 ± 0.08	0.86 ± 0.05	2.69 ± 0.76	0.7	-4.56
HD18352	B1V	137.73 2.16	0.81	8.03	6.99	6.84	6.36	6.45	6.38	0.45 ± 0.08	1.29 ± 0.05	2.85 ± 0.55	5.8	-3.98
HD16832	O9.2III	138 -2.88	2.32	10.29	9.21	8.87	8.01	7.95	7.95	0.66 ± 0.07	1.99 ± 0.04	2.99 ± 0.35	2.4	-4.95
HD18076	B0II-III	138.44 0.05	2.4	10.82	9.48	9.04	7.75	7.64	7.52	0.76 ± 0.08	2.43 ± 0.04	3.21 ± 0.36	4.1	-5.29
HD168571	B1Iab/b	14.07 -1.39	1.68	8.1	8.51	7.99	6.47	6.24	6.12	0.78 ± 0.08	2.89 ± 0.05	3.71 ± 0.42	1.1	-6.03
HD168552	B2/3Ib/II	14.26 -1.25	1.49	7.89	8.37	8.13	7.35	7.24	7.2	0.49 ± 0.08	1.75 ± 0.05	3.55 ± 0.66	0.9	-4.49
HD171012	B0.5Ia	14.52 -4.38	1.8	6.9	7.49	6.99	5.82	5.7	5.58	0.75 ± 0.08	2.22 ± 0.05	2.95 ± 0.34	1.7	-6.51
HD166539	B1/2Ib	14.58 1.45	1.62	8.33	8.99	8.8	8.21	8.19	8.14	0.51 ± 0.07	1.68 ± 0.05	3.3 ± 0.54	1.9	-3.93

Table 5.2: Complete information relative to each star for the B-Sgs sample: SpT and galactic coordinates (l and b); distances in kpc (d); photometry values (U Mag, B Mag, V Mag, J Mag, H Mag, K Mag); extinction parameters with corresponding uncertainty ($E(B-V)$, A_V, R_V and χ^2) and absolute magnitude taking into account interstellar extinction: M_V.

ID	SpT	l [º] b	d [kpc]	U Mag	B Mag	V Mag	J Mag	H Mag	K Mag	$E(B-V)$	A_V [mag]	R_V	χ^2	M_V [mag]
HD171432	B0.5Ib	14.62 -4.98	1.51	6.59	7.3	7.12	6.54	6.53	6.46	0.45 ± 0.08	1.55 ± 0.05	3.46 ± 0.66	2.1	-5.33
BD-175190	B1Ia	14.86 -2.23	1.87	9.93	10.01	9.28	7.25	7.02	6.79	1.02 ± 0.08	3.61 ± 0.04	3.53 ± 0.3	3.2	-5.69
HD168987	B1Ia/ab	14.99 -1.44	1.83	8.73	8.99	8.13	5.85	5.53	5.35	1.12 ± 0.08	3.84 ± 0.04	3.43 ± 0.25	1.8	-7.02
HD20508	B1.5IV	140.6 2.39	1.06	9.99	8.75	8.41	7.37	7.3	7.23	0.64 ± 0.07	2.09 ± 0.04	3.26 ± 0.4	3.2	-3.81
HD25090	B0.5III	143.19 7.34	3.59	7.01	7.64	7.34	6.66	6.65	6.63	0.6 ± 0.07	1.61 ± 0.05	2.66 ± 0.35	2.3	-7.04
HD25639	B0III	143.68 7.66	1.15	6.87	7.24	6.86	6.05	5.95	5.93	0.66 ± 0.07	1.88 ± 0.05	2.87 ± 0.35	0.6	-5.32
HD25443	B0.5III	143.68 7.35	1.13	6.45	7	6.77	6.11	6.14	6.11	0.55 ± 0.07	1.6 ± 0.04	2.88 ± 0.42	4	-5.1
HD30614	O9Ia	144.07 14.04	1.72	3.47	4.34	4.29	4.2	4.38	4.24	0.28 ± 0.07	0.71 ± 0.04	2.56 ± 0.83	7.4	-7.59
HD22253	B0.5III	144.28 0.92	0.68	7.81	6.76	6.53	5.84	5.82	5.79	0.51 ± 0.08	1.59 ± 0.05	3.13 ± 0.54	2.6	-4.23
HD237211	O9.5Iab	147.14 2.97	3.84	10.58	9.41	9.05	7.95	7.83	7.77	0.67 ± 0.08	2.38 ± 0.05	3.57 ± 0.48	2	-6.25
HD23675	B0.5III	148.1 -1.29	1.04	8.27	7.12	6.82	5.87	5.79	5.78	0.61 ± 0.08	2.08 ± 0.04	3.42 ± 0.51	3	-5.34
HD23800	B1IV	148.33 -1.33	0.65	8.4	7.2	6.98	6.17	6.12	6	0.49 ± 0.07	1.9 ± 0.05	3.84 ± 0.61	2.6	-3.99
HD166803	B1/2Ib	15.06 1.38	1.44	7.54	8.29	8.18	7.82	7.87	7.77	0.4 ± 0.07	1.31 ± 0.05	3.25 ± 0.65	3.4	-3.92
HD165319	O9.7Ib	15.12 3.33	1.39	8.15	8.63	8.04	6.53	6.36	6.27	0.86 ± 0.08	2.78 ± 0.04	3.22 ± 0.31	1.9	-5.46
HD167838	B3Ia/ab	15.39 0.27	1.67	6.83	7.19	6.73	5.58	5.43	5.28	0.62 ± 0.07	2.09 ± 0.04	3.35 ± 0.44	1.5	-6.47
HD170604	B1Ib	15.88 -3.1	1.75	7.95	9.52	9.16	8.11	8.15	8.13	0.72 ± 0.08	2.05 ± 0.05	2.84 ± 0.34	9.6	-4.1
HD167543	B1Ib/II	15.92 0.94	1.5	8.46	8.87	8.56	7.51	7.44	7.32	0.61 ± 0.07	2.23 ± 0.05	3.63 ± 0.47	3.2	-4.55
HD24432	B3II	151.12 -3.5	1.09	8.99	7.34	6.86	5.58	5.47	5.38	0.7 ± 0.08	2.09 ± 0.05	2.96 ± 0.38	3	-5.43
HD28446B	B1IV:	151.91 3.95	0.87	5.2	6.9	6.8	6.61	6.68	6.68	0.41 ± 0.07	1 ± 0.05	2.48 ± 0.54	2.2	-3.91
HD27795	B1V	156.81 -2.17	0.72	7.15	7.64	7.42	6.8	6.8	6.78	0.5 ± 0.07	1.45 ± 0.05	2.91 ± 0.5	2.8	-3.32
HD169673	B1Ib	16.21 -1.68	1.59	6.66	9.03	8.85	7.19	7.2	7.2	0.64 ± 0.08	2.94 ± 0.05	4.62 ± 0.65	32.1	-5.09
HD168183	O9.5III+B3-5V/III	16.81 0.67	1.92	7.92	8.55	8.28	7.54	7.45	7.39	0.56 ± 0.08	1.92 ± 0.05	3.41 ± 0.53	0.9	-5.06
HD167451	B1Ib	16.83 1.52	1.71	8.75	9.02	8.23	6.49	6.24	6.09	1.06 ± 0.08	3.23 ± 0.04	3.04 ± 0.24	0.4	-6.17
HD170938	B1Ia	16.84 -3.05	2.07	8.58	8.84	7.99	5.82	5.51	5.36	1.13 ± 0.08	3.72 ± 0.05	3.31 ± 0.26	1.8	-7.31
HD168917	B0/0.5II/III	16.91 -0.31	1.54	8.29	9.77	8.87	7.54	7.46	7.41	1.23 ± 0.08	2.49 ± 0.04	2.03 ± 0.15	0.9	-4.56
BD-145037	B1.5Ia	16.93 -0.95	1.88	9.87	9.72	8.41	4.97	4.5	4.17	1.54 ± 0.07	5.33 ± 0.04	3.45 ± 0.18	2.8	-8.29
BD-134930	O9.7IIIp	16.94 0.77	1.59	9.04	9.71	9.45	8.79	8.77	8.76	0.58 ± 0.08	1.73 ± 0.04	2.97 ± 0.44	2	-3.29
HD24398	B1Ib	162.29 -16.69	0.26	2.19	2.97	2.85	2.6	2.62	2.6	0.37 ± 0.07	1 ± 0.05	2.68 ± 0.59	1.2	-5.26
HD31327	B2.5Ib	168.14 -4.4	0.91	6.03	6.43	6.09	5.21	5.17	5.1	0.6 ± 0.08	1.78 ± 0.05	2.96 ± 0.42	2.8	-5.48
HD169454	B1Ia	17.54 -0.67	1.94	7.39	7.61	6.71	4.45	4.09	3.89	1.1 ± 0.07	3.64 ± 0.04	3.3 ± 0.23	0.7	-8.37
HD167330	O9.5/B0Ia/ab	17.66 2.16	1.64	8.44	8.89	8.23	6.71	6.56	6.41	0.94 ± 0.08	2.89 ± 0.04	3.06 ± 0.28	1.6	-5.73
HD169034	B2Ia	17.66 -0.07	1.69	9.57	9.42	8.24	5.15	4.77	4.42	1.37 ± 0.08	4.72 ± 0.04	3.45 ± 0.22	3.8	-7.62
HD167311	B0Ib	17.69 2.18	1.69	9.43	9.56	8.61	6.43	6.15	5.99	1.24 ± 0.08	3.76 ± 0.04	3.02 ± 0.22	1.2	-6.28
BD-124970	B0.5Ia	17.99 1.63	1.98	9.69	9.8	8.78	6.39	6.13	5.89	1.29 ± 0.08	4.02 ± 0.05	3.11 ± 0.21	2.3	-6.73
HD34078	O9.5V	172.08 -2.26	0.38	5.48	6.18	5.96	5.34	5.36	5.29	0.54 ± 0.08	1.69 ± 0.05	3.12 ± 0.51	2.8	-3.64
HD36483	O9.5IV(n)	172.29 1.88	1.63	8.06	8.55	8.24	7.25	7.15	7.13	0.64 ± 0.08	2.23 ± 0.05	3.46 ± 0.46	2.9	-5.05
HD36212	B3II	173.4 0.69	2.11	7.61	7.98	7.81	7.14	7.14	7.05	0.42 ± 0.07	1.46 ± 0.05	3.5 ± 0.68	3.4	-5.27
HD37737	O9.5II-III(n)	173.46 3.24	1.41	8.02	8.3	8.06	7.32	7.32	7.25	0.56 ± 0.07	1.81 ± 0.05	3.24 ± 0.43	3.3	-4.49
HD35653	B0.5V	173.73 -0.51	2.03	6.81	7.56	7.49	7.15	7.2	7.12	0.33 ± 0.07	1.17 ± 0.05	3.56 ± 0.93	3.4	-5.21
HD37032	B0.5V	174.06 1.58	2.38	7.42	8.18	8.15	7.9	7.91	7.94	0.35 ± 0.07	1.18 ± 0.04	3.34 ± 0.74	1.8	-4.91
HD38131	B0.5V	174.62 3.15	1.64	7.71	8.35	8.2	7.74	7.77	7.74	0.45 ± 0.07	1.35 ± 0.05	2.98 ± 0.56	2.6	-4.22
HD36371	B4Iab	175.77 -0.61	1.19	4.68	5.15	4.79	4.25	4.08	4	0.45 ± 0.08	1.24 ± 0.04	2.76 ± 0.53	1.7	-6.82
HD172510	B2Ib	18.62 -4.45	1.54	8.45	9	8.72	8.14	8.16	8.1	0.54 ± 0.08	1.36 ± 0.05	2.51 ± 0.42	2.4	-3.58
HD169227	B1.5Ia	18.96 0.38	2.01	9.86	10.06	8.84	5.77	5.38	5.08	1.51 ± 0.08	4.97 ± 0.04	3.29 ± 0.18	2.5	-7.65
HD39746	B1II	182.18 1.27	1.49	6.58	7.26	7.04	6.48	6.47	6.41	0.47 ± 0.07	1.43 ± 0.05	3 ± 0.54	2	-5.26
HD41398	B2Ib	182.26 3.87	3.65	7.13	7.75	7.49	6.68	6.61	6.53	0.49 ± 0.08	1.76 ± 0.05	3.58 ± 0.66	1.7	-7.08
HD93521	O9.5IIInn	183.14 62.15	1.25	5.67	6.79	7.03	7.5	7.65	7.7	0.04 ± 0.04	0.11 ± 0.04	2.77 ± 2.62	1.9	-3.56
HD40111	B0/1II/III	183.97 0.84	1.42	3.82	4.76	4.82	4.96	5.04	5.03	0.17 ± 0.07	0.56 ± 0.05	3.25 ± 1.69	1.4	-6.5
HD250289	B2III:e	186.58 0.15	2.03	7.74	8.71	8.23	6.92	6.77	6.61	0.72 ± 0.07	2.47 ± 0.04	3.42 ± 0.35	1.9	-5.78
HD250290	B3Ib	186.62 0.14	1.89	7.74	7.9	7.41	5.85	5.67	5.55	0.71 ± 0.08	2.56 ± 0.04	3.62 ± 0.43	3.1	-6.53
HD251847	B1IV	186.96 1.64	1.39	8.25	9.02	9.01	8.73	8.77	8.72	0.29 ± 0.1	1.2 ± 0.06	4.03 ± 1.57	2.7	-2.91

Table 5.2: Complete information relative to each star for the B-Sgs sample: SpT and galactic coordinates (l and b); distances in kpc (d); photometry values (U Mag, B Mag, V Mag, J Mag, H Mag, K Mag); extinction parameters with corresponding uncertainty ($E(B-V)$, A_V, R_V and χ^2) and absolute magnitude taking into account interstellar extinction: M_V.

ID	**SpT**	**l [º] b**	**d [kpc]**	**U Mag**	**B Mag**	**V Mag**	**J Mag**	**H Mag**	**K Mag**	$E(B-V)$	A_V **[mag]**	R_V	χ^2	M_V **[mag]**
HD44674	B1Vne	187.26 5.74	1.4	7.69	8.54	8.46	8.04	7.92	7.75	0.28 ± 0.07	1.57 ± 0.05	5.64 ± 1.48	3	-3.84
HD42087	B3Ia	187.75 1.77	2.31	5.33	5.96	5.75	5.39	5.21	5.23	0.37 ± 0.07	1.21 ± 0.05	3.23 ± 0.72	0.7	-7.28
HD43384	B3Iab	187.99 3.53	1.75	6.31	6.7	6.25	5.19	5.09	4.97	0.62 ± 0.07	1.87 ± 0.05	3.01 ± 0.41	1.9	-6.83
HD43818	B0II	188.49 3.87	1.99	6.52	7.21	6.92	6.15	6.04	6.01	0.54 ± 0.07	1.8 ± 0.05	3.35 ± 0.54	0.6	-6.37
HD41690	B1V	188.6 0.75	1.6	7.31	7.93	7.71	7.2	7.23	7.2	0.5 ± 0.07	1.32 ± 0.05	2.63 ± 0.45	2.3	-4.62
HD255134	B1IVp	188.73 3.9	1.65	9.01	9.46	9.18	8.24	8.21	8.14	0.6 ± 0.08	2.04 ± 0.05	3.38 ± 0.49	4	-3.95
HD43703	B1IVp(e)	188.82 3.52	1.77	8.51	8.98	8.65	7.57	7.47	7.36	0.62 ± 0.08	2.29 ± 0.05	3.71 ± 0.52	2.5	-4.88
HD43753	B0.5III	188.87 3.59	1.87	7.58	8.14	7.89	7.08	7.05	6.96	0.54 ± 0.07	1.86 ± 0.04	3.48 ± 0.5	3.1	-5.34
HD42379	B1II	189.28 1.34	1.64	7.21	7.68	7.43	6.68	6.7	6.6	0.55 ± 0.08	1.71 ± 0.04	3.13 ± 0.48	4.2	-5.36
HD41117	B2Ia	189.69 -0.86	1.33	4.24	4.91	4.63	4.04	4.04	3.84	0.45 ± 0.08	1.39 ± 0.04	3.07 ± 0.6	5	-7.37
HD30677	B1II-III((n))	190.18 -22.22	1.53	5.94	6.82	6.84	6.87	6.93	6.94	0.19 ± 0.07	0.57 ± 0.05	3.03 ± 1.44	1.2	-4.65
HD43837	B2Ibp?	191.04 2.51	4.1	8.82	8.99	8.49	7.11	6.91	6.79	0.74 ± 0.08	2.65 ± 0.05	3.57 ± 0.42	0.8	-7.23
ALS47	O9.5V	192.32 3.36	2.27	9.97	10.65	10.5	10.04	10.01	9.98	0.42 ± 0.07	1.48 ± 0.04	3.48 ± 0.62	1.2	-2.76
HD30836	B2III	192.89 -23.52	0.26	2.7	3.5	3.68	4.03	4.09	4.13	0.05 ± 0.04	0.15 ± 0.04	2.99 ± 2.5	0.6	-3.57
HD36822	B0III	195.4 -12.29	0.39	3.29	4.26	4.41	4.81	4.85	4.86	0.09 ± 0.06	0.35 ± 0.05	3.74 ± 2.51	0.8	-3.91
HD44965	B3II	199.56 -0.41	1.7	7.81	8.24	7.95	7.14	7.13	7.03	0.54 ± 0.07	1.6 ± 0.04	2.98 ± 0.46	3.3	-4.8
HD163613	B1I/II	2.09 -1.96	1.99	8.31	8.88	8.59	7.71	7.69	7.6	0.58 ± 0.08	1.91 ± 0.04	3.33 ± 0.48	3.5	-4.82
HD169754	B0.5Ia	20.02 0.24	1.67	9.61	9.64	8.6	6.11	5.81	5.65	1.35 ± 0.08	4.1 ± 0.05	3.03 ± 0.2	3.7	-6.61
HD36486	O9.5IINwk	203.86 -17.74	0.21	0.96	2.02	2.41	2.72	2.84	2.88	0.05 ± 0.01	0.38 ± 0.04	6.72 ± 2.01	5.2	-4.6
HD37128	B0Ia	205.21 -17.24	0.61	0.48	1.51	1.69	2.07	2.07	2.16	0.06 ± 0.04	0.23 ± 0.04	3.9 ± 2.54	0.1	-7.45
HD47417	B0IV	205.35 0.35	1.34	6.12	6.91	6.95	6.92	6.96	7	0.25 ± 0.08	0.86 ± 0.05	3.47 ± 1.22	1.3	-4.54
HD46202	O9.2V	206.31 -2	1.47	7.6	8.33	8.27	7.78	7.78	7.72	0.39 ± 0.07	1.58 ± 0.05	4.05 ± 0.79	2.4	-4.15
HD46484	B2Ib	206.78 -1.76	1.36	7.49	8.1	7.74	7	6.95	6.87	0.65 ± 0.07	1.82 ± 0.05	2.79 ± 0.36	1.4	-4.75
HD37479	B2IV-Vp_He	206.82 -17.32	0.43	5.66	6.38	6.46	6.97	6.95	6.95	0.02 ± 0.02	0.02 ± 0.01	1.45 ± 2.17	3.1	-1.71
HD47240	B1Ib	206.98 -0.75	4.1	5.65	6.35	6.2	5.8	5.76	5.69	0.34 ± 0.08	1.23 ± 0.05	3.61 ± 1.02	1	-8.1
HD47382	B6Ib	207.35 -0.77	0.93	6.55	7.31	7.14	6.75	6.69	6.71	0.44 ± 0.07	1.37 ± 0.05	3.12 ± 0.58	0.4	-4.07
HD48434	B0II	208.54 0.06	1.33	4.99	5.88	5.9	5.94	6.01	5.98	0.23 ± 0.07	0.74 ± 0.05	3.19 ± 1.19	1.6	-5.46
HD46847	A9V	208.72 -2.25	0.87	9.26	9.56	8.97	7.42	7.29	7.1	0.91 ± 0.07	3.03 ± 0.04	3.32 ± 0.3	3.1	-3.76
HD47432	O9.7Ib	210.03 -2.11	1.6	5.67	6.44	6.31	5.93	5.95	5.87	0.36 ± 0.07	1.27 ± 0.05	3.52 ± 0.78	2.2	-5.98
HD48691	B5/7Ib	211.63 -1.25	1.62	7.08	7.88	7.87	7.67	7.73	7.73	0.31 ± 0.07	1.03 ± 0.05	3.3 ± 0.93	2.5	-4.21
BD+001617A	O9	212.29 -0.41	4.26	11.28	11.83	11.31	10.1	9.96	9.87	0.84 ± 0.08	2.54 ± 0.05	3.04 ± 0.32	1	-4.38
BD+001617C	O9	212.31 -0.4	8.24	11.12	11.24	10.82	9.94	9.8	9.71	0.7 ± 0.08	2.14 ± 0.05	3.06 ± 0.36	0.5	-5.9
HD42259	B1/2Ib	212.7 -11.62	1.58	8.29	8.87	8.49	7.8	7.75	7.67	0.63 ± 0.07	1.59 ± 0.05	2.55 ± 0.35	1.1	-4.1
HD38771	B0.5Ia	214.51 -18.5	0.2	0.87	1.88	2.06	2.47	2.69	2.6	0.06 ± 0.06	0.13 ± 0.04	2.54 ± 2.75	5.8	-4.56
HD66665	B1V	215.77 19.12	1.69	6.5	7.58	7.81	8.38	8.58	8.61	0.01 ± 0.01	0.01 ± 0.01	2.11 ± 2.53	4.2	-3.34
HD52266	O9.5IIIn	219.13 -0.68	1.35	6.32	7.22	7.23	7.2	7.24	7.26	0.27 ± 0.07	0.85 ± 0.04	3.19 ± 0.89	1	-4.26
HD52382	B0.5Ia	222.17 -2.15	2.33	6.07	6.76	6.57	6.04	5.99	5.88	0.41 ± 0.08	1.46 ± 0.05	3.57 ± 0.76	1.4	-6.73
HD53667	B0/1Ib	222.31 -0.86	2.46	7.28	7.99	7.75	7.13	7.1	6.92	0.47 ± 0.08	1.68 ± 0.04	3.55 ± 0.66	3.6	-5.88
HD53754	B0/1Ib	222.41 -0.84	2.51	7.73	8.36	8.21	7.66	7.62	7.59	0.41 ± 0.07	1.47 ± 0.05	3.55 ± 0.71	1.6	-5.25
HD59882	B2Ib/II	222.55 6.36	1.98	7.73	8.64	8.82	9.15	9.24	9.29	0.09 ± 0.06	0.3 ± 0.04	3.21 ± 2.25	1.1	-2.96
HD48038	B2III	222.66 -7.82	1.1	6.26	6.96	6.92	6.69	6.66	6.69	0.28 ± 0.08	0.93 ± 0.04	3.35 ± 1.05	0.8	-4.21
HD53367	B0IV/Ve	223.71 -1.9	1.6	6.81	7.4	6.96	6.33	6.22	6.12	0.68 ± 0.08	1.72 ± 0.05	2.53 ± 0.35	1.3	-5.78
HD53974	B0IIIn	224.71 -1.79	0.93	4.59	5.44	5.39	5.29	5.31	5.3	0.3 ± 0.08	0.87 ± 0.05	2.94 ± 0.94	0.9	-5.33
HD55879	O9.7III	224.73 0.35	0.93	4.88	5.85	6.03	6.36	6.45	6.5	0.1 ± 0.05	0.39 ± 0.04	3.83 ± 2.34	1.2	-4.21
HD44743	B1II-III	226.06 -14.27	0.15	0.77	1.73	1.97	2.53	2.62	2.65	0.01 ± 0.01	0.02 ± 0.01	2.36 ± 2.61	0.7	-3.95
HD51309	B3Ib	228.7 -6.68	1.14	3.62	4.3	4.38	4.7	4.62	4.54	0.05 ± 0.03	0.23 ± 0.04	4.85 ± 2.65	4.9	-6.12
HD54911	B1III	229 -3.06	1.11	6.45	7.27	7.34	7.46	7.57	7.57	0.17 ± 0.07	0.47 ± 0.05	2.73 ± 1.35	2.1	-3.36
HD54764	B1Ib/II	229.42 -3.44	1.39	5.32	6.12	6.08	5.89	5.95	5.91	0.29 ± 0.07	0.88 ± 0.05	3.09 ± 0.9	2.3	-5.52
HD161961	B0/1Ib	23.64 12.9	1.67	7.45	8.12	7.89	7.32	7.33	7.33	0.53 ± 0.07	1.48 ± 0.04	2.79 ± 0.42	2.7	-4.7
HD173010	O9.7Ia	23.73 -2.49	4.18	9.64	9.87	9.21	7.38	7.18	7.03	0.95 ± 0.08	3.07 ± 0.04	3.22 ± 0.29	4.3	-6.97
HD172488	B0Iab/b	23.96 -1.62	1.06	7.76	8.16	7.62	6.5	6.4	6.34	0.81 ± 0.08	2.16 ± 0.04	2.67 ± 0.29	1.3	-4.67

Table 5.2: Complete information relative to each star for the B-Sgs sample: SpT and galactic coordinates (l and b); distances in kpc (d); photometry values (U Mag, B Mag, V Mag, J Mag, H Mag, K Mag); extinction parameters with corresponding uncertainty ($E(B-V)$, A_V, R_V and χ^2) and absolute magnitude taking into account interstellar extinction: M_V.

ID	**SpT**	**l [º] b**	**d [kpc]**	**U Mag**	**B Mag**	**V Mag**	**J Mag**	**H Mag**	**K Mag**	$E(B-V)$	A_V **[mag]**	R_V	χ^2	M_V **[mag]**
HD60325	B2II	230.45 2.52	1.11	5.46	6.17	6.21	6.23	6.25	6.27	0.18 ± 0.07	0.57 ± 0.05	3.26 ± 1.52	0.7	-4.58
HD50707	B1Ib	231.3 -8.62	0.37	3.66	4.62	4.83	5.3	5.4	5.46	0.04 ± 0.04	0.08 ± 0.04	2.31 ± 2.31	0.6	-3.1
LS516	OB+	231.4 1.94	4.28	10.47	11.15	10.8	10.11	10.01	9.97	0.61 ± 0.07	1.79 ± 0.04	2.91 ± 0.39	0.3	-4.15
HD60308	B2Ia	231.41 1.95	4.23	8.09	8.59	8.21	7.14	7.03	6.9	0.58 ± 0.07	2.07 ± 0.05	3.55 ± 0.51	1.6	-6.99
HD51283	B2/3III	234.01 -9.33	0.67	4.36	5.12	5.3	5.63	5.65	5.68	0.05 ± 0.03	0.18 ± 0.04	3.86 ± 2.52	0.3	-4.01
HD91316	B1Iab	234.89 52.77	0.63	2.78	3.72	3.87	4.19	4.22	4.28	0.08 ± 0.04	0.27 ± 0.04	3.59 ± 2.37	0.2	-5.38
HD58510	B1Ia	235.52 -2.47	2.35	6.15	9.1	8.84	6.48	6.49	6.45	0.75 ± 0.07	3.78 ± 0.04	5.07 ± 0.53	56.9	-6.8
HD53138	B3Ia	235.55 -8.23	1.45	2.14	2.94	3.02	3.21	3.24	3.25	0.06 ± 0.04	0.2 ± 0.04	3.25 ± 2.49	0.6	-7.99
HD52089	B1.5II	239.83 -11.33	0.12	0.36	1.29	1.5	1.97	2.16	2.15	0.02 ± 0.02	0.02 ± 0.03	2.01 ± 2.36	3.4	-3.99
HD64993	B1Ib/II	241.5 2.22	3.3	6.87	7.67	7.68	7.62	7.66	7.64	0.24 ± 0.06	0.8 ± 0.04	3.39 ± 1.04	1.2	-5.71
HD60479	O9.5Ib	242.43 -4.03	2.85	8.08	8.74	8.41	7.7	7.66	7.56	0.59 ± 0.08	1.8 ± 0.05	3.04 ± 0.45	1.6	-5.66
HD58350	B5Ia	242.62 -6.49	0.61	1.65	2.37	2.45	2.57	2.56	2.61	0.07 ± 0.06	0.17 ± 0.04	2.71 ± 2.43	0.3	-6.65
HD60369	B7Ib	242.68 -4.3	2.56	7.28	8.87	9.01	8.09	8.19	8.18	0.29 ± 0.06	2.07 ± 0.04	7.05 ± 1.42	24.2	-5.1
HD62844	B2Ia	247.32 -4.03	2.67	8.45	9.06	9.05	6.47	6.27	6.09	0.46 ± 0.04	4.29 ± 0.04	9.08 ± 0.64	39.1	-7.37
HD59864	B1/2Ib/II	247.53 -7.49	1.51	6.7	7.55	7.62	7.83	7.89	7.92	0.17 ± 0.07	0.44 ± 0.05	2.57 ± 1.45	0.6	-3.72
HD71771	B2II	248.47 6.45	1.33	6.59	7.37	7.5	7.77	7.87	7.85	0.09 ± 0.04	0.28 ± 0.04	3.06 ± 2.04	1.6	-3.39
CD-324967	B2.5Iab	250.65 0.76	4.69	8.46	9.88	9.3	7.51	7.36	7.27	0.84 ± 0.08	2.88 ± 0.04	3.4 ± 0.33	7.5	-6.93
HD68450	O9.7II	254.47 -2.02	1.31	5.58	6.42	6.44	6.43	6.44	6.47	0.24 ± 0.07	0.85 ± 0.05	3.53 ± 1.23	0.5	-5
HD74575	B1.5III	254.99 5.77	0.24	2.65	3.5	3.68	4.11	4.17	4.25	0.05 ± 0.04	0.12 ± 0.04	2.5 ± 2.34	0.3	-3.38
HD75222	O9.7Iab	258.29 4.18	2.02	7.24	7.8	7.42	6.53	6.49	6.4	0.64 ± 0.07	1.92 ± 0.05	2.98 ± 0.37	2.5	-6.02
HD173987	B0.5Ia	26.85 -2.31	3.33	8.64	9.14	8.89	8.26	8.28	8.18	0.52 ± 0.08	1.55 ± 0.05	3 ± 0.51	3.2	-5.27
HD63922	B0III	260.18 -10.19	0.3	2.92	3.93	4.11	4.57	4.69	4.67	0.08 ± 0.04	0.22 ± 0.04	2.75 ± 1.92	1.9	-3.53
HD71304	O9II	261.76 -3.77	2.1	8.52	8.98	8.45	7.13	7.02	6.93	0.84 ± 0.08	2.61 ± 0.04	3.12 ± 0.31	2.2	-5.77
HD64760	B0.5Ib	262.06 -10.42	0.68	3.11	4.1	4.24	4.56	4.61	4.67	0.09 ± 0.04	0.28 ± 0.04	3.28 ± 2.2	0.4	-5.21
HD76341	O9.2IV	263.53 1.52	1.14	6.88	7.39	7.16	6.44	6.41	6.32	0.49 ± 0.07	1.74 ± 0.04	3.54 ± 0.56	2.4	-4.86
HD22586	B1/2III	264.19 -50.36	2.27	6.93	7.85	8.03	8.42	8.64	8.56	0.04 ± 0.04	0.06 ± 0.03	2.01 ± 2.38	5.8	-3.81
HD75149	B5Iab	265.33 -1.69	1.47	5.25	5.68	5.46	4.83	4.68	4.59	0.37 ± 0.07	1.49 ± 0.04	4.02 ± 0.89	0.6	-6.86
HD79186	B5Ia	267.36 2.25	1.81	4.65	5.22	5	4.46	4.37	4.27	0.35 ± 0.08	1.22 ± 0.04	3.5 ± 0.85	1.1	-7.51
HD76968	O9.2Ib	270.22 -3.37	2.2	6.53	7.33	7.21	6.75	6.76	6.66	0.38 ± 0.07	1.44 ± 0.05	3.81 ± 0.8	2.4	-5.94
HD70839	B2III	272.87 -11.91	0.64	5.06	5.85	5.95	6.09	6.18	6.19	0.15 ± 0.07	0.45 ± 0.05	3.1 ± 1.97	2	-3.53
HD89137	ON9.7II(n)	279.69 4.45	2.44	7.02	7.93	7.97	8.07	8.13	8.12	0.18 ± 0.08	0.66 ± 0.05	3.75 ± 2.21	1.2	-4.63
HD173438	B0/1Iab	28.16 -0.77	3.07	8.66	8.97	8.2	6.56	6.38	6.23	1.04 ± 0.08	3 ± 0.04	2.9 ± 0.23	1.2	-7.23
HD89767	B0.5/1Iab	281.02 3.72	2.81	6.63	8.82	7.21	6.82	6.78	6.73	1.74 ± 0.08	0.83 ± 0.05	0.48 ± 0.04	22.9	-5.86
HD90087	O9.2III(n)	285.16 -2.13	2.19	6.91	9.49	8.92	7.72	7.74	7.76	0.93 ± 0.08	2.21 ± 0.05	2.37 ± 0.22	8.6	-5
HD91943	B0.7Ib	285.82 0.1	2.37	5.91	6.74	6.7	6.51	6.5	6.49	0.26 ± 0.08	0.98 ± 0.05	3.73 ± 1.33	0.8	-6.16
CD-573344	OB	285.83 0.08	2.41	7.93	8.75	8.73	8.75	8.75	8.81	0.26 ± 0.07	0.69 ± 0.05	2.61 ± 0.89	0.3	-3.87
CPD-573507	B1	285.84 0.09	2.22	8.35	9.23	9.28	9.36	9.39	9.46	0.18 ± 0.07	0.58 ± 0.04	3.2 ± 1.48	0.8	-3.03
HD91969	B0I+	285.85 0.08	2.31	5.57	6.41	6.43	6.43	6.5	6.42	0.2 ± 0.07	0.72 ± 0.05	3.66 ± 1.46	2.5	-6.11
CD-573348B	B2.5V	285.85 0.06	2.29	8.36	9.37	9.23	9.17	9.14	9.21	0.4 ± 0.08	0.81 ± 0.05	2.05 ± 0.49	0.1	-3.38
CPD-573517	B1V	285.87 0.06	2.4	8.44	9.26	9.22	9.1	9.16	9.14	0.3 ± 0.07	0.82 ± 0.05	2.76 ± 0.8	1.9	-3.51
HD92007	B1III	285.89 0.07	2.27	8.26	9	8.92	8.8	8.82	8.83	0.34 ± 0.08	0.84 ± 0.05	2.49 ± 0.79	0.8	-3.7
HD92850	B0Ia	285.98 1.54	2.92	7.26	8.98	8.96	7.89	7.93	7.92	0.41 ± 0.08	2.22 ± 0.04	5.33 ± 1.02	18.3	-5.59
HD92712	B2/3II/III	285.99 1.26	3.15	7.11	7.95	7.93	7.82	7.89	7.88	0.29 ± 0.07	0.88 ± 0.04	2.99 ± 0.85	2.2	-5.44
HD91651	ON9.5IIIn	286.55 -1.72	1.85	7.96	9.64	9.52	8.76	8.81	8.81	0.48 ± 0.08	1.8 ± 0.05	3.73 ± 0.67	9	-3.61
HD92964	B2.5Ia	287.11 -0.36	2.1	5.12	5.78	5.51	4.71	4.62	4.51	0.45 ± 0.07	1.66 ± 0.05	3.67 ± 0.68	1.5	-7.76
HD93027	O9.5IV	287.61 -1.13	2.92	7.86	8.72	8.72	8.67	8.72	8.67	0.29 ± 0.08	0.98 ± 0.05	3.41 ± 1.21	1.6	-4.59
HD305523	O9II-III	287.66 -0.9	2.41	7.82	8.64	8.5	7.78	7.69	7.63	0.44 ± 0.07	1.94 ± 0.05	4.38 ± 0.8	1.2	-5.35
HD305619	O9.7II	288.22 -0.96	2.45	9.28	9.86	9.44	7.96	7.77	7.62	0.7 ± 0.08	2.97 ± 0.05	4.21 ± 0.49	1.8	-5.48
HD91452	B0III	288.32 -5.1	2.69	7	8.83	8.6	6.98	6.91	6.93	0.62 ± 0.07	2.89 ± 0.05	4.68 ± 0.56	22.8	-6.44
HD94493	B0.5Iab/b	289.01 -1.18	2.15	6.43	7.75	7.59	7.18	7.25	7.21	0.43 ± 0.07	1.21 ± 0.05	2.78 ± 0.55	3.2	-5.28
HD95880	B3Ib/II	289.63 0.29	2.27	6.87	7.29	6.95	6.13	5.98	5.9	0.49 ± 0.07	1.58 ± 0.04	3.21 ± 0.51	0.3	-6.41

Table 5.2: Complete information relative to each star for the B-Sgs sample: SpT and galactic coordinates (l and b); distances in kpc (d); photometry values (U Mag, B Mag, V Mag, J Mag, H Mag, K Mag); extinction parameters with corresponding uncertainty ($E(B-V)$, A_V, R_V and χ^2) and absolute magnitude taking into account interstellar extinction: M_V.

ID	SpT	l [º] b	d [kpc]	U Mag	B Mag	V Mag	J Mag	H Mag	K Mag	$E(B-V)$	A_V [mag]	R_V	χ^2	M_V [mag]
HD96248	B1Iab	289.93 0.3	2.45	5.97	6.73	6.57	6.07	6.01	5.92	0.37 ± 0.07	1.38 ± 0.05	3.77 ± 0.78	1	-6.76
HD165174	O9.7IIn	29.27 11.29	0.98	5.23	6.08	6.15	6.15	6.22	6.24	0.21 ± 0.07	0.76 ± 0.04	3.61 ± 1.35	2	-4.57
HD96622	O9.2IV	290.09 0.57	2.16	8.37	9.05	8.87	8.48	8.53	8.5	0.49 ± 0.07	1.34 ± 0.05	2.73 ± 0.48	2.4	-4.14
HD97400	B1	290.92 0.08	2.55	7.32	7.92	7.79	7.5	7.51	7.47	0.35 ± 0.07	0.91 ± 0.04	2.64 ± 0.66	1.4	-5.15
HD306097	B2	291.06 -0.38	2.48	9.27	9.58	8.91	7.42	7.25	7.14	0.97 ± 0.08	2.89 ± 0.04	2.96 ± 0.26	1	-5.95
HD99146	OBe	291.96 1.69	6.1	7.71	9.06	8.94	7.4	7.31	7.03	0.46 ± 0.07	3.08 ± 0.04	6.72 ± 1.06	11	-8.07
HD97522	B0.5II	292.78 -4.32	2.29	7.46	8.05	7.76	7.06	7.01	6.96	0.54 ± 0.08	1.64 ± 0.05	3.01 ± 0.46	1.3	-5.68
HD99953	B2Ia	293.93 -2.13	2.45	6.28	6.88	6.57	5.61	5.47	5.41	0.53 ± 0.08	1.98 ± 0.05	3.74 ± 0.6	1.1	-7.36
HD100943	B1Iab/b	294.16 -0.08	2.1	6.66	6.8	6.66	6.82	6.79	6.73	0.21 ± 0.08	0.21 ± 0.05	1.05 ± 0.68	3.8	-5.16
HD99857	B1Ib	294.78 -4.94	1.8	6.81	7.57	7.49	7.15	7.17	7.08	0.31 ± 0.08	1.19 ± 0.05	3.89 ± 1.15	2.4	-4.97
HD102997	B5Ia	295.89 0.2	4.03	6.31	6.79	6.56	5.73	5.66	5.54	0.38 ± 0.07	1.55 ± 0.04	4.06 ± 0.83	2.4	-8.02
HD103779	B0/1II	296.85 -1.02	2.02	6.35	7.18	7.22	7.13	7.2	7.2	0.22 ± 0.08	0.87 ± 0.05	3.91 ± 1.5	2.2	-5.18
HD103338	B3Ib	296.95 -3.09	2.39	7.03	9.35	9.01	7.12	7.14	7.08	0.73 ± 0.08	2.92 ± 0.04	4 ± 0.46	32.6	-5.8
HD29138	B1.5III	297.99 -30.54	2.24	6.26	7.09	7.2	7.37	7.42	7.41	0.12 ± 0.06	0.49 ± 0.04	4.03 ± 2.08	1	-5.05
HD106343	B1.5Ia	298.93 -1.83	2.33	5.58	6.29	6.24	5.94	5.92	5.85	0.28 ± 0.08	1.13 ± 0.05	4.06 ± 1.35	1.4	-6.73
HD160430	B2II	3.78 3.59	1.22	7.78	8.93	8.74	7.08	7.05	6.96	0.58 ± 0.07	2.92 ± 0.04	5.02 ± 0.66	21.3	-4.62
HD108002	B2Ia/ab	300.16 -2.48	2.43	6.3	7.01	6.96	6.63	6.59	6.54	0.27 ± 0.08	1.16 ± 0.05	4.29 ± 1.38	1	-6.13
HD108639	B1III	300.22 1.95	1.98	7.09	8.74	8.57	7.57	7.62	7.6	0.55 ± 0.08	2.06 ± 0.05	3.77 ± 0.57	12.2	-4.98
HD109867	B0.5/1Iab	301.71 -4.35	2.54	5.5	6.26	6.26	6.1	6.09	6.05	0.23 ± 0.08	0.99 ± 0.04	4.26 ± 1.53	1	-6.75
HD109399	B0.5III	301.71 -9.88	2.33	6.85	7.67	7.67	7.62	7.69	7.66	0.26 ± 0.08	0.77 ± 0.06	2.95 ± 1.09	2	-4.94
HD111123	B1IV	302.46 3.18	0.09	0.03	1.02	1.25	1.8	1.92	1.99	0.01 ± 0.02	0.02 ± 0.02	1.92 ± 2.32	0.9	-3.43
HD111822	B0.5/1Ib	303.1 10.2	1.92	6.89	7.84	7.87	7.98	8.05	8.04	0.22 ± 0.08	0.67 ± 0.05	3.06 ± 1.42	1.4	-4.21
HD111973	B5I	303.23 2.49	1.94	5.62	6.12	5.94	5.36	5.3	5.21	0.38 ± 0.08	1.34 ± 0.05	3.57 ± 0.85	1.5	-6.84
HD111990	B1.5I+	303.25 2.53	2.44	6.46	6.95	6.78	6.12	6.05	6.01	0.39 ± 0.08	1.48 ± 0.05	3.76 ± 0.83	1.5	-6.64
HD112481	B2II/III	303.95 13.08	2.14	7.66	8.36	8.33	8.29	8.36	8.39	0.31 ± 0.07	0.71 ± 0.04	2.29 ± 0.61	1.6	-4.03
HD117024	B2Ib	307.06 -1.3	1.98	6.44	7.13	7.11	6.95	6.99	6.97	0.25 ± 0.08	0.86 ± 0.05	3.43 ± 1.28	1.7	-5.23
HD115842	B0.5Ia/ab	307.08 6.83	1.68	5.7	6.39	6.09	5.34	5.3	5.17	0.52 ± 0.07	1.72 ± 0.04	3.29 ± 0.5	2.1	-6.76
HD117460	B0/1(III)	307.52 -0.53	1.88	6.53	9.35	7.5	7.29	7.3	7.25	1.91 ± 0.05	0.35 ± 0.04	0.18 ± 0.03	36.3	-4.23
HD116084	B2Ib	307.73 10.4	1.95	5.3	6.02	5.91	5.58	5.54	5.47	0.29 ± 0.07	1.1 ± 0.05	3.83 ± 1.06	1.3	-6.64
HD117490	ON9.5IInn	307.88 1.66	2.11	8.13	8.94	8.92	8.78	8.84	8.83	0.32 ± 0.08	1.01 ± 0.05	3.17 ± 0.89	2.1	-3.72
HD120680	B2II	309.05 -4.38	1.05	6.63	7.16	7.11	6.84	6.83	6.77	0.25 ± 0.07	0.93 ± 0.04	3.75 ± 1.1	1.3	-3.92
HD119646	B1.5Ib	309.23 -0.25	1.74	6.03	6.67	6.62	6.34	6.31	6.25	0.27 ± 0.08	1.06 ± 0.05	3.9 ± 1.27	1	-5.65
HD149881	B0.5III	31.37 36.23	1.76	5.87	6.84	7.03	7.37	7.48	7.54	0.1 ± 0.06	0.26 ± 0.04	2.7 ± 2.04	1.5	-4.46
HD184915	B0.5IIIn	31.77 -13.29	0.51	4.05	4.93	4.96	4.96	5.17	4.96	0.19 ± 0.08	0.64 ± 0.04	3.34 ± 1.6	11.3	-4.2
HD123008	ON9.2Iab	311.02 -2.8	3.24	8.58	10	9.5	7.91	7.84	7.71	0.84 ± 0.07	2.89 ± 0.04	3.42 ± 0.33	8.2	-5.95
HD121228	B1Ib	311.07 2.48	1.68	7.34	8	7.86	7.43	7.43	7.38	0.4 ± 0.08	1.27 ± 0.04	3.2 ± 0.68	1.7	-4.53
HD123056	O9.5IV(n)	312.17 1.03	2.4	7.54	8.28	8.14	7.81	7.79	7.84	0.46 ± 0.08	1.28 ± 0.05	2.8 ± 0.51	1.2	-5.04
HD122879	B0Ia	312.26 1.79	2.22	5.9	6.64	6.5	6.13	6.09	6.07	0.37 ± 0.08	1.28 ± 0.05	3.42 ± 0.79	0.6	-6.51
HD125545	B1Iab/b	314.62 2.51	2.17	6.84	8.01	7.91	7	6.97	6.95	0.4 ± 0.07	1.88 ± 0.05	4.7 ± 0.96	7.5	-5.65
HD119608	B1Ib	320.35 43.13	2.84	6.65	7.47	7.53	7.59	7.59	7.62	0.17 ± 0.07	0.62 ± 0.04	3.73 ± 1.94	0.4	-5.36
HD134959	B2Ia	320.51 -1.21	3.58	9.05	9.14	8.1	5.77	5.48	5.24	1.24 ± 0.07	3.76 ± 0.04	3.03 ± 0.2	1.6	-8.43
HD129056	B1.5III	321.61 11.44	0.14	1.22	2.13	2.29	2.63	2.72	2.67	0.07 ± 0.04	0.24 ± 0.04	3.7 ± 2.56	2.1	-3.72
HD142758	B1Ia	325.31 -4.28	3.21	6.62	7.24	7.07	6.55	6.48	6.39	0.39 ± 0.07	1.43 ± 0.05	3.64 ± 0.77	1.1	-6.89
HD141318	B2III	326.79 -0.73	0.6	5.13	5.76	5.77	5.7	5.72	5.7	0.23 ± 0.07	0.78 ± 0.05	3.32 ± 1.14	1.1	-3.9
CPD-546791	O9.5V	327.56 -0.83	2.29	10.51	10.95	10.41	9.03	8.86	8.75	0.86 ± 0.08	2.83 ± 0.05	3.3 ± 0.33	1.1	-4.22
HD150898	B0Ia/ab	329.98 -8.47	1.13	4.7	5.55	5.61	5.69	5.73	5.75	0.19 ± 0.07	0.68 ± 0.04	3.58 ± 1.37	0.8	-5.33
HD145794	B2II/III	330.88 -1.5	1.28	8.34	8.92	8.77	8.21	8.19	8.21	0.44 ± 0.07	1.41 ± 0.05	3.19 ± 0.57	3	-3.17
HD148878	B1/2Ia	332.61 -3.67	3.21	7.57	8.02	7.69	6.89	6.82	6.73	0.54 ± 0.07	1.68 ± 0.05	3.14 ± 0.48	1.4	-6.52
HD157246	B1Ib	334.64 -11.48	0.26	2.25	3.21	3.34	3.63	3.69	3.73	0.09 ± 0.05	0.3 ± 0.04	3.34 ± 2.41	0.6	-4.03
HD150168	B1Iab/Ib	336.08 -2.2	1.01	4.88	5.67	5.68	5.69	5.76	5.72	0.21 ± 0.08	0.72 ± 0.05	3.41 ± 1.64	1.9	-5.06
HD150041	B1/2Ib	336.65 -1.5	1.11	6.39	7.16	7.07	6.79	6.83	6.81	0.39 ± 0.07	1.18 ± 0.05	3.02 ± 0.63	2.2	-4.34

Table 5.2: Complete information relative to each star for the B-Sgs sample: SpT and galactic coordinates (l and b); distances in kpc (d); photometry values (U Mag, B Mag, V Mag, J Mag, H Mag, K Mag); extinction parameters with corresponding uncertainty ($E(B-V)$, A_V, R_V and χ^2) and absolute magnitude taking into account interstellar extinction: M_V.

ID	SpT	l [º] b	d [kpc]	U Mag	B Mag	V Mag	J Mag	H Mag	K Mag	$E(B-V)$	A_V [mag]	R_V	χ^2	M_V [mag]
HD148379	B2Iab	337.25 1.58	1.61	5.51	5.95	5.37	4.05	3.83	3.69	0.74 ± 0.08	2.39 ± 0.04	3.21 ± 0.36	0.5	-8.06
HD158243	B1Ib	337.59 -10.64	4.06	7.33	8.12	8.15	8.09	8.12	8.12	0.19 ± 0.07	0.7 ± 0.04	3.74 ± 1.58	1.3	-5.59
HD150574	ON9III(n)	339 -0.2	2.2	8.01	8.74	8.5	7.93	7.89	7.86	0.51 ± 0.07	1.58 ± 0.04	3.08 ± 0.48	0.8	-4.8
HD149038	O9.7Iab	339.38 2.51	0.91	4.05	4.99	4.94	4.74	4.68	4.61	0.25 ± 0.07	1.15 ± 0.05	4.58 ± 1.36	0.8	-5.99
HD151018	O9Ib	339.51 -0.41	2.05	8.9	9.93	9.37	7.28	7.17	7.02	0.93 ± 0.08	3.63 ± 0.05	3.92 ± 0.36	13.5	-5.82
HD148688	B1Iaeqp	340.72 4.35	1.36	5.16	5.78	5.39	4.37	4.24	4.13	0.62 ± 0.08	2.07 ± 0.05	3.36 ± 0.47	1.1	-7.35
HD154811	OC9.7Ib	341.06 -4.22	1.22	6.71	7.32	6.98	5.95	5.85	5.79	0.6 ± 0.08	2.17 ± 0.05	3.59 ± 0.53	2.1	-5.62
HD155756	O9Ibp	342.57 -4.39	3.37	9.39	9.81	9.55	8.14	8.03	7.92	0.58 ± 0.07	2.76 ± 0.04	4.79 ± 0.58	6.8	-5.85
HD152147	O9.7IbNwk	343.15 1.1	1.57	7.2	7.76	7.34	6.35	6.25	6.17	0.68 ± 0.08	2.13 ± 0.05	3.14 ± 0.4	1.3	-5.77
HD152235	B0.5Ia	343.31 1.1	1.63	6.47	6.92	6.38	5.03	4.94	4.8	0.81 ± 0.07	2.49 ± 0.04	3.07 ± 0.32	3.3	-7.18
HD165024	B2Ib	343.33 -13.82	0.34	2.73	3.58	3.66	3.85	3.9	3.94	0.14 ± 0.08	0.4 ± 0.04	2.87 ± 1.97	0.6	-4.41
HD152003	O9.7IabNwk	343.33 1.41	1.54	6.9	7.47	7.08	6.1	6.01	5.91	0.66 ± 0.08	2.08 ± 0.05	3.14 ± 0.41	1.8	-5.94
HD148546	O9Iab	343.38 7.15	2.35	7.28	7.99	7.71	6.96	6.9	6.81	0.53 ± 0.07	1.83 ± 0.04	3.44 ± 0.52	1.4	-5.97
HD152200	O9.7IV(n)	343.41 1.22	1.39	7.74	8.49	8.39	8.12	8.08	8.06	0.37 ± 0.07	1.26 ± 0.05	3.39 ± 0.79	0.4	-3.59
HD152076	B0/1III	343.42 1.4	1.61	7.98	9.1	8.9	7.93	7.93	7.89	0.57 ± 0.08	2.12 ± 0.05	3.7 ± 0.56	7.5	-4.25
HD152249	OC9Iab	343.45 1.16	1.47	5.91	6.65	6.45	5.9	5.84	5.75	0.44 ± 0.08	1.59 ± 0.05	3.59 ± 0.71	1.1	-5.97
HD152234	B0.5Ia	343.46 1.22	3.25	4.92	5.64	5.45	4.95	4.93	4.77	0.39 ± 0.08	1.46 ± 0.05	3.7 ± 0.82	3.4	-8.57
HD152247	O9.2III	343.61 1.3	1.38	6.62	7.35	7.16	6.65	6.61	6.59	0.47 ± 0.07	1.52 ± 0.05	3.22 ± 0.56	1	-5.06
HD155985	B0.5Ib	343.63 -3.92	1.08	6.04	6.66	6.49	5.92	5.86	5.81	0.43 ± 0.08	1.57 ± 0.05	3.66 ± 0.77	1	-5.24
HD152685	B1Ib	344.29 1.23	0.9	7.06	8.79	8.83	6.96	6.98	6.91	0.42 ± 0.07	3.22 ± 0.05	7.48 ± 1.21	45.7	-4.17
HD152405	O9.7II	344.56 1.89	1.68	6.71	7.42	7.29	6.83	6.86	6.8	0.4 ± 0.08	1.43 ± 0.05	3.6 ± 0.74	2.6	-5.26
HD154385	B1Ib	349.49 2.8	1.26	7.17	7.74	7.43	6.58	6.57	6.46	0.6 ± 0.07	1.89 ± 0.04	3.15 ± 0.42	3.5	-4.96
HD163522	B1Ia	349.57 -9.09	4.01	7.57	8.43	8.43	8.39	8.46	8.34	0.22 ± 0.08	0.81 ± 0.05	3.61 ± 1.53	3.8	-5.4
HD157038	B3Iap	349.95 -0.79	2.18	6.99	7.2	6.44	4.54	4.29	4.11	0.92 ± 0.07	3.01 ± 0.04	3.27 ± 0.27	1.4	-8.26
HD154368	O9.5Iab	349.97 3.22	1.03	6.1	6.63	6.13	5.02	4.85	4.75	0.74 ± 0.08	2.37 ± 0.05	3.19 ± 0.36	0.3	-6.3
HD154643	O9.7III	350.54 3.19	0.93	6.76	7.42	7.2	6.57	6.54	6.53	0.53 ± 0.07	1.67 ± 0.05	3.15 ± 0.51	1.9	-4.32
HD154090	B2Iab	350.83 4.29	1.05	4.44	5.13	4.87	4.25	4.19	4.13	0.49 ± 0.07	1.53 ± 0.05	3.1 ± 0.52	1	-6.76
HD156134	B0Ib	351.2 1.37	1.75	8.26	8.7	8.05	6.58	6.41	6.3	0.94 ± 0.08	2.81 ± 0.05	3 ± 0.28	1	-5.98
HD147165	B1III+B1:V	351.31 17	0.21	2.32	3.02	2.89	2.49	2.4	2.4	0.39 ± 0.07	1.4 ± 0.05	3.59 ± 0.73	0.2	-5.16
HD155450	B1Ib	353.2 3.92	1.1	5.36	6.02	6	5.78	5.79	5.75	0.26 ± 0.08	1.02 ± 0.06	3.95 ± 1.41	1.6	-5.23
HD160575	B1/2II	353.78 -3	1.22	7.47	8.82	8.88	6.77	6.7	6.62	0.43 ± 0.05	3.65 ± 0.04	8.42 ± 0.94	45.5	-5.2
HD161789	B2/3II	357 -2.67	1.32	9.19	9.66	9.22	8.24	8.16	8.13	0.77 ± 0.07	2.16 ± 0.04	2.81 ± 0.3	1.8	-3.54
HD159090	B0.5Ia/ab	357.41 1.35	1.33	6.79	7.56	7.4	7.01	7	7.03	0.46 ± 0.08	1.31 ± 0.05	2.81 ± 0.62	1.7	-4.53
HD156212	B0Iab	357.59 5.83	1.4	7.91	9.13	8.74	6.71	6.57	6.5	0.77 ± 0.08	3.57 ± 0.05	4.61 ± 0.49	18.7	-5.57
HD177812	B1/2Ib	37.51 -1.76	2.64	8.86	9.11	8.64	7.31	7.22	7.08	0.75 ± 0.08	2.51 ± 0.04	3.34 ± 0.38	3.6	-5.98
HD178129	B3Ia	37.81 -1.95	2.45	7.63	7.85	7.45	6.33	6.21	6.07	0.59 ± 0.07	2.03 ± 0.04	3.43 ± 0.47	2.2	-6.53
HD214080	B1/2Ib	44.8 -56.92	1.49	6	6.81	6.93	7.1	7.25	7.21	0.12 ± 0.07	0.38 ± 0.04	3.19 ± 2.13	4.1	-4.31
HD164741	B2Ib/II	5.16 -1.64	1.36	8.74	9.48	9.19	8.17	8.14	8.09	0.61 ± 0.07	2.06 ± 0.04	3.37 ± 0.44	5.4	-3.53
HD173502	B1/2Ib	5.36 -12.27	3.91	8.77	9.61	9.7	9.97	10.06	10.09	0.16 ± 0.08	0.37 ± 0.05	2.32 ± 1.73	0.8	-3.63
HD156779	B2II	5.43 10.32	2.86	8.95	9.57	9.38	8.84	8.85	8.78	0.43 ± 0.07	1.2 ± 0.04	2.82 ± 0.53	2.7	-4.1
HD168941	O9.5IVp	5.82 -6.31	4	8.53	9.36	9.37	9.19	9.21	9.22	0.3 ± 0.07	1.12 ± 0.05	3.72 ± 0.96	1.4	-4.76
HD165016	B2Ib	5.85 -1.58	1.03	6.42	9.01	8.73	7.38	7.42	7.43	0.72 ± 0.08	2.53 ± 0.04	3.52 ± 0.41	20.9	-3.87
HD180968	B3IV+	56.36 4.85	0.54	4.64	5.43	5.43	5.34	5.41	5.4	0.26 ± 0.08	0.78 ± 0.05	3.01 ± 1.06	2.4	-4.01
HD185859	B3I+	56.64 -1	1	6.29	6.89	6.52	5.72	5.67	5.65	0.65 ± 0.07	1.82 ± 0.05	2.78 ± 0.35	1.5	-5.3
HD187320	B2III	56.9 -3.09	1.86	6.89	7.5	7.4	7	7.01	7	0.36 ± 0.07	1.16 ± 0.04	3.22 ± 0.76	2.4	-5.11
HD344776	B0.5Ib	59.51 0	2.05	9.04	9.41	8.76	7.22	7.05	6.99	0.99 ± 0.08	2.91 ± 0.04	2.93 ± 0.25	2.6	-5.71
HD168750	B1Ib	6.19 -5.85	1.71	7.61	8.31	8.21	8	8.02	7.97	0.35 ± 0.07	1.04 ± 0.04	2.94 ± 0.68	1.4	-4
HD149757	O9.2IVnn	6.28 23.59	0.14	1.73	2.58	2.56	2.59	2.59	2.62	0.28 ± 0.07	0.81 ± 0.05	2.88 ± 0.91	0.2	-3.96
HD164018	B1/2Ib	6.65 0.16	1.23	9.55	9.86	9.26	7.75	7.56	7.48	0.92 ± 0.08	2.94 ± 0.04	3.21 ± 0.3	1.7	-4.13
HD165132	B5/6Ib	6.75 -1.21	1.43	7.38	9.11	9.12	7.79	7.8	7.77	0.44 ± 0.07	2.68 ± 0.05	6.05 ± 1.01	23.8	-4.34
HD164971	B0Ia	6.89 -0.93	2.83	9.03	9.88	9.66	8.63	8.54	8.55	0.56 ± 0.07	2.22 ± 0.05	3.94 ± 0.56	6.1	-4.82

Table 5.2: Complete information relative to each star for the B-Sgs sample: SpT and galactic coordinates (l and b); distances in kpc (d); photometry values (U Mag, B Mag, V Mag, J Mag, H Mag, K Mag); extinction parameters with corresponding uncertainty ($E(B-V)$, A_V, R_V and χ^2) and absolute magnitude taking into account interstellar extinction: M_V.

ID	**SpT**	**l [º] b**	**d [kpc]**	**U Mag**	**B Mag**	**V Mag**	**J Mag**	**H Mag**	**K Mag**	$E(B-V)$	A_V **[mag]**	R_V	χ^2	M_V **[mag]**
HD186841	B1Ia	60.41 -0.29	2.08	8.55	8.86	8.01	6.21	6.03	5.91	1.15 ± 0.08	3.15 ± 0.04	2.75 ± 0.22	2.1	-6.73
HD190066	B1Iab	60.69 -4.54	1.58	6.07	6.78	6.6	6.07	6.12	6.1	0.47 ± 0.07	1.35 ± 0.05	2.91 ± 0.53	4	-5.75
HD183561	B2III	60.86 4.27	1.2	7.68	8.22	8.05	7.7	7.75	7.7	0.42 ± 0.08	1.03 ± 0.05	2.43 ± 0.52	2.3	-3.37
HD191877	B1Ib	61.57 -6.45	1.73	5.51	6.22	6.27	6.27	6.39	6.35	0.19 ± 0.08	0.63 ± 0.05	3.24 ± 1.55	3.9	-5.55
HD203664	B0.5IIIn	61.93 -27.46	2.4	7.37	8.33	8.53	9.07	9.17	9.24	0.04 ± 0.04	0.05 ± 0.03	1.64 ± 2.1	0.4	-3.42
HD332407	B1Ibp	64.28 3.11	2.69	7.99	8.65	8.52	8.04	8.06	8.02	0.42 ± 0.07	1.41 ± 0.04	3.39 ± 0.65	2.9	-5.04
HD189779	B2III	67.06 -0.13	1.52	7.69	8.28	8.23	7.98	7.98	7.98	0.28 ± 0.08	0.94 ± 0.05	3.36 ± 1.08	1.2	-3.62
HD187459	B0.5II	68.81 3.85	1.4	5.99	6.58	6.46	6.03	6.03	6.03	0.39 ± 0.08	1.32 ± 0.05	3.35 ± 0.7	2.3	-5.58
HD331759	B1Ib	69.39 0.43	1.86	8.77	9.08	8.72	7.69	7.67	7.6	0.69 ± 0.07	2.16 ± 0.04	3.11 ± 0.36	5	-4.79
HD190603	B1.5Ia	69.49 0.39	1.91	5.73	6.19	5.65	4.5	4.14	4.04	0.65 ± 0.08	2.3 ± 0.05	3.5 ± 0.46	1.9	-8.06
HD163892	O9.5IV(n)	7.15 0.62	1.27	6.81	7.61	7.44	7.08	7.1	7.08	0.47 ± 0.07	1.3 ± 0.05	2.74 ± 0.47	1.6	-4.38
HD164402	B0Iab/b	7.16 -0.03	0.76	4.88	5.77	5.77	5.75	5.75	5.76	0.25 ± 0.07	0.89 ± 0.05	3.52 ± 1.22	0.4	-4.51
HD164637	B0Ib/II	7.34 -0.23	1.08	5.8	6.65	6.72	6.77	6.81	6.85	0.21 ± 0.07	0.76 ± 0.05	3.54 ± 1.35	0.9	-4.21
HD164359	B1II	7.7 0.34	1.21	6.71	8.89	8.67	7.5	7.57	7.53	0.63 ± 0.07	2.3 ± 0.04	3.62 ± 0.47	16.9	-4.04
HD190336	B0.7II-III	70.38 1.28	2.08	7.94	8.68	8.62	8.38	8.41	8.4	0.34 ± 0.07	1.06 ± 0.04	3.13 ± 0.78	1.5	-4.03
HD192539	B2III	70.41 -1.45	1.09	6.79	7.38	7.29	6.96	6.96	7	0.37 ± 0.07	1.08 ± 0.05	2.93 ± 0.62	1.8	-3.98
HD226868	O9.7Iabpvar	71.33 3.07	2.15	9.38	9.72	8.91	6.87	6.65	6.5	1.1 ± 0.08	3.55 ± 0.05	3.22 ± 0.24	2.6	-6.3
HD227704	B0III	71.99 1.47	1.88	8.31	8.95	8.7	7.68	7.64	7.6	0.59 ± 0.07	2.21 ± 0.04	3.71 ± 0.49	5.8	-4.88
HD190919	B0.7Ib	72.55 2.01	1.97	6.86	7.54	7.29	6.68	6.69	6.65	0.54 ± 0.07	1.52 ± 0.05	2.83 ± 0.43	2.4	-5.71
HD227634	B0.2II	72.64 2.04	1.84	7.03	8.17	7.92	7.4	7.42	7.41	0.55 ± 0.08	1.42 ± 0.05	2.61 ± 0.42	2.3	-4.82
BD+353955	B0.7Iab	72.66 2.07	1.74	6.99	7.63	7.38	6.79	6.8	6.75	0.52 ± 0.08	1.47 ± 0.05	2.81 ± 0.47	2.3	-5.29
HD191495	B0IV-V(n)	72.74 1.41	1.66	7.56	8.47	8.42	8.19	8.23	8.25	0.36 ± 0.08	1.13 ± 0.05	3.08 ± 0.76	2.3	-3.81
HD199140	B2IIIv	72.75 -10.48	0.82	5.47	6.4	6.54	6.8	6.94	6.98	0.13 ± 0.07	0.23 ± 0.05	1.95 ± 1.56	2.7	-3.27
HD190467	B5II:n	72.95 2.79	1.1	7.92	8.27	8.18	7.76	7.73	7.67	0.3 ± 0.07	1.17 ± 0.04	3.95 ± 1.09	1.5	-3.21
HD191139	B0.5III	73.27 2.22	2.21	7.48	8.17	8.02	7.37	7.35	7.33	0.45 ± 0.07	1.68 ± 0.05	3.69 ± 0.69	3	-5.38
HD191611	B	73.62 1.85	2.97	8.36	8.87	8.57	7.74	7.73	7.66	0.6 ± 0.08	1.87 ± 0.05	3.12 ± 0.48	3.2	-5.66
HD191456	B0.5III	73.68 2.09	1.08	6.7	7.5	7.43	7.22	7.29	7.29	0.37 ± 0.08	0.98 ± 0.05	2.68 ± 0.66	2.6	-3.72
HD228053	B1II	73.86 1.87	3.17	8.95	9.24	8.87	7.74	7.63	7.57	0.67 ± 0.08	2.33 ± 0.05	3.48 ± 0.46	2.7	-5.96
HD185780	B0III	74.17 9.05	1.73	6.72	7.63	7.72	7.92	8.02	8.07	0.2 ± 0.07	0.49 ± 0.04	2.44 ± 1.07	1.5	-3.96
HD191396	B0.5II	74.88 2.93	1.84	7.64	8.3	8.12	7.49	7.47	7.46	0.48 ± 0.08	1.63 ± 0.04	3.38 ± 0.59	2.9	-4.83
HD187879	B1.1III+B2.5/3V:	75.22 7.13	1.12	4.86	5.61	5.68	5.71	5.76	5.77	0.16 ± 0.08	0.6 ± 0.04	3.7 ± 2.15	1.2	-5.16
HD193007	B0III	75.36 1.31	4.08	7.95	8.4	7.95	7.17	7.12	7.11	0.74 ± 0.08	1.79 ± 0.05	2.43 ± 0.3	0.9	-6.9
HD193076	B0.5II	75.45 1.25	1.69	7.38	7.88	7.65	6.95	6.94	6.89	0.51 ± 0.08	1.67 ± 0.05	3.24 ± 0.54	2.7	-5.16
HD194303	B3II	75.57 -0.26	1.27	9.23	9.25	8.67	7.06	6.9	6.8	0.87 ± 0.08	2.83 ± 0.05	3.23 ± 0.32	3.8	-4.69
HD229033	B0II-III	75.93 0.64	1.67	9.26	9.43	8.82	7.28	7.14	7.06	0.93 ± 0.08	2.89 ± 0.05	3.1 ± 0.31	2.9	-5.18
HD192422	B0.5Ib	75.95 2.45	2.22	7.13	7.61	7.1	5.92	5.83	5.75	0.79 ± 0.08	2.31 ± 0.04	2.91 ± 0.33	2.4	-6.94
BD+364063	ON9.7Ib	76.17 -0.34	1.72	10.93	10.67	9.66	7.17	6.85	6.64	1.26 ± 0.08	4.03 ± 0.04	3.21 ± 0.22	1.6	-5.55
HD190991	B0IVp	76.28 4.34	2.23	7.58	8.3	8.22	7.8	7.83	7.84	0.4 ± 0.07	1.39 ± 0.04	3.49 ± 0.72	3.4	-4.91
HD193032	B0III	76.42 1.98	1.89	8.09	8.62	8.31	7.55	7.5	7.46	0.61 ± 0.08	1.83 ± 0.05	3.01 ± 0.43	1.4	-4.9
HDE229234	O9III	76.92 0.59	1.67	9.5	9.58	8.94	7.34	7.18	7.1	0.96 ± 0.08	3 ± 0.05	3.12 ± 0.29	2.6	-5.17
HD194280	OC9.7Iab	77.2 0.92	1.68	8.94	9.08	8.42	6.74	6.6	6.49	0.95 ± 0.07	2.97 ± 0.04	3.11 ± 0.26	4	-5.68
HD229159	B	77.36 1.16	1.65	9.54	9.43	8.62	6.44	6.22	6.09	1.13 ± 0.07	3.66 ± 0.04	3.25 ± 0.23	5.1	-6.13
HD192660	B0Ib	77.37 3.14	1.86	7.83	8.07	7.56	6.15	6	5.91	0.79 ± 0.08	2.65 ± 0.04	3.33 ± 0.36	2.7	-6.44
HD197460	B0.5III	77.41 -3.66	1.64	7.93	8.42	8.15	7.37	7.34	7.3	0.56 ± 0.07	1.78 ± 0.05	3.2 ± 0.45	2.5	-4.71
HD189957	O9.7III	77.43 6.17	2.02	6.93	7.84	7.82	7.72	7.71	7.74	0.3 ± 0.08	0.98 ± 0.05	3.28 ± 0.99	0.6	-4.68
HD228712	B0.5Ia	78.06 3.11	1.79	9.86	9.81	8.67	5.89	5.51	5.28	1.42 ± 0.08	4.62 ± 0.05	3.26 ± 0.2	1.4	-7.21
HD193117	O9.5II	78.07 3.02	1.7	8.89	9.26	8.79	7.24	7.09	6.97	0.79 ± 0.08	3 ± 0.05	3.79 ± 0.39	3.8	-5.37
HD192039	B0IV	78.41 4.53	1.75	8.28	8.95	8.79	8.3	8.32	8.3	0.49 ± 0.07	1.48 ± 0.05	3.02 ± 0.51	2.9	-3.91
HD192001	O9.5IV	78.53 4.66	1.69	7.97	8.52	8.29	7.68	7.68	7.68	0.56 ± 0.08	1.64 ± 0.05	2.92 ± 0.47	2.7	-4.49
HD186994	B0III	78.62 10.06	1.73	6.43	7.37	7.5	7.78	7.89	7.92	0.14 ± 0.07	0.42 ± 0.04	2.92 ± 1.74	1.6	-4.11
HD194279	B2Ia	78.68 1.99	1.83	8.01	8.04	7.01	4.64	4.19	4	1.22 ± 0.08	3.98 ± 0.05	3.26 ± 0.23	0.1	-8.28

Table 5.2: Complete information relative to each star for the B-Sgs sample: SpT and galactic coordinates (l and b); distances in kpc (d); photometry values (U Mag, B Mag, V Mag, J Mag, H Mag, K Mag); extinction parameters with corresponding uncertainty ($E(B-V)$, A_V, R_V and χ^2) and absolute magnitude taking into account interstellar extinction: M_V.

ID	**SpT**	**l [º] b**	**d [kpc]**	**U Mag**	**B Mag**	**V Mag**	**J Mag**	**H Mag**	**K Mag**	$E(B-V)$	A_V **[mag]**	R_V	χ^2	M_V **[mag]**
HD192832	B5Ia	79.2 4.13	1.78	10.82	9.37	8.64	6.43	6.12	5.98	0.97 ± 0.08	3.57 ± 0.05	3.68 ± 0.3	3.1	-6.19
HD194779	B3II	79.43 1.92	1.27	7.48	7.98	7.8	7.18	7.16	7.13	0.45 ± 0.08	1.46 ± 0.05	3.24 ± 0.66	2.3	-4.19
HD194839	B0.5Iae	79.52 1.87	1.5	8.4	8.49	7.49	5.24	4.96	4.72	1.25 ± 0.07	3.82 ± 0.04	3.05 ± 0.2	1.5	-7.21
HD158661	B0II	8.29 9.05	3.1	7.66	9.02	8.81	7.73	7.72	7.68	0.55 ± 0.07	2.19 ± 0.05	3.98 ± 0.6	9.8	-5.84
HD165812	B1/2II	8.48 -1.11	1.25	7.2	7.93	7.94	7.84	7.91	7.89	0.26 ± 0.07	0.82 ± 0.04	3.13 ± 1.04	2.5	-3.37
HD166852	B0Ia/ab	8.51 -2.32	1.82	8.11	9.2	8.99	7.9	7.9	7.82	0.57 ± 0.07	2.3 ± 0.04	4.05 ± 0.57	8.6	-4.61
HD159864	B1Ib	8.52 7.38	2.19	8.09	8.81	8.57	8.09	8.11	8.04	0.52 ± 0.07	1.4 ± 0.05	2.71 ± 0.43	2.1	-4.53
HD165516	B1/2Ib	8.93 -0.44	1.24	5.73	6.45	6.33	6	6	5.9	0.37 ± 0.07	1.27 ± 0.05	3.47 ± 0.77	1.9	-5.41
HD195229	B	80.26 1.91	1.43	7.11	7.82	7.66	7.34	7.36	7.32	0.44 ± 0.08	1.21 ± 0.05	2.74 ± 0.54	1.4	-4.33
HD201638	B0.5Ib	80.29 -8.45	3.01	7.98	8.92	9.05	9.47	9.52	9.6	0.13 ± 0.07	0.22 ± 0.05	1.88 ± 1.64	0.1	-3.56
HD186618	B0V	80.48 11.48	1.74	6.57	7.59	7.75	8.18	8.31	8.34	0.07 ± 0.06	0.15 ± 0.04	2.46 ± 2.4	1.3	-3.61
HD188209	O9.5Iab	80.99 10.09	1.92	4.61	5.55	5.63	5.72	5.83	5.82	0.19 ± 0.07	0.61 ± 0.05	3.31 ± 1.47	2.5	-6.4
HD190427	B0III	81.04 7.94	1.87	7.73	8.47	8.37	7.95	7.96	7.97	0.42 ± 0.07	1.38 ± 0.04	3.3 ± 0.68	2.6	-4.37
HD201819	B1Vp	81.05 -8.08	0.96	5.46	6.37	6.51	6.75	6.85	6.9	0.11 ± 0.06	0.31 ± 0.04	2.84 ± 1.64	1.9	-3.72
HD191781	ON9.7Iab	81.18 6.61	2.79	10.1	10.06	9.53	8	7.76	7.66	0.83 ± 0.07	3.04 ± 0.05	3.66 ± 0.34	1.2	-5.74
HD188439	B0.5IIIn	81.77 10.32	1.02	5.24	6.15	6.28	6.48	6.6	6.62	0.13 ± 0.07	0.38 ± 0.04	2.89 ± 1.76	2.3	-4.15
HD194057	B1Ib	81.85 4.54	1.53	8.21	8.2	7.52	5.58	5.36	5.17	0.98 ± 0.08	3.48 ± 0.05	3.54 ± 0.33	2.8	-6.89
HD195592	O9.7Ia	82.36 2.96	1.73	7.75	7.95	7.08	5.08	4.8	4.62	1.13 ± 0.08	3.37 ± 0.04	2.98 ± 0.22	1	-7.48
HD204172	B0Ib	83.39 -9.96	2.06	4.89	5.86	5.94	6.08	6.08	6.14	0.16 ± 0.07	0.6 ± 0.05	3.82 ± 2.06	0.2	-6.23
HD215733	B1II	85.16 -36.35	3.85	6.37	7.21	7.34	7.6	7.72	7.76	0.11 ± 0.07	0.29 ± 0.05	2.74 ± 2.46	2	-5.88
HD198479	B	85.37 1.18	5.08	8.43	8.9	8.62	7.69	7.65	7.61	0.61 ± 0.08	2.04 ± 0.05	3.34 ± 0.47	4.3	-6.95
HD198478	B4Ia	85.75 1.49	1.84	4.83	5.28	4.86	3.89	3.78	3.75	0.62 ± 0.08	1.81 ± 0.05	2.91 ± 0.42	1.2	-8.27
BD+453341	B1II	86.98 0.69	2.55	8.73	9.11	8.73	7.75	7.65	7.63	0.66 ± 0.08	2.06 ± 0.05	3.13 ± 0.43	1.8	-5.37
HD202124	O9Iab	87.29 -2.66	3.21	7.33	7.94	7.76	7.18	7.13	7.09	0.42 ± 0.07	1.56 ± 0.04	3.7 ± 0.72	1.1	-6.33
HD199216	B1II	88.92 3.03	1.1	7.05	7.51	7.03	6.05	6.03	5.97	0.77 ± 0.08	1.94 ± 0.05	2.52 ± 0.29	2.8	-5.12
HD165892	B2II	9.17 -0.81	1.4	9.07	9.55	9.12	8.09	8	7.91	0.69 ± 0.07	2.03 ± 0.05	2.94 ± 0.35	1.6	-3.64
HD149363	B1/2Ib	9.85 26.69	2.19	7.06	7.86	7.81	7.68	7.72	7.73	0.34 ± 0.07	0.93 ± 0.04	2.75 ± 0.68	1.5	-4.82
HD203938	B0.5IV	90.56 -2.23	2.96	7.13	7.54	7.08	5.96	5.88	5.81	0.77 ± 0.07	2.27 ± 0.04	2.94 ± 0.3	2.2	-7.55
BD+483437	B1Ib	93.56 -2.06	3	8.15	8.83	8.73	8.29	8.34	8.3	0.39 ± 0.07	1.28 ± 0.04	3.3 ± 0.68	3.4	-4.94
HD200857	B3IIIv	94.25 5.58	0.85	7.42	7.68	7.13	5.95	5.89	5.84	0.82 ± 0.08	2.06 ± 0.05	2.51 ± 0.28	3.2	-4.58
HD206259	B3III	95.93 -0.13	1.31	7.02	7.59	7.54	7.34	7.39	7.36	0.27 ± 0.07	0.66 ± 0.04	2.5 ± 0.84	2.3	-3.7
HD207793	B0.5III	97.39 -0.94	0.85	6.42	6.9	6.57	5.81	5.77	5.7	0.58 ± 0.07	1.67 ± 0.05	2.87 ± 0.41	1.8	-4.75
HD214993	B2III	97.65 -16.18	0.38	4.24	5.08	5.23	5.48	5.58	5.62	0.11 ± 0.07	0.33 ± 0.05	3.11 ± 2.17	1.7	-3.01
HD205196	B0Ib	98.57 4.41	1.01	7.57	7.92	7.43	5.91	5.74	5.59	0.77 ± 0.07	2.94 ± 0.05	3.83 ± 0.39	2.2	-5.53
HD206183	O9.5IV-V	98.89 3.4	0.9	6.75	7.55	7.41	7.19	7.19	7.23	0.45 ± 0.07	1.13 ± 0.04	2.5 ± 0.45	0.8	-3.5
HD205794	B0.5V	98.95 4.01	0.91	8.22	8.71	8.43	7.54	7.54	7.49	0.6 ± 0.07	1.94 ± 0.05	3.21 ± 0.44	4.7	-3.3
HD209678	B2I	99.33 -1.79	4.47	8.34	8.72	8.44	7.52	7.44	7.38	0.53 ± 0.08	1.87 ± 0.05	3.52 ± 0.56	2.3	-6.68
HD210809	O9Iab	99.85 -3.13	3.66	6.7	7.61	7.56	7.37	7.4	7.41	0.34 ± 0.08	1.05 ± 0.05	3.07 ± 0.93	1.4	-6.31
HD198781	B0.5V	99.94 12.61	0.91	5.75	6.47	6.45	6.3	6.38	6.4	0.31 ± 0.08	0.85 ± 0.05	2.74 ± 0.91	3	-4.21

References

Arp, Halton C. (Jan. 1958). "The Hertzsprung-Russell Diagram." In: *Handbuch der Physik* 51, p. 75. DOI: 10.1007/978-3-642-45908-5_2.

Bailer-Jones, C. A. L. et al. (Mar. 2021). "Estimating Distances from Parallaxes. V. Geometric and Photogeometric Distances to 1.47 Billion Stars in Gaia Early Data Release 3". In: 161.3, 147, p. 147. DOI: 10.3847/1538-3881/abd806.

Blaauw, Adriaan (Jan. 1964). "The O Associations in the Solar Neighborhood". In: 2, p. 213. DOI: 10.1146/annurev.aa.02.090164.001241.

Bouy, H. and J. Alves (Dec. 2015). "Cosmography of OB stars in the solar neighbourhood". In: 584, A26, A26. DOI: 10.1051/0004-6361/201527058.

Cardelli, J. A., G. C. Clayton, and J. S. Mathis (Dec. 1989). "The relationship between IR, optical, and UV extinction." In: *Interstellar Dust*. Ed. by Louis J. Allamandola and A. G. G. M. Tielens. Vol. 135, pp. 5–10.

Chen, B. -Q. et al. (July 2019). "The Galactic spiral structure as revealed by O- and early B-type stars". In: 487.1, pp. 1400–1409. DOI: 10.1093/mnras/stz1357. arXiv: 1905.05542 [astro-ph.GA].

Deno Stelter, R. and Stephen S. Eikenberry (Apr. 2020). "Extinction at the Galactic Center Using Near- and Mid-infrared Broadband Photometry: A Twist on the Rayleigh-Jeans Color Excess Method". In: *arXiv e-prints*, arXiv:2004.01338, arXiv:2004.01338. DOI: 10.48550/arXiv.2004.01338. arXiv: 2004.01338 [astro-ph.GA].

Dong, Ting, Dawn An, and Nam H. Kim (2019). "Prognostics 102: Efficient Bayesian-Based Prognostics Algorithm in MATLAB". In: *Fault Detection, Diagnosis and Prognosis*. Ed. by Fausto Pedro García Márquez. Rijeka: IntechOpen. Chap. 2. DOI: 10.5772/intechopen.82781. URL: https://doi.org/10.5772/intechopen.82781.

Egret, D., M. Wenger, and P. Dubois (Jan. 1991). "The SIMBAD astronomical database." In: *Databases and On-line Data in Astronomy*. Ed. by M. A. Albrecht and D. Egret. Vol. 171. Astrophysics and Space Science Library, pp. 79–88. DOI: 10.1007/978-94-011-3250-3_9.

Elias, F., J. Cabrera-Caño, and E. J. Alfaro (June 2006). "OB Stars in the Solar Neighborhood. I. Analysis of their Spatial Distribution". In: 131.5, pp. 2700–2709. DOI: 10.1086/503110. arXiv: astro-ph/0602484 [astro-ph].

Fitzpatrick, Edward L. (Dec. 1996). "The Composition of the Diffuse Interstellar Medium". In: 473, p. L55. DOI: 10.1086/310392.

— (Jan. 1999). "Correcting for the Effects of Interstellar Extinction". In: 111.755, pp. 63–75. DOI: 10.1086/316293.

Gaia Collaboration (Apr. 2018). "VizieR Online Data Catalog: Gaia DR2 (Gaia Collaboration, 2018)". In: *VizieR Online Data Catalog*, I/345, pp. I/345.

Green, Gregory M. et al. (Sept. 2015). "A Three-dimensional Map of Milky Way Dust". In: 810.1, 25, p. 25. DOI: 10.1088/0004-637X/810/1/25.

Holgado, Gonzalo, Sergio Simón-Dıaz, and Rodolfo Barbá (Nov. 2017). "Quantitative spectroscopic analyses in the IACOB+OWN project: Massive O-type stars in the Galaxy with the current Gaia information". In: *The Lives and Death-Throes of Massive Stars*. Ed. by J. J. Eldridge et al. Vol. 329, pp. 407–407. DOI: 10.1017/S1743921317001120.

Hoogerwerf, Ronnie (May 2000). "Hipparcos and the nearby OB associations. Space astrometry and high-mass star formation." PhD thesis. Leiden Observatory.

Kurucz, R. L. (Oct. 1993). "VizieR Online Data Catalog: Model Atmospheres (Kurucz, 1979)". In: *VizieR Online Data Catalog*, VI/39, pp. VI/39.

Maız Apellániz, J. and R. H. Barbá (May 2018). "Optical-NIR dust extinction towards Galactic O stars". In: 613, A9, A9. DOI: 10.1051/0004-6361/201732050. arXiv: 1712.09228 [astro-ph.GA].

Maız Apellániz, J., R. H. Barbá, et al. (Feb. 2021). "Galactic extinction laws - II. Hidden in plain sight, a new interstellar absorption band at 7700 Å broader than any known DIB". In: 501.2, pp. 2487–2503. DOI: 10.1093/mnras/staa2371. arXiv: 2008.00834 [astro-ph.GA].

Maız Apellániz, J., C. J. Evans, et al. (Apr. 2014). "The VLT-FLAMES Tarantula Survey. XVI. The optical and NIR extinction laws in 30 Doradus and the photometric determination of the effective temperatures of OB stars". In: 564, A63, A63. DOI: 10.1051/0004-6361/201423439. arXiv: 1402.3062 [astro-ph.GA].

Maız Apellániz, J., M. Pantaleoni González, et al. (Aug. 2020). "Galactic extinction laws - I. A global NIR analysis with 2MASS photometry". In: 496.4, pp. 4951–4963. DOI: 10.1093/mnras/staa1790. arXiv: 2006.09206 [astro-ph.GA].

Maız-Apellániz, Jesús (Sept. 2004). "CHORIZOS: A χ^2 Code for Parameterized Modeling and Characterization of Photometry and Spectrophotometry". In: 116.823, pp. 859–875. DOI: 10.1086/424021. arXiv: astro-ph/0408361 [astro-ph].

Morgan, W. W., S. Sharpless, and D. Osterbrock (Apr. 1952). "Some features of galactic structure in the neighborhood of the Sun." In: 57, pp. 3–3. DOI: 10.1086/106673.

Quintana, Alexis L., Nicholas J. Wright, and Robin D. Jeffries (June 2023). "Mapping the distribution of OB stars and associations in Auriga". In: 522.2, pp. 3124–3137. DOI: 10.1093/mnras/stad1160. arXiv: 2304.08370 [astro-ph.SR].

Simón-Dıaz, Sergio (2020). "A Modern Guide to Quantitative Spectroscopy of Massive OB Stars". In: *Reviews in Frontiers of Modern Astrophysics; From Space Debris to Cosmology*, pp. 155–187. DOI: 10.1007/978-3-030-38509-5_6.

Simón-Dıaz, Sergio et al. (July 2011). "The IACOB spectroscopic database of galactic OB stars". In: *Active OB Stars: Structure, Evolution, Mass Loss, and Critical Limits*. Ed. by Coralie Neiner et al. Vol. 272, pp. 310–312. DOI: 10.1017/S1743921311010714. arXiv: 1009.3750 [astro-ph.SR].

Skrutskie, M. F. et al. (Feb. 2006). "The Two Micron All Sky Survey (2MASS)". In: 131.2, pp. 1163–1183. DOI: 10.1086/498708.

Taylor, David K., R. L. Dickman, and N. Z. Scoville (Apr. 1987). "Molecular Clouds and the Gould Belt". In: 315, p. 104. DOI: 10.1086/165117.

Urbaneja, M. A. et al. (Sept. 2017). "LMC Blue Supergiant Stars and the Calibration of the Flux-weighted Gravity-Luminosity Relationship". In: 154.3, 102, p. 102. DOI: 10.3847/1538-3881/aa79a8. arXiv: 1706.03967 [astro-ph.SR].

Zhang, M. and J. Kainulainen (Dec. 2022). "Dust extinction map of the Galactic plane based on the VVV survey data". In: 517.4, pp. 5180–5215. DOI: 10.1093/mnras/stac3012. arXiv: 2210.09621 [astro-ph.GA].